Engineering artificial quantum matter with two-dimensional materials

Jose Lado

Department of Applied Physics, Aalto University, Finland

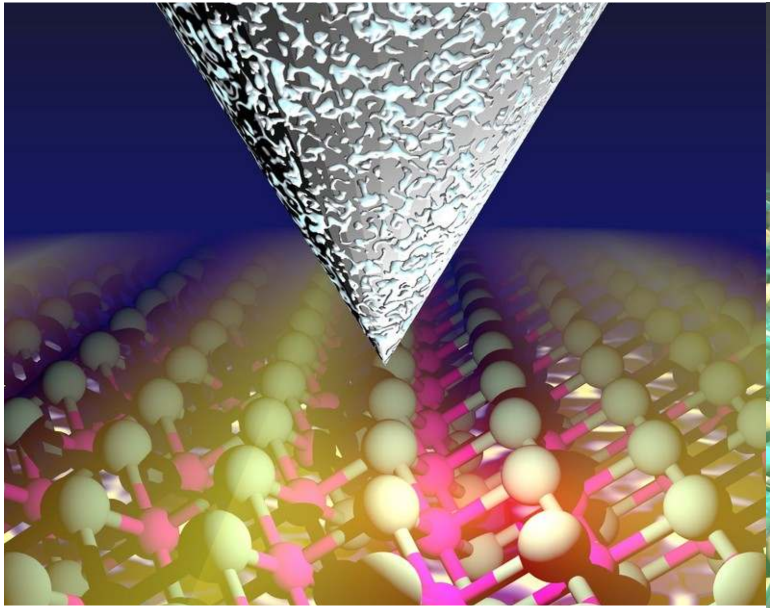

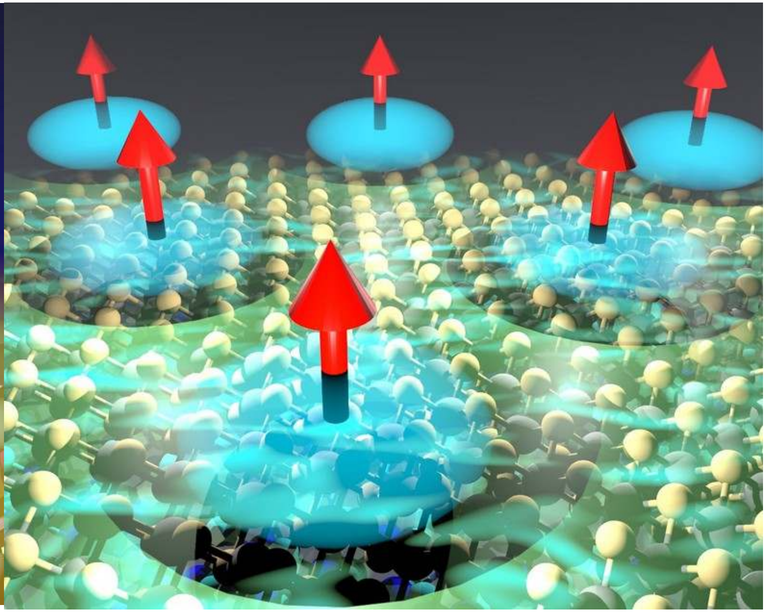

2D Materials 9 (2), 025010 (2022)
2D Materials 10 (2), 025026 (2023)
Advanced Materials, 2311342 (2024)

Phys. Rev. Lett. 127, 026401 (2021)
Nature 599, 582–586 (2021)
Nano Letters 24 (14), 4272–4278 (2024)

17th European School on Molecular Nanoscience (ESMolNa2024), Spain, May 23rd 2024

Building quantum matter with artificial lattices

Atomic lattices

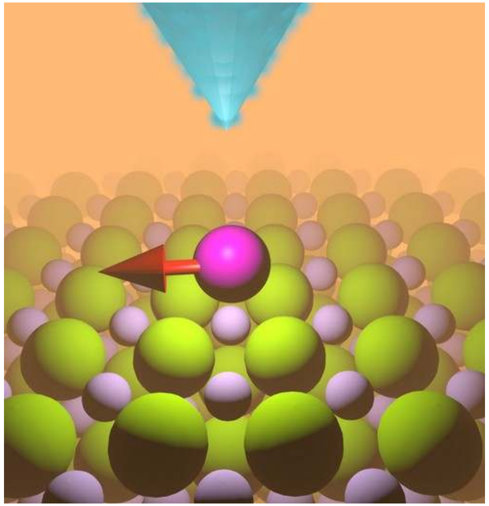

a = 0.5 nm

Nature Physics 12 (7), 656 (2016)
Nature Physics 13 (7) 668 (2017)
Science 335 (6065), 196-199 (2012)

Molecular lattices

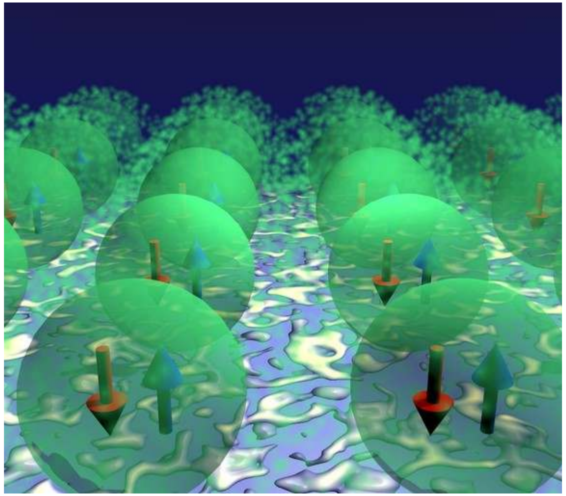

a = 3 nm

Nature 408, 447–449 (2000)
Nature Rev. Mat. 5 (2), 87-104 (2020)
Nature 598, 287–292 (2021)
Phys. Rev. Lett. 130, 100401 (2023)

Twisted 2D moire materials

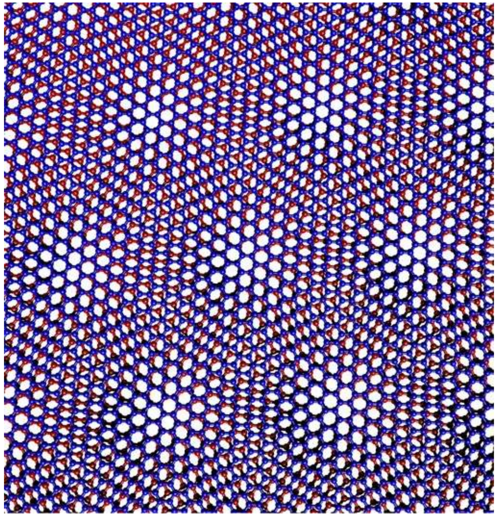

a = 30 nm

Phys. Rev. Lett. 99, 256802 (2007)
Nature Physics 6, 109–113 (2010)
PNAS 108 (30) 12233-12237 (2011)
Nature 556, 80–84 (2018)

The world of two-dimensional materials

Semimetal

Graphene

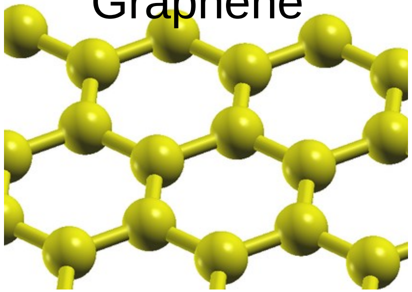

Insulator

BN

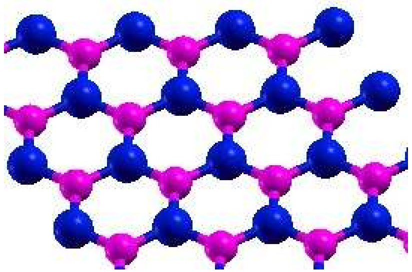

Superconductor

$NbSe_2$

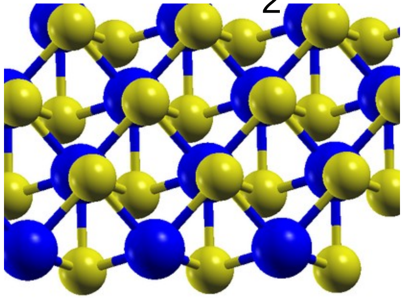

Ferroelectric

SnTe

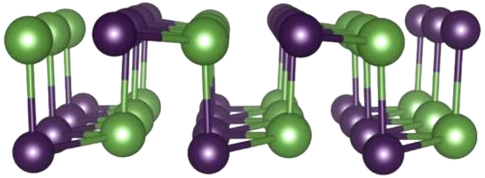

Semiconductor

WSe_2

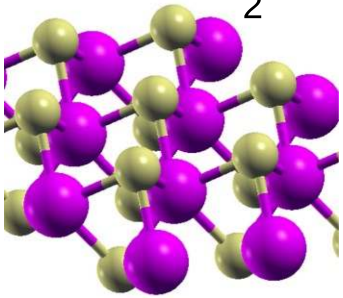

Ferromagnet

CrI_3

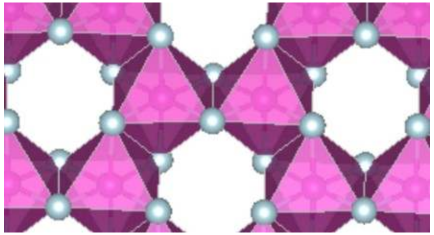

Quantum spin Hall insulator

WTe_2

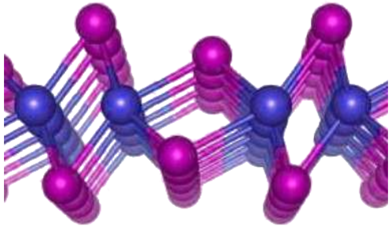

Multiferroic

NiI_2

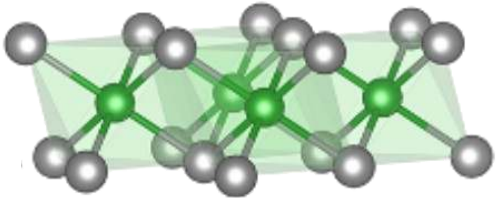

The flexibility of two-dimensional materials

They can be stacked

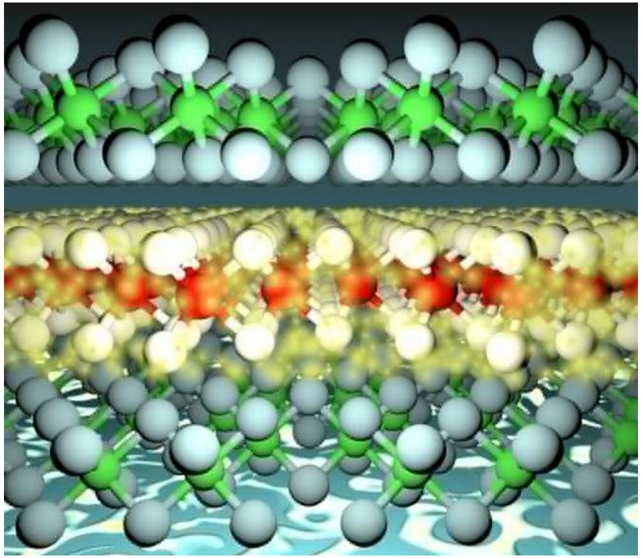

They can be rotated

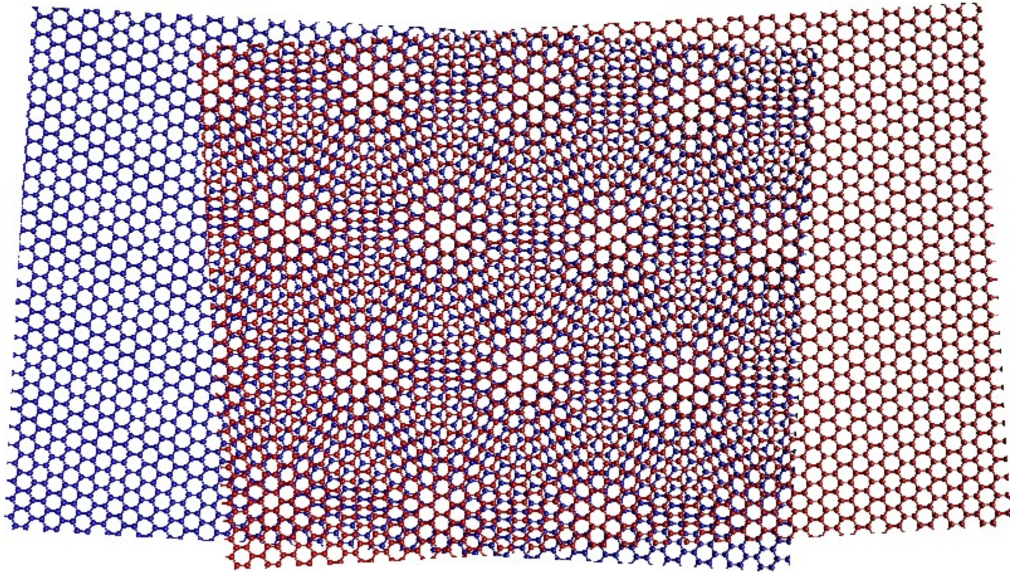

These are unique features of two-dimensional materials

Moire in twisted bilayer graphene

Upper graphene layer

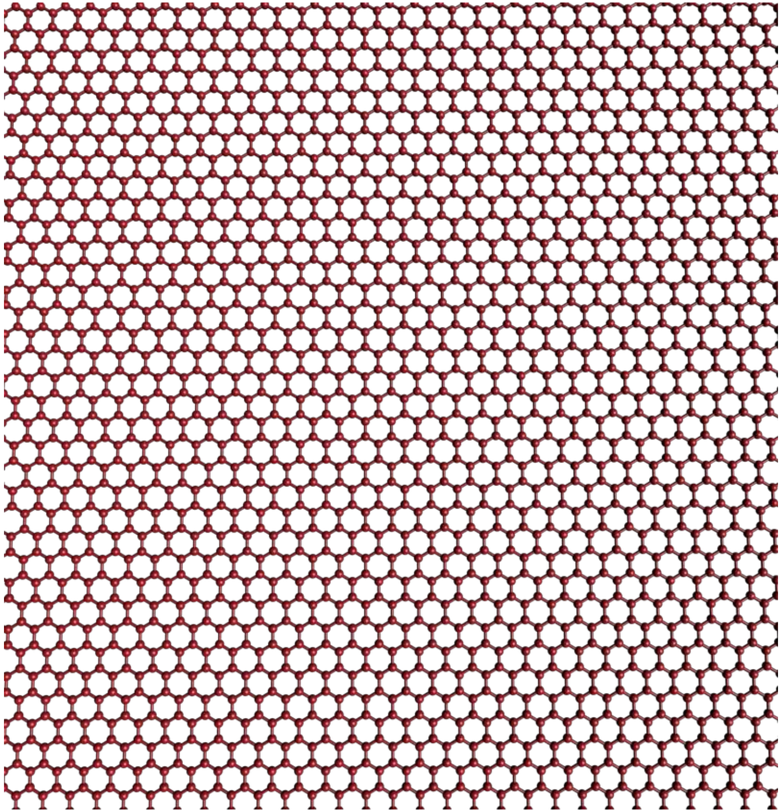

Lower graphene layer

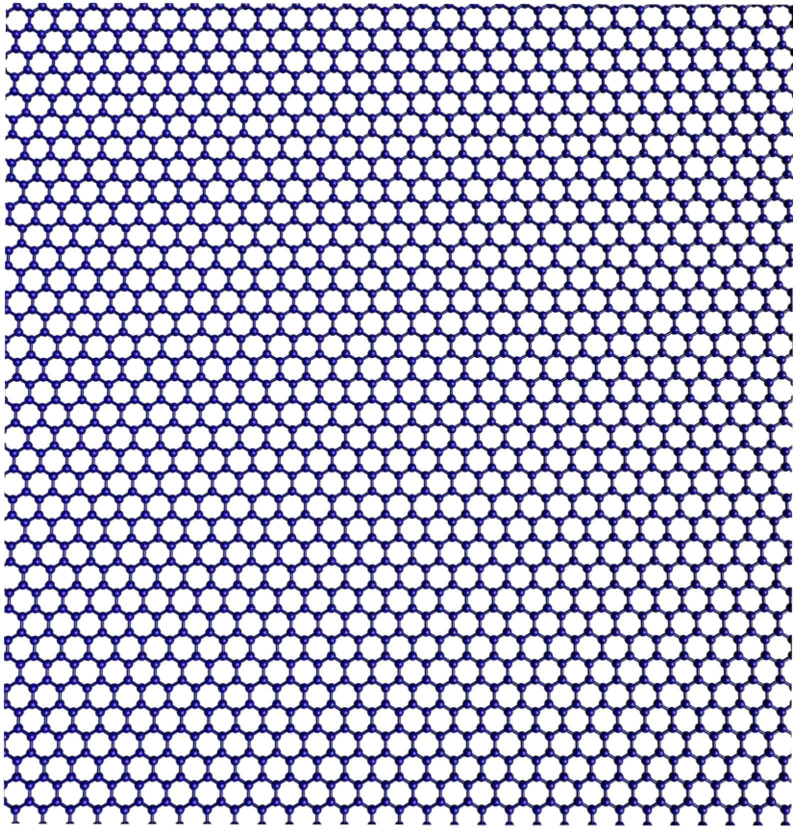

Moire in twisted bilayer graphene

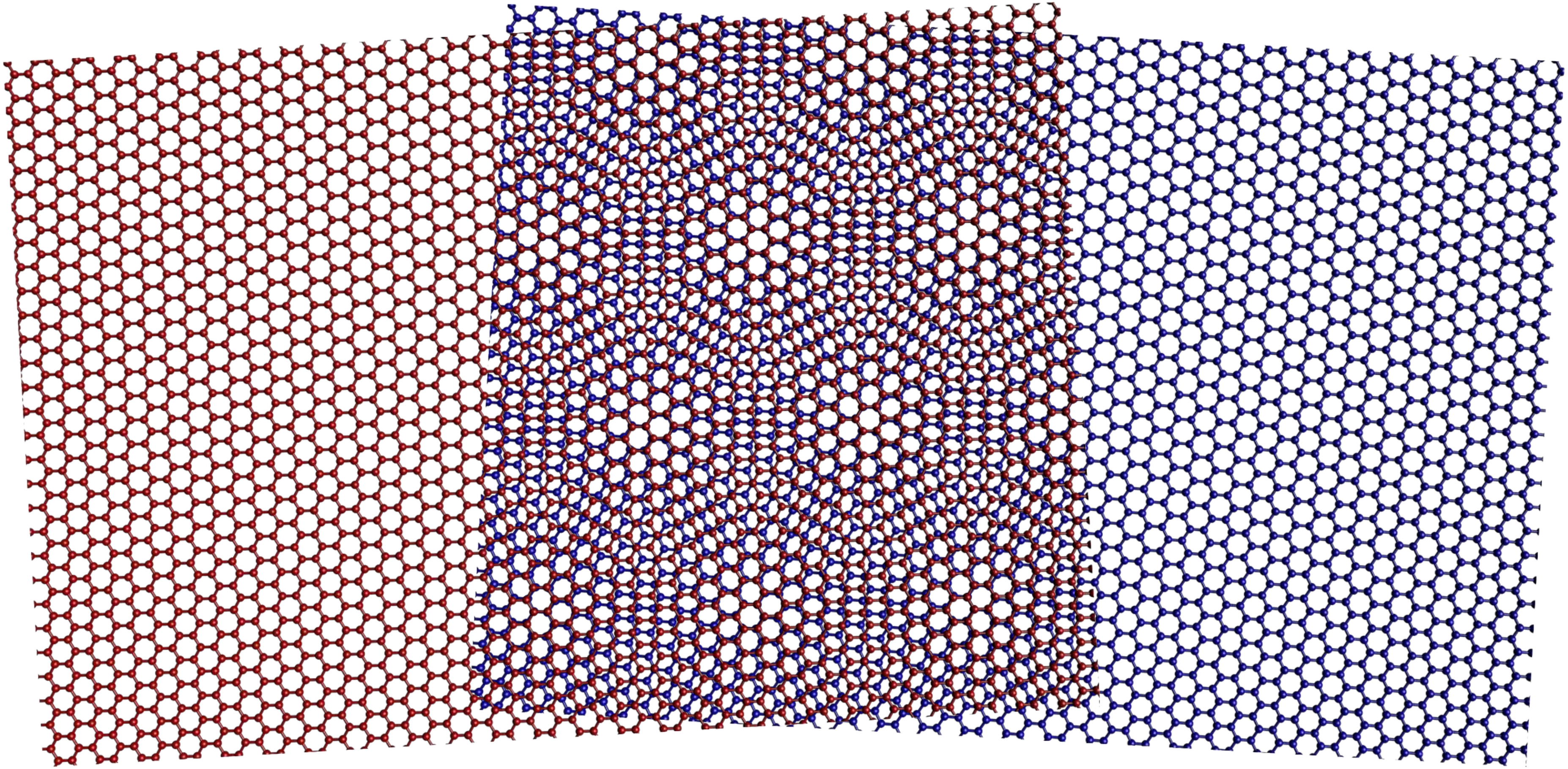

Moire in twisted bilayer graphene

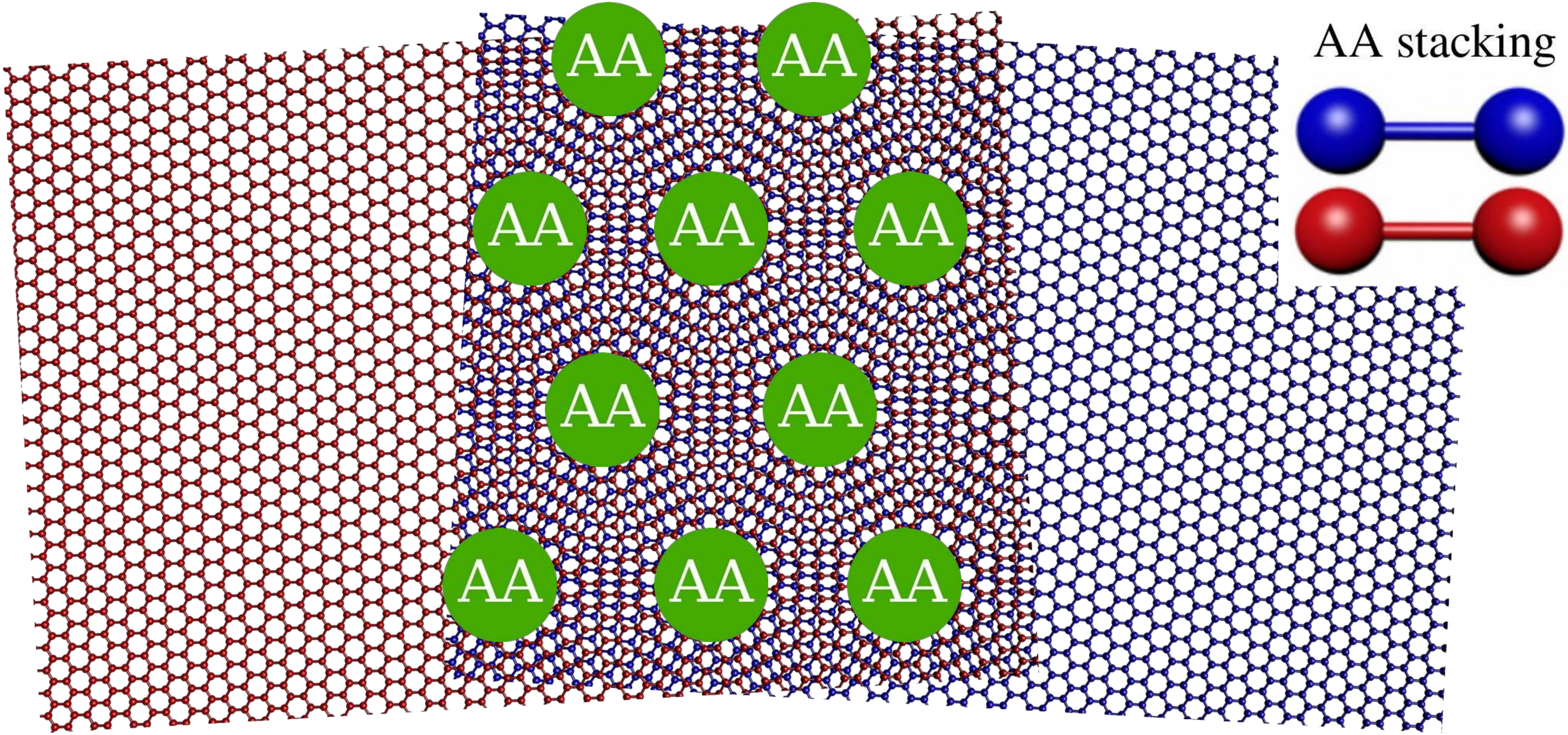

Moire in twisted bilayer graphene

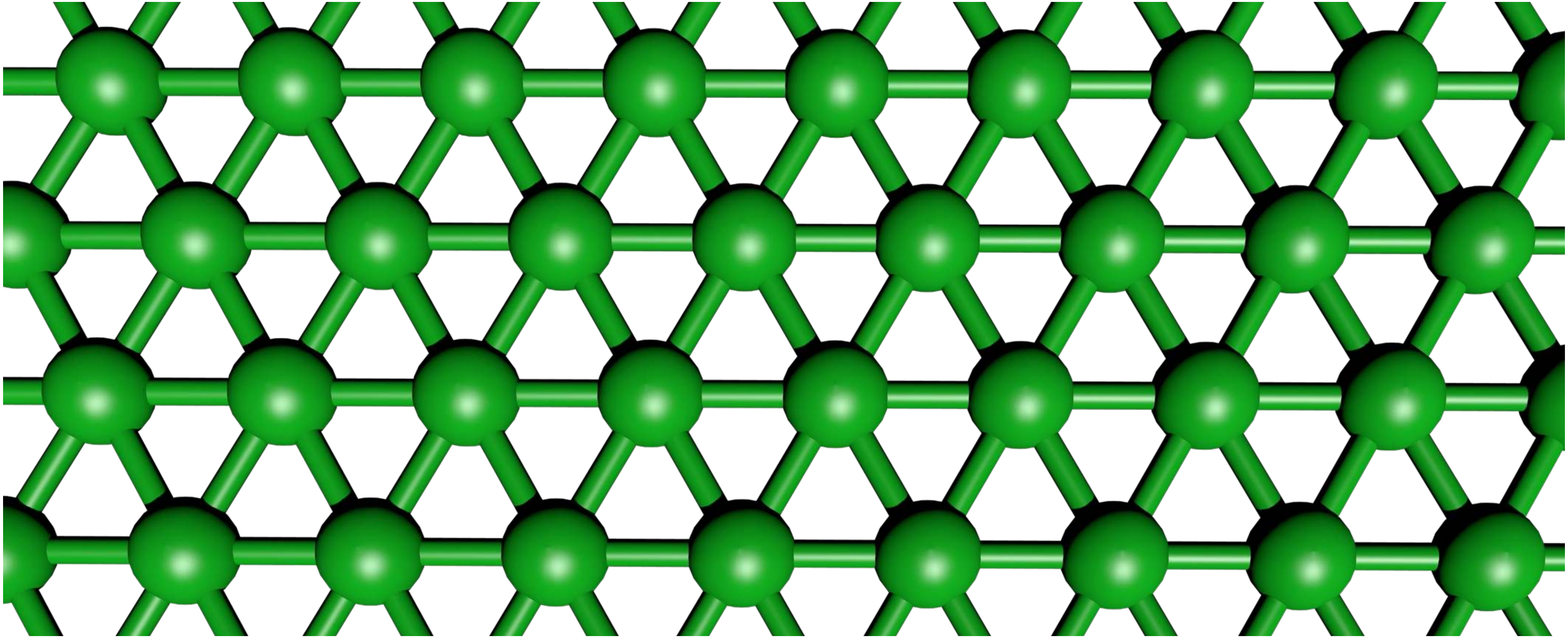

One material, a zoo of electronic phases

Twisted bilayer graphene

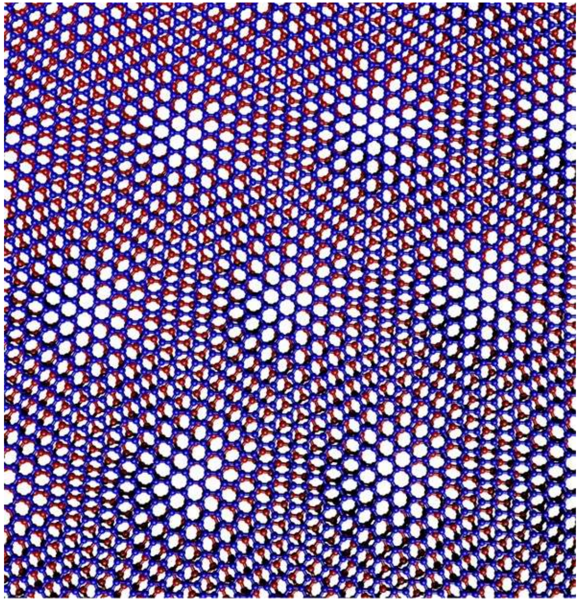

Superconductivity

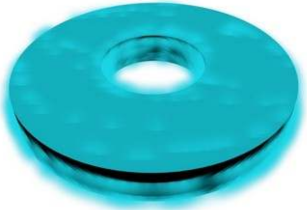

Nature 556, 43–50 (2018)
Nature 600, 240–245 (2021)

Topological networks

Nano Lett. 18, 11, 6725-6730 (2018)

Chern insulators

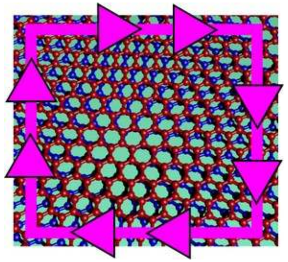

Science 365, 605-608 (2019)

Correlated insulators

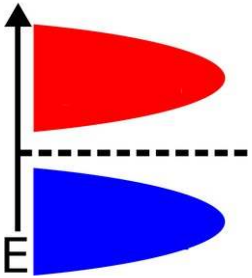

Nature 556, 80–84 (2018)

Quasicrystalline physics

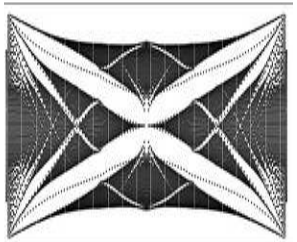

Science 361, 782-786 (2018)

Fractional Chern insulators

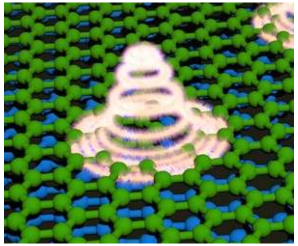

Nature 600, 439–443 (2021)

A bilayer of a van der Waals material realizes a variety of widely different electronic states

Van der Waals magnetic materials

Ferromagnet, antiferromagnets

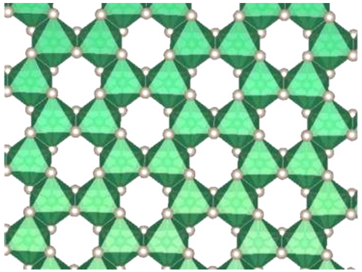

CrI_3, $CrCl_3$, $CrBr_3$

Nature 546, 270–273 (2017)

Break time-reversal

(proximal) Quantum spin-liquids

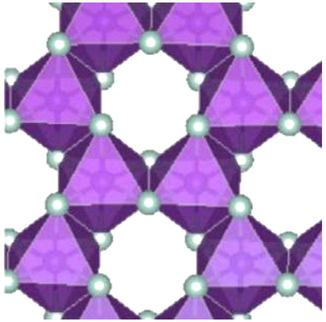

$RuCl_3$, 1T-TaS_2

Nature Physics 17, 1154–1161 (2021)

Heavy-fermion Kondo insulators

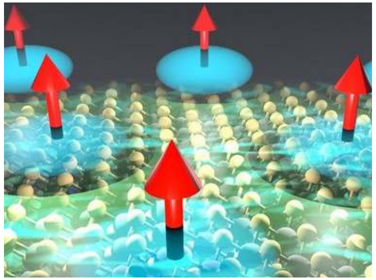

1T-TaS_2/1H-TaS_2

Nature 599, 582–586 (2021)

Do not break time-reversal

Multiferroics

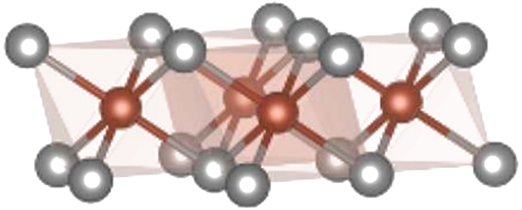

NiI_2

Nature 602, 601–605 (2022)

Break time-reversal and inversion symmetry

Emergent excitations in van der Waals magnets

Magnons

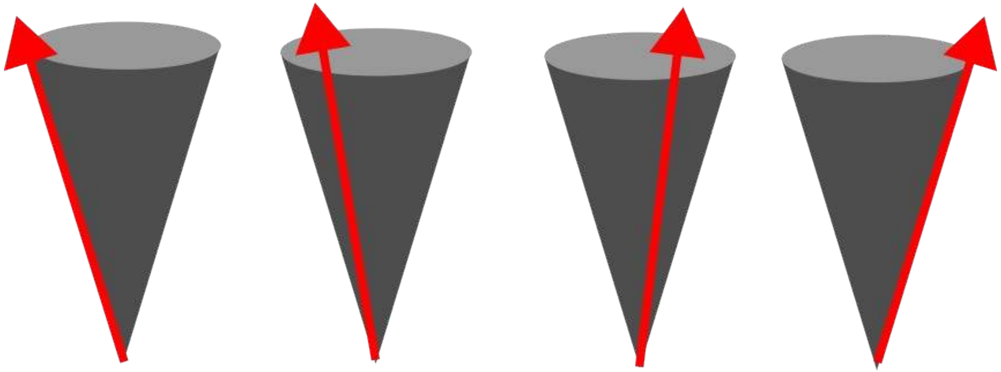

S=1
No charge

Instrumental for magnonics

Spinons

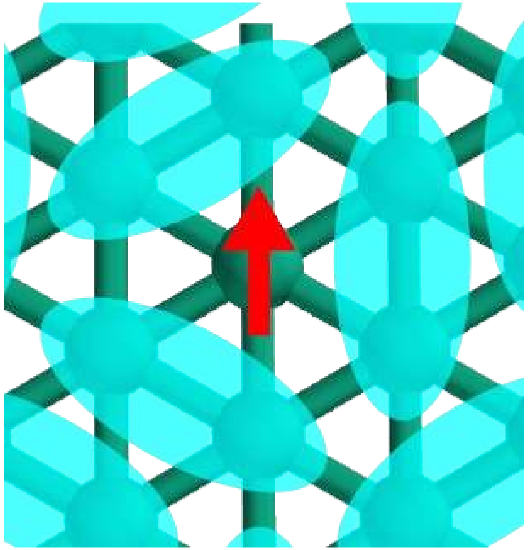

S=1/2
No charge

Plan for today

Engineering and probing van der Waals multiferroics

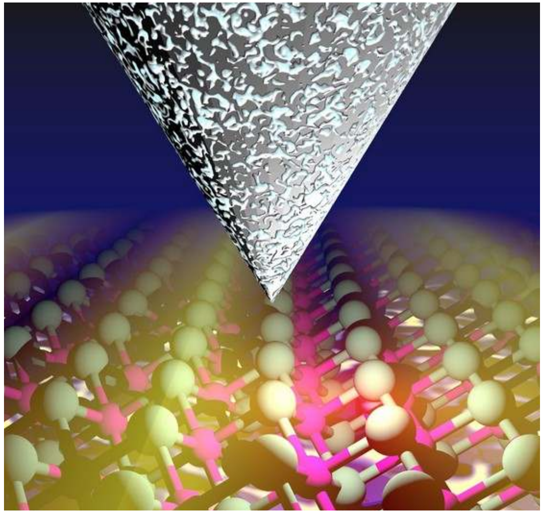

2D Materials 9 (2), 025010 (2022)
2D Materials 10 (2), 025026 (2023)
Advanced Materials, 2311342 (2024)

Engineering and probing van der Waals heavy fermion Kondo magnets

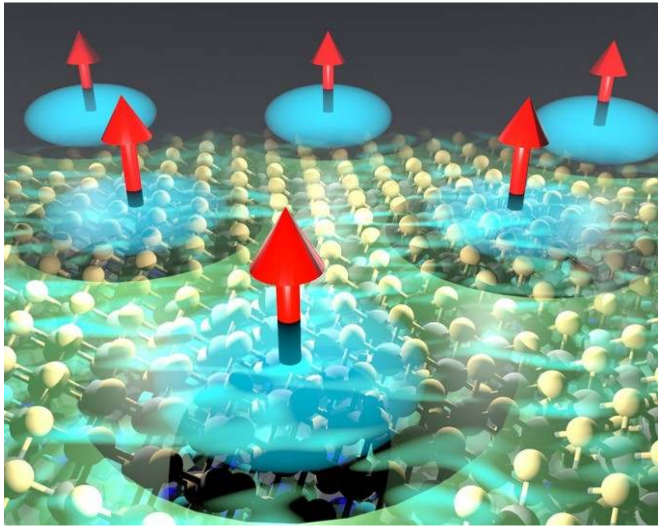

Phys. Rev. Lett. 127, 026401 (2021)
Nature 599, 582–586 (2021)
Nano Letters 24 (14), 4272–4278 (2024)

A reminder about magnetism

A reminder about magnetism, the origin of local moments

Let us start with a Hubbard model dimer

$$H = t[c^\dagger_{0\uparrow}c_{1\uparrow} + c^\dagger_{0\downarrow}c_{1\downarrow}] + \sum_i U c^\dagger_{i\uparrow}c_{i\uparrow}c^\dagger_{i\downarrow}c_{i\downarrow} + h.c.$$

Levels 

The full Hilbert space at half filling is

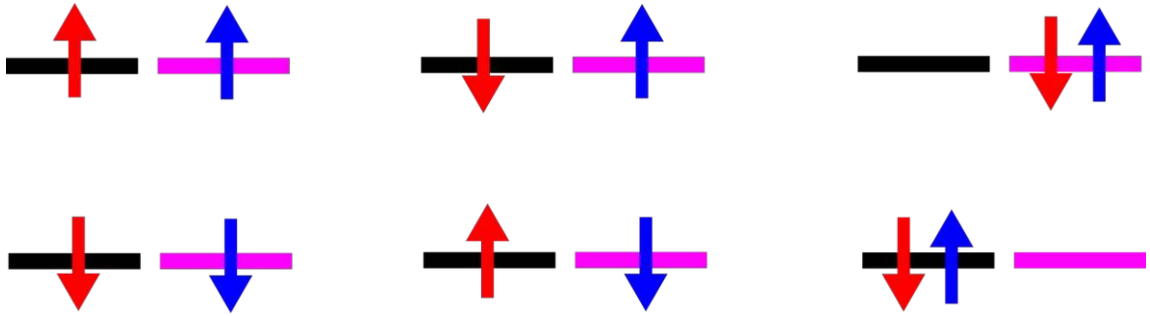

A reminder about magnetism, the origin of local moments

Let us start with a Hubbard model dimer

$$H = t[c^\dagger_{0\uparrow}c_{1\uparrow} + c^\dagger_{0\downarrow}c_{1\downarrow}] + \sum_i U c^\dagger_{i\uparrow}c_{i\uparrow}c^\dagger_{i\downarrow}c_{i\downarrow} + h.c.$$

The energies in the strongly interacting limit are $U \gg t$

~ 0 $\sim U$

A reminder about magnetism, the origin of local moments

Let us start with a Hubbard model dimer

$$H = t[c^{\dagger}_{0\uparrow} c_{1\uparrow} + c^{\dagger}_{0\downarrow} c_{1\downarrow}] + \sum_i U c^{\dagger}_{i\uparrow} c_{i\uparrow} c^{\dagger}_{i\downarrow} c_{i\downarrow} + h.c.$$

The low energy manifold is

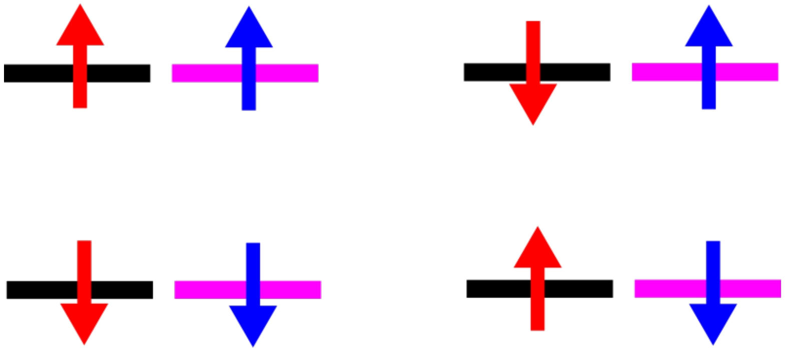

Just one electron in each site for $U \gg t$

Local S=1/2 at each site

A reminder about magnetism, the origin of the Heisenberg model

Let us start with a Hubbard model dimer

$$H = t[c^\dagger_{0\uparrow} c_{1\uparrow} + c^\dagger_{0\downarrow} c_{1\downarrow}] + \sum_i U c^\dagger_{i\uparrow} c_{i\uparrow} c^\dagger_{i\downarrow} c_{i\downarrow} + h.c.$$

In the strongly correlated (half-filled) limit we obtain a Heisenberg model

$$\mathcal{H} = J \vec{S}_0 \cdot \vec{S}_1$$

$$J \sim \frac{|t|^2}{U}$$

The lattice Heisenberg model

For a generic lattice and a generic interacting model, the Hamiltonian is

$$\mathcal{H} = \sum_{ij} J_{ij} \vec{S}_i \cdot \vec{S}_j$$

In those generic cases, the exchange couplings can be positive or negative

$$J_{ij} > 0$$

Antiferromagnetic coupling

$$J_{ij} < 0$$

Ferromagnetic coupling

Spin-orbit coupling introduces anisotropic couplings

$$\mathcal{H} = \sum_{ij} J_{ij}^{\alpha\beta} S_i^{\alpha} S_j^{\beta}$$

The classical Heisenberg model

Ferromagnetism

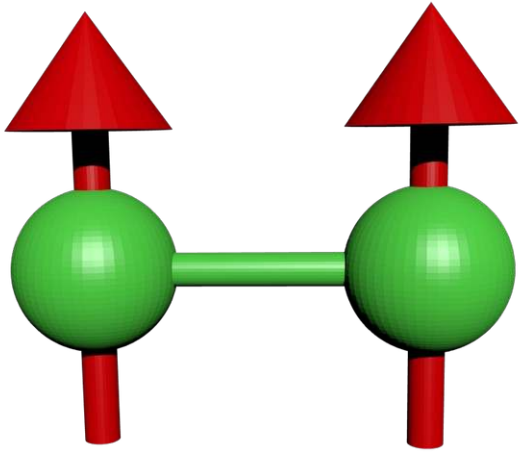

Antiferromagnetism

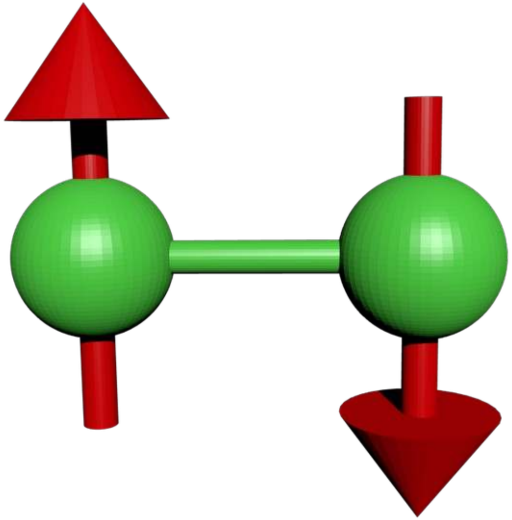

Frustrated magnetism

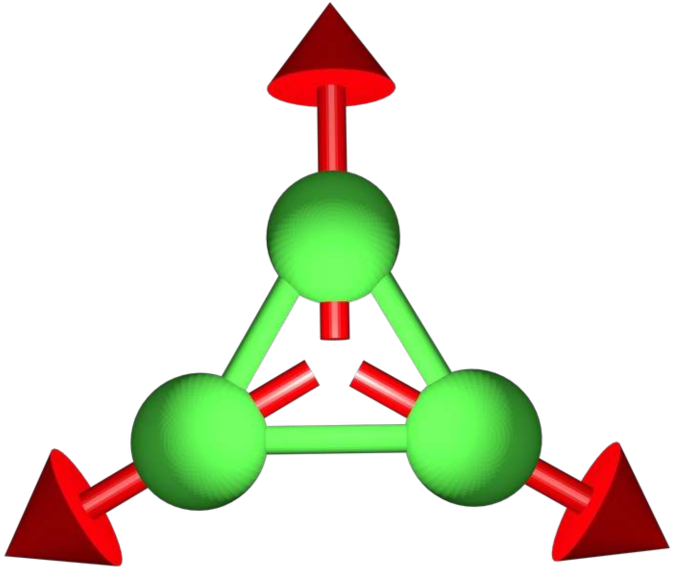

The quantum Heisenberg model

What is the ground state of the quantum Heisenberg Hamiltonian?

$$\mathcal{H} = J\vec{S}_0 \cdot \vec{S}_1$$

$$[S_j^\alpha, S_j^\beta] = i\epsilon_{\alpha\beta\gamma}S_j^\gamma$$

The ground state is unique, and does not break time-reversal

$$|GS\rangle = \frac{1}{\sqrt{2}}[|\uparrow\downarrow\rangle - |\downarrow\uparrow\rangle]$$

$$\langle \vec{S}_i \rangle = 0$$

The state is maximally entangled

A quantum magnet is the macroscopic version of the previous state $\langle \vec{S}_i \rangle = 0$

Classical and quantum magnets

Ferromagnet, antiferromagnets & helimagnets

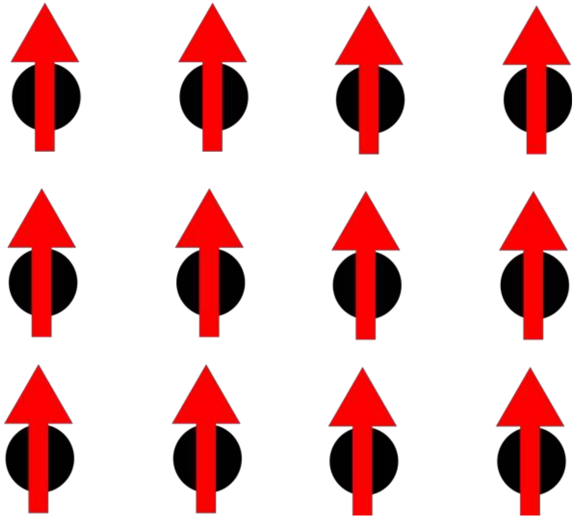

$$\langle \vec{S}_n \rangle \neq 0$$

They break time-reversal symmetry

Classical magnets

Quantum spin liquids and heavy ferrmion Kondo magnets

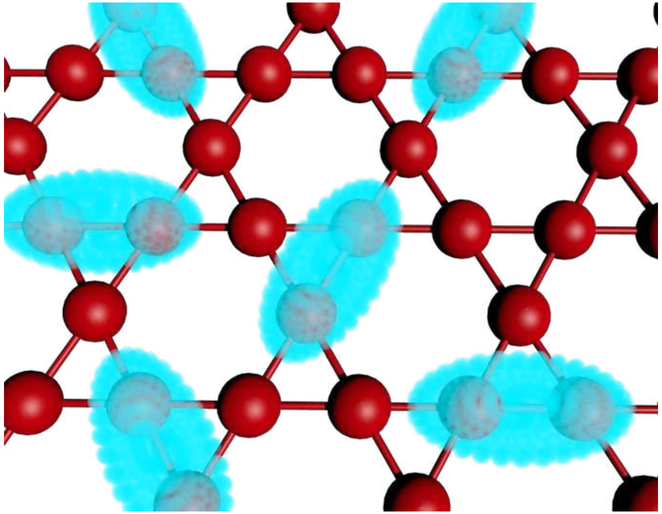

$$\langle \vec{S}_n \rangle = 0$$

They no not break time-reversal symmetry

Quantum entangled magnets

Van der Waals multiferroic magnets

Plan for 2D multiferroics

Multiferroicity in NiI_2

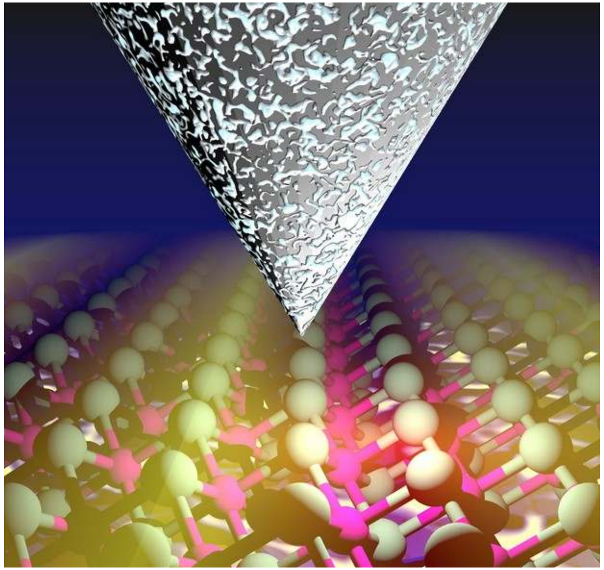

2D Materials 9 (2), 025010 (2022)
Advanced Materials, 2311342 (2024)

Artificial multiferroicity by twisting 2D magnets

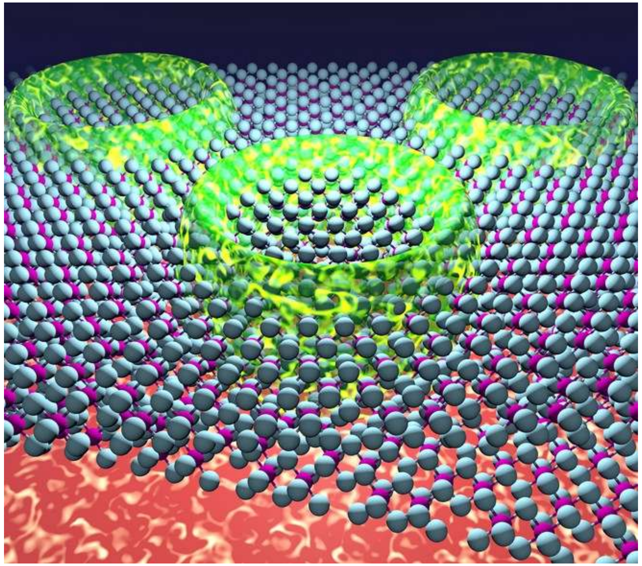

2D Materials 10 (2), 025026 (2023)

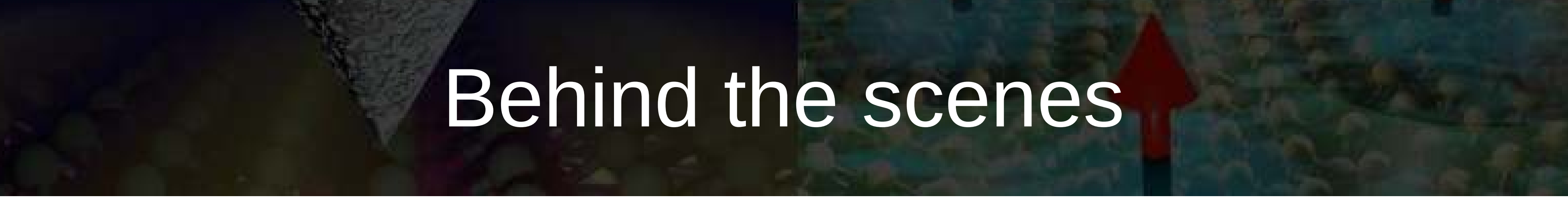

Behind the scenes

Intrinsic multiferroics, NiI_2

(theory and experiment)

V. Vaňo

M. Amini

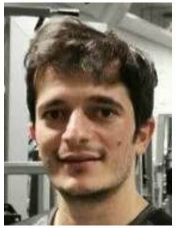

A. Fumega

H. Gonzalez Herrero

S. Kezilebieke

P. Liljeroth

2D Materials 9 (2), 025010 (2022)
Advanced Materials, 2311342 (2024)

Artificial multiferroics, twisted $CrBr_3$ bilayers

(theory)

A. Fumega

2D Materials 10 (2), 025026 (2023)

Origin and visualization of multiferroicity in NiI_2

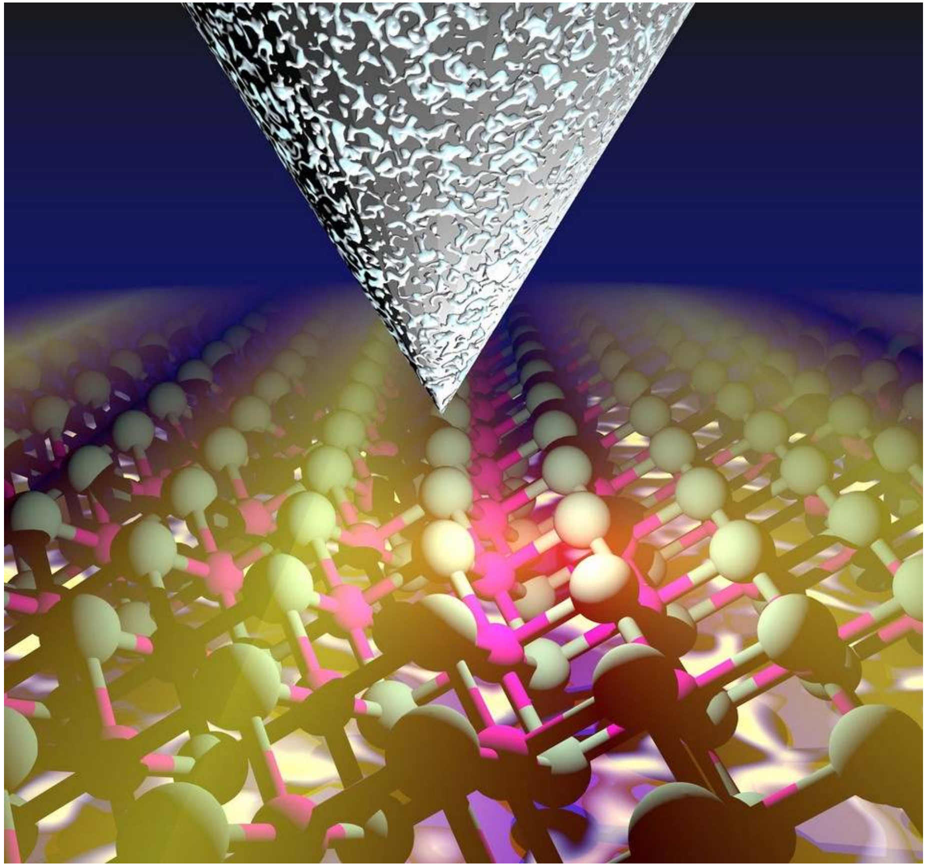

V. Vaňo

M. Amini

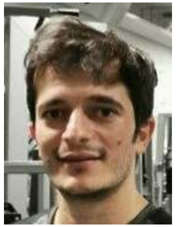

A. Fumega

H. Gonzalez Herrero

S. Kezilebieke

P. Liljeroth

2D Materials 9 (2), 025010 (2022)
Advanced Materials, 2311342 (2024)

Monolayer NiI_2

Structure

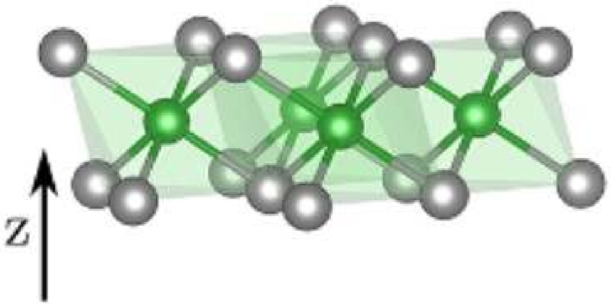

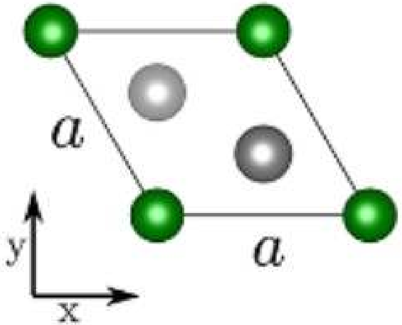

Nature 602, 601–605 (2022)

Frustrated magnetic Heisenberg model

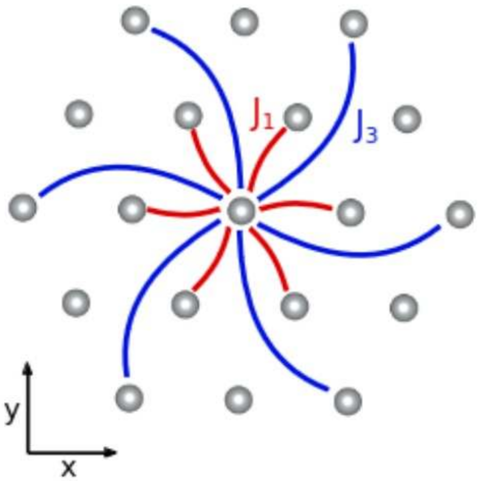

Magnetic structure

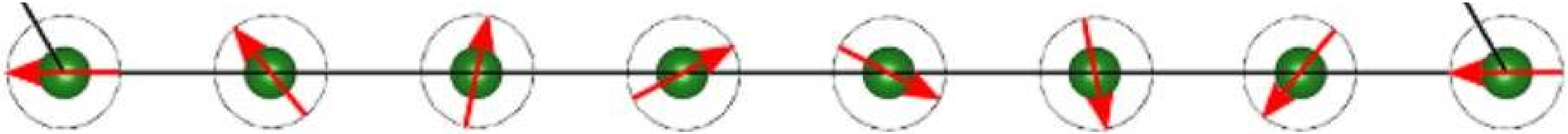

Multiferroicity in monolayer NiI_2

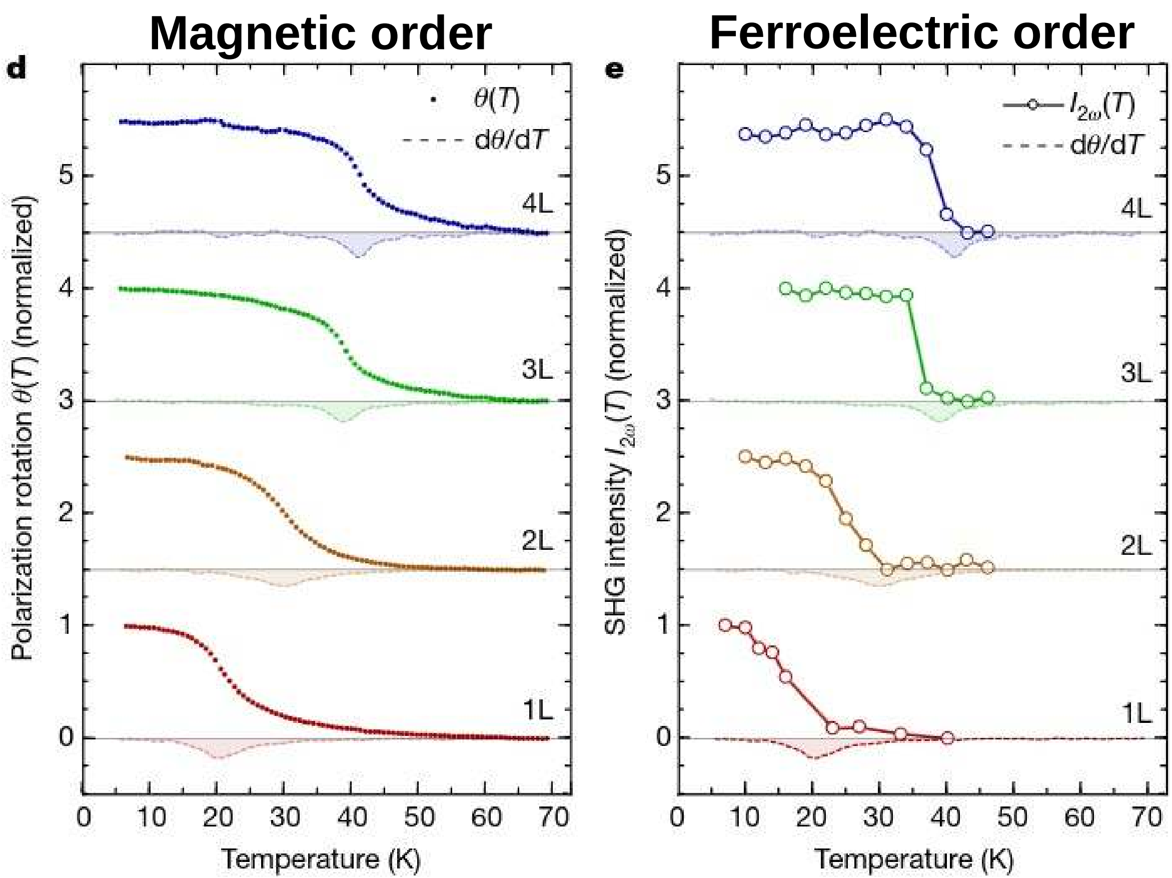

Probe of magnetic order
Magneto-optic Kerr effect

Probe of ferroelectric order
Second harmonic generation

Nature 602, 601–605 (2022)

The impact of spin-orbit coupling in magnetic ordering

In the presence of spin-orbit coupling, new terms can appear in the Hamiltonian

Antisymmetric exchange

$$(\mathbf{r}_{ik} \times \mathbf{r}_{kj}) \cdot \vec{S}_i \times \vec{S}_j$$

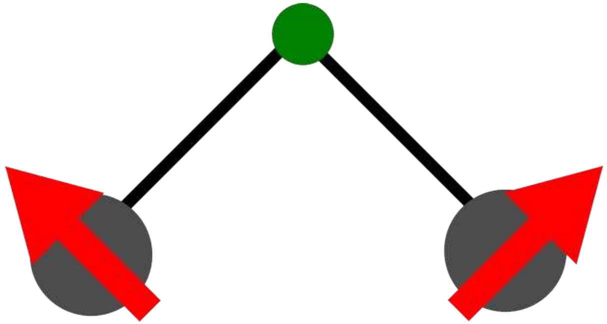

Anisotropic exchange

$$S_i^z S_j^z$$

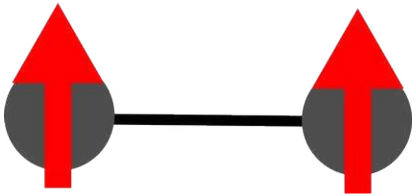

Kitaev interaction

$$S_i^{\alpha(i)} S_j^{\alpha(j)}$$

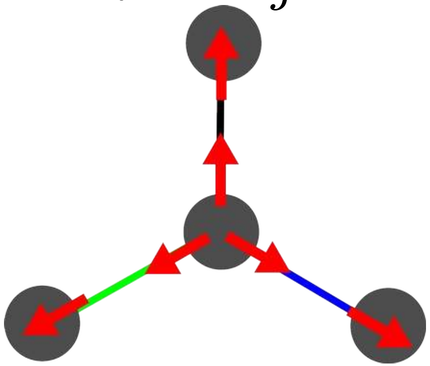

In NiI_2, the non-collinear order is promoted by isotropic exchange

In NiI_2, the ferroelectricity is created by inverse antisymmetric exchange

The origin of ferroelectricity in NiI_2

Magnetically driven ferroelectric order

$$\mathbf{P} = \xi \mathbf{q} \times \mathbf{e},$$

$$\mathbf{M}(\mathbf{r}) = e^{i(\mathbf{e}\cdot\mathbf{S})(\mathbf{q}\cdot(\mathbf{r}-\mathbf{r}_0))}\mathbf{M}(\mathbf{r}_0)$$

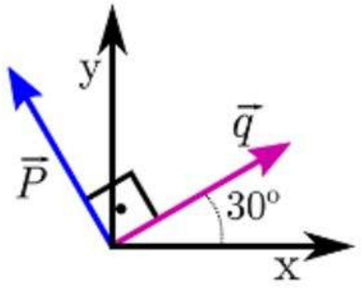

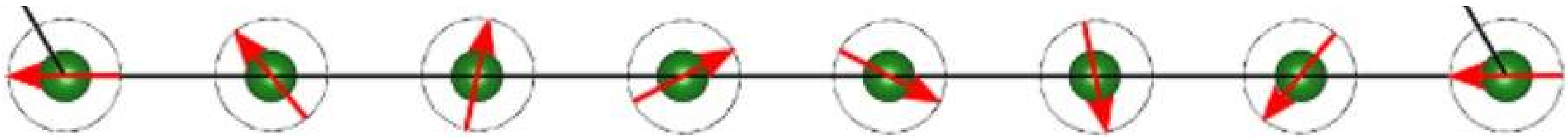

The emergence of non-collinear order is drives ferroelectricity

The origin of ferroelectricity in NiI_2

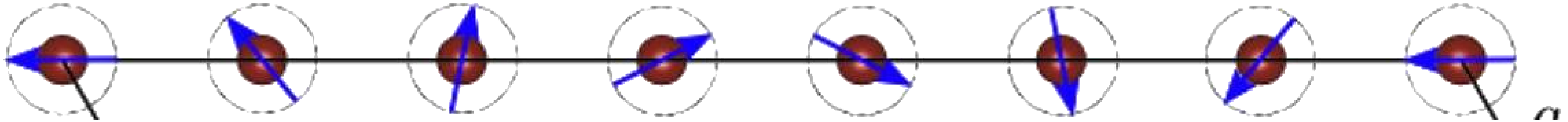

$$\mathbf{P} = \xi \mathbf{q} \times \mathbf{e}$$

Electric polarization

SOC driven

Wavevector of the spin spiral

Spin rotation axis

The impact of spin-orbit coupling in the electronic structure

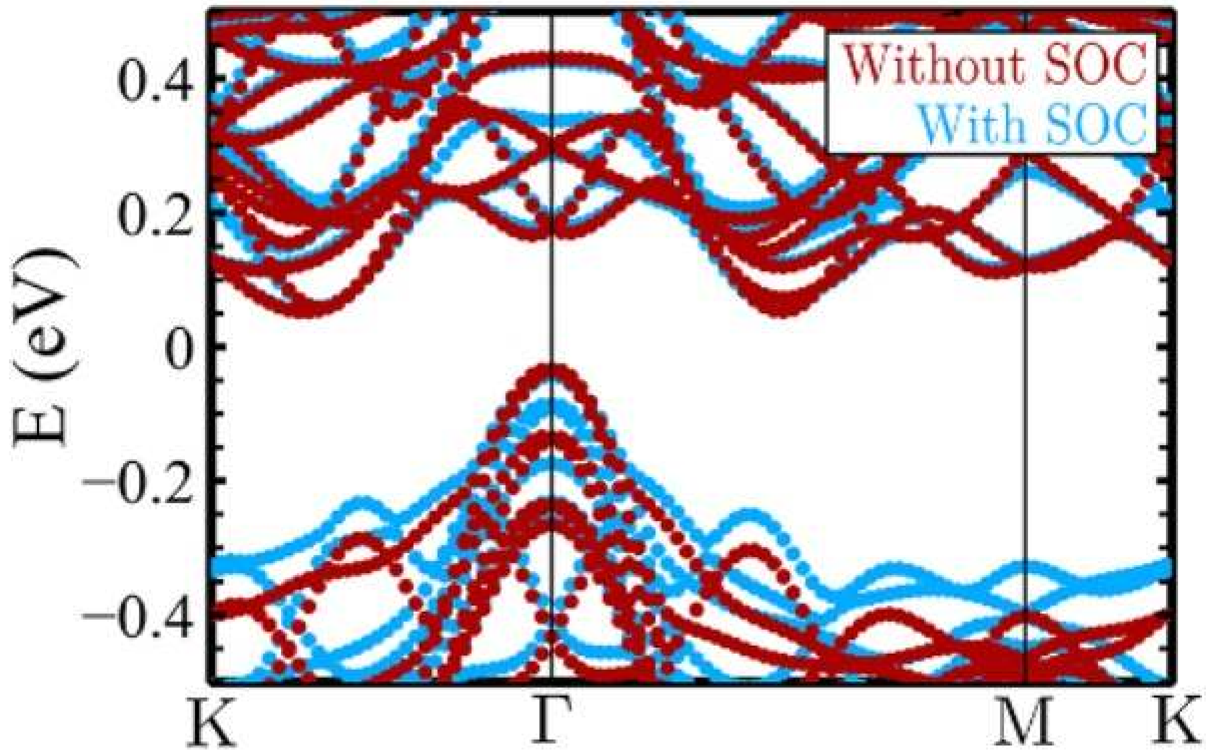

Spin-orbit coupling introduces corrections of 100 meV close to the Fermi level

There is a major role of the halide close to the Fermi level

Ferroelectric correction to the electronic density

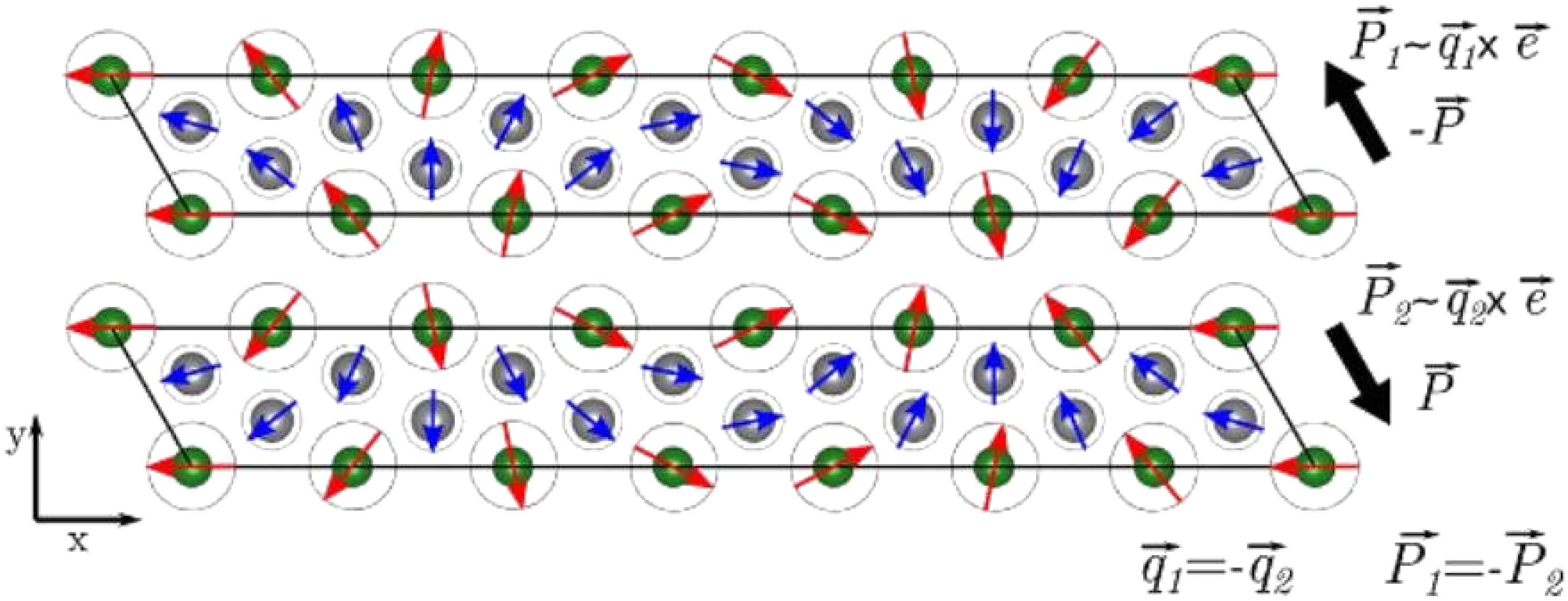

We will examine the ferroelectric density correction $\delta\rho = \rho[\vec{q}_1] - \rho[-\vec{q}_1]$

Ferroelectric correction to the electronic density

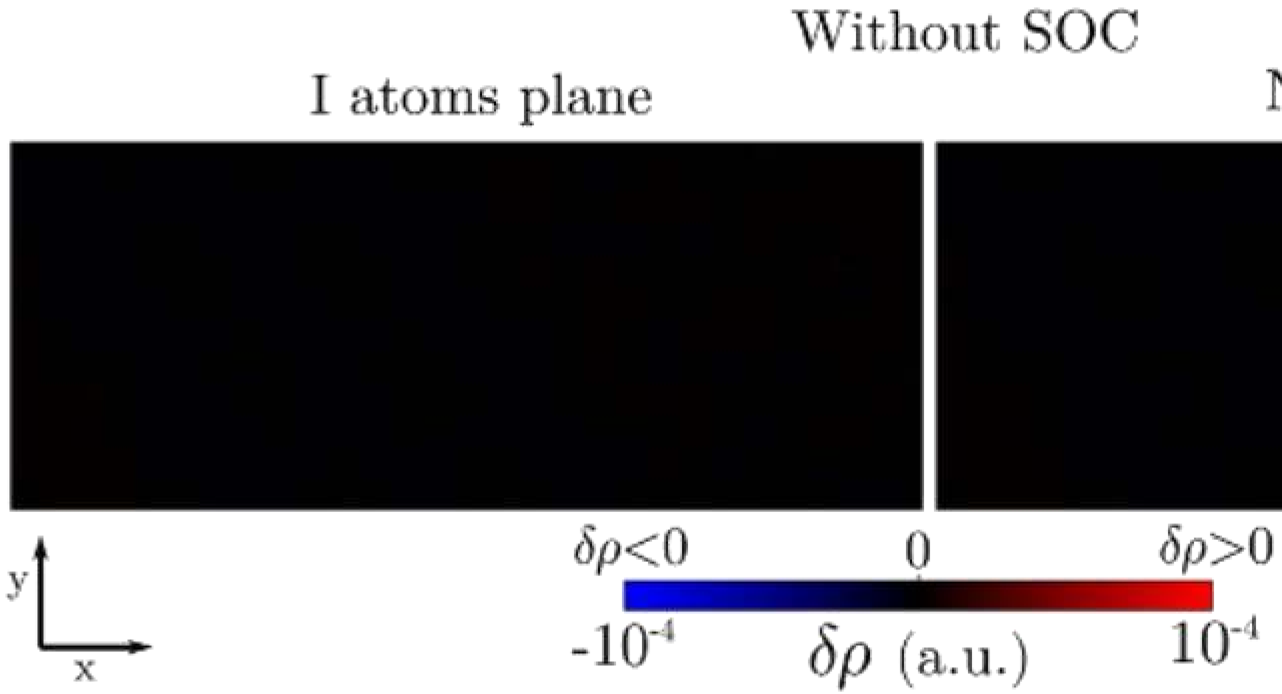

$$\delta\rho = \rho[\vec{q}_1] - \rho[-\vec{q}_1]$$

In the absence of SOC, no ferroelectric density appears

Ferroelectric correction to the electronic density

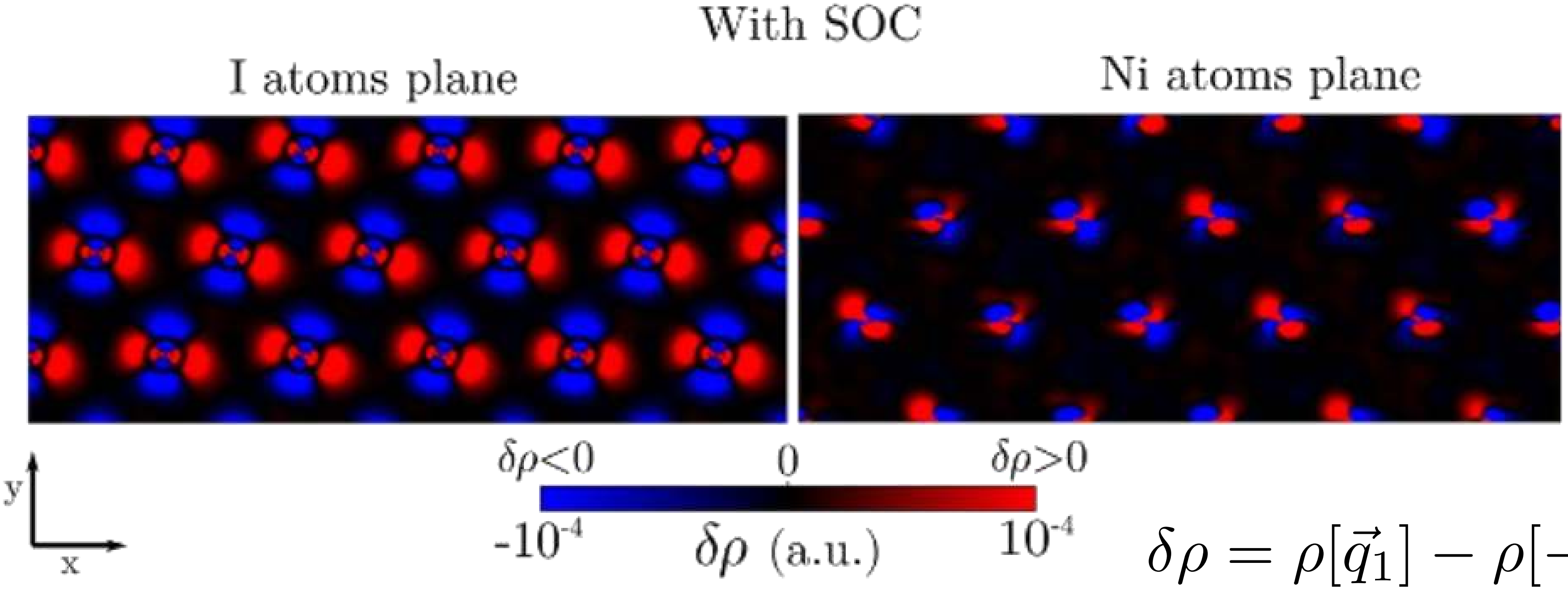

$$\delta\rho = \rho[\vec{q}_1] - \rho[-\vec{q}_1]$$

In the presence of SOC, a ferroelectric density appears both in Ni and I

The ferroelectric force

$$\mathcal{F}_\alpha = \frac{1}{2}(\mathbf{F}_\alpha[\mathbf{q}_1] - \mathbf{F}_\alpha[\mathbf{q}_2]),$$

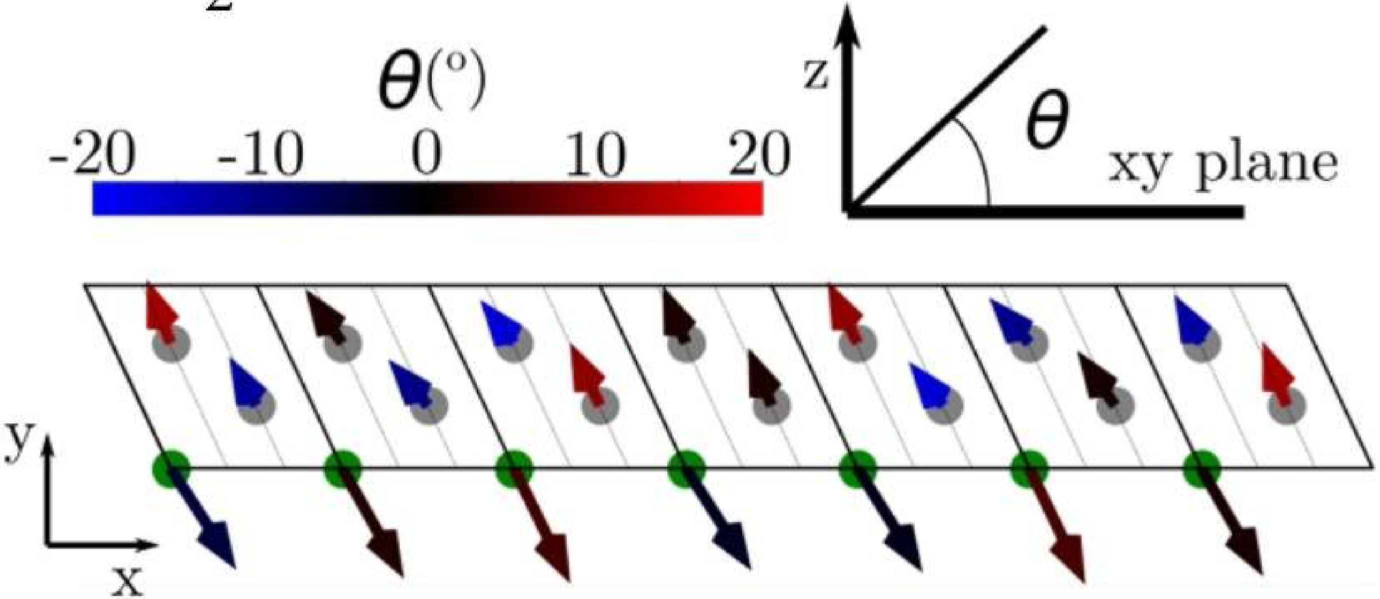

The forces between the two magnetic configuration account for the ferroelectric displacement

The ferroelectric force

$$\mathcal{H} = \mathcal{H}_0 + \lambda^{\mathrm{Ni}}_{\mathrm{SOC}}\mathcal{H}^{\mathrm{Ni}}_{\mathrm{SOC}} + \lambda^{\mathrm{I}}_{\mathrm{SOC}}\mathcal{H}^{\mathrm{I}}_{\mathrm{SOC}},$$

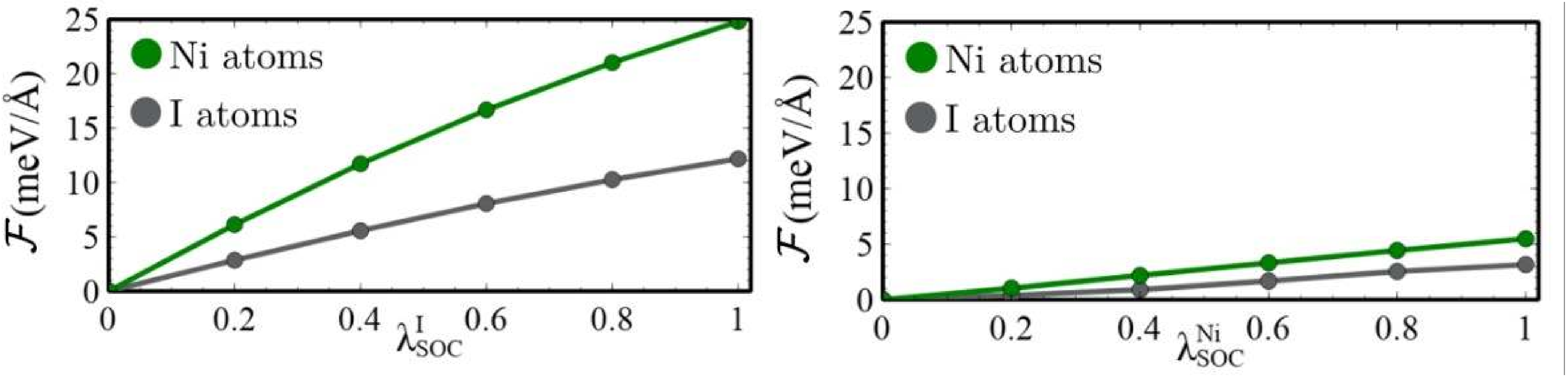

The dominant contribution to the ferroelectric force comes from iodine

Modulated multiferroicity in monolayer NiI_2

The ferroelectric order has actually a modulation in real space

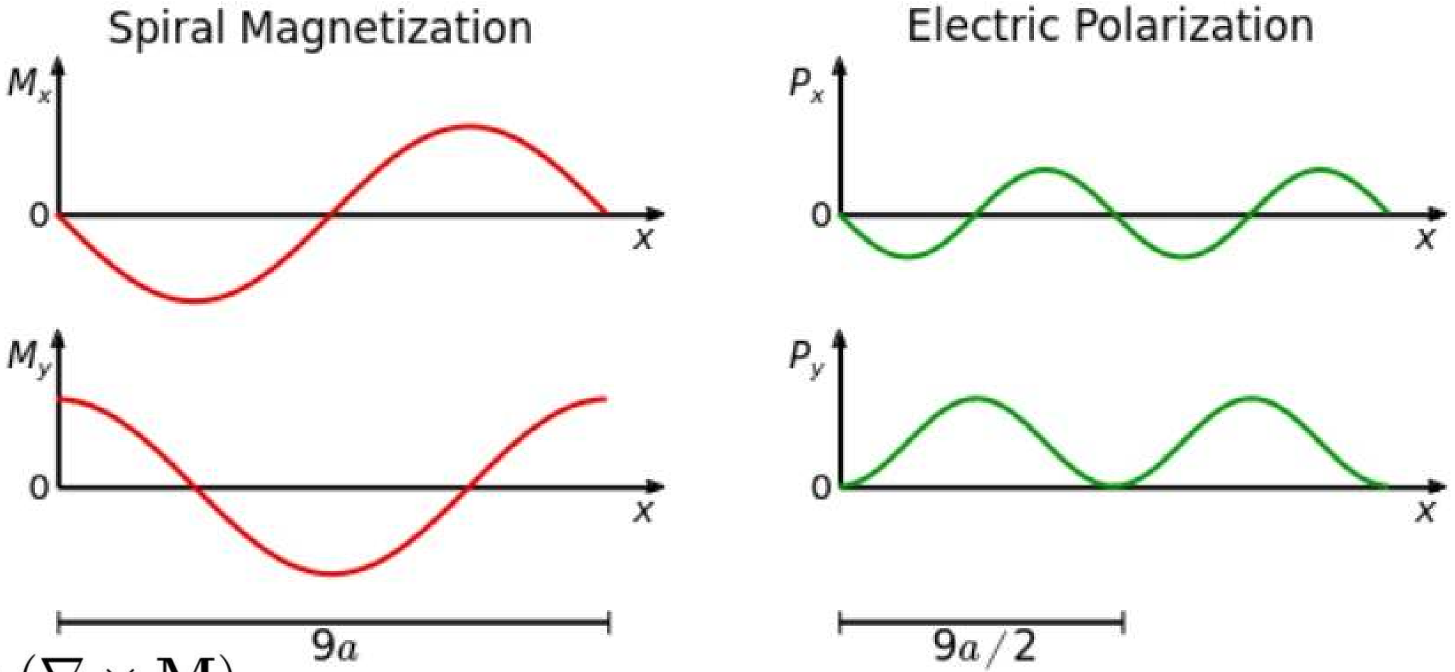

$$\mathbf{P} = \Lambda \frac{\mathbf{M} \times (\nabla \times \mathbf{M})}{\mathrm{M}^2} = \Lambda \mathrm{q}(-\sin(2\mathbf{q}\cdot\mathbf{r}), \sin^2(\mathbf{q}\cdot\mathbf{r}), 0)$$

Advanced Materials, 2311342 (2024)

Visualizing multiferroicity in monolayer NiI_2

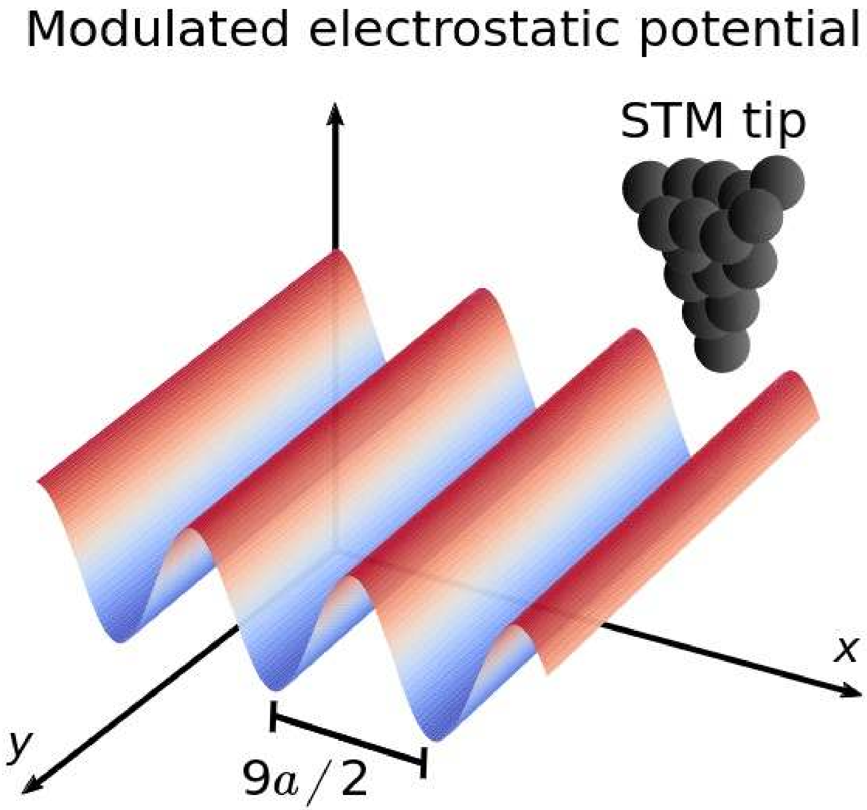

Advanced Materials, 2311342 (2024)

Visualizing multiferroicity in monolayer NiI_2

Experiment

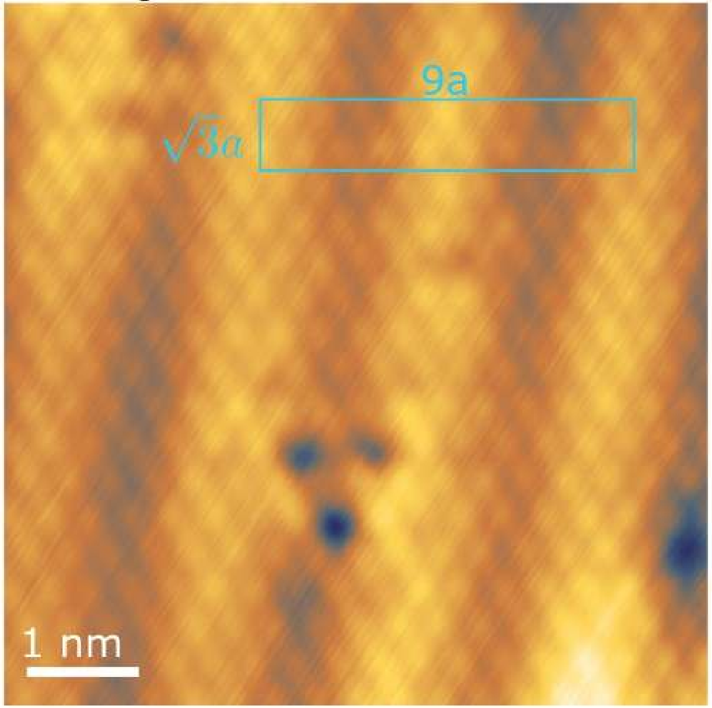

Theory

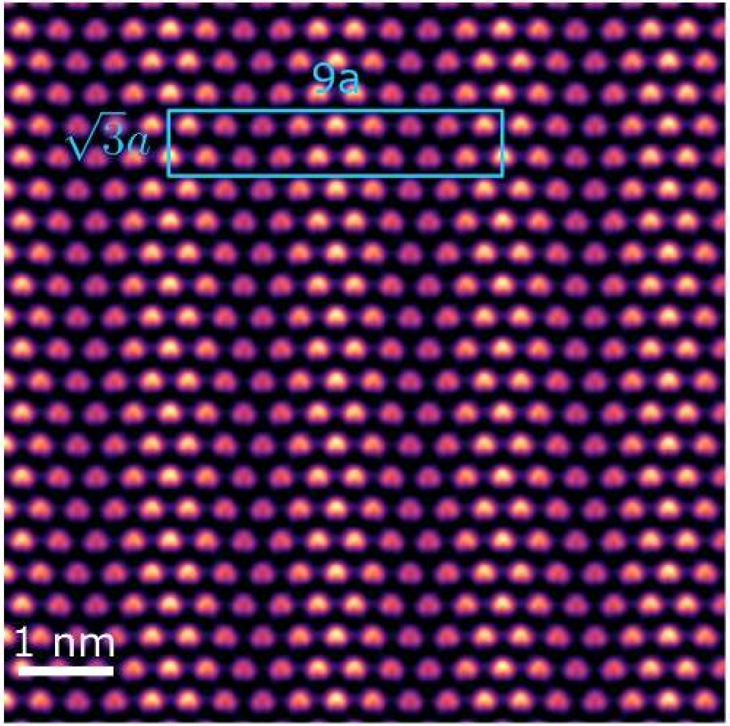

$$\Lambda \mathrm{q}(-\sin(2\mathbf{q}\cdot\mathbf{r}), \sin^2(\mathbf{q}\cdot\mathbf{r}), 0)$$

Ferroelectricity from modulated band offset

Band offset (experiment)

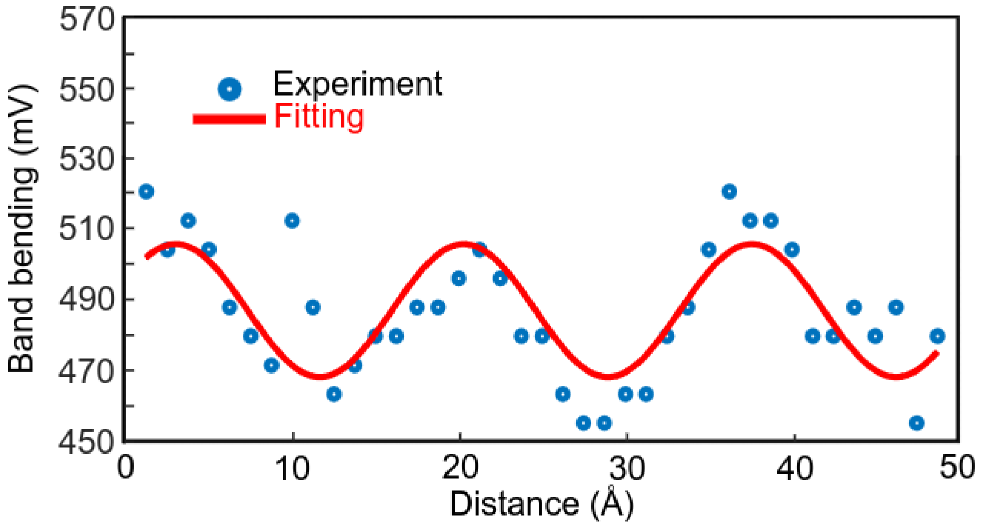

Band offset (theory)

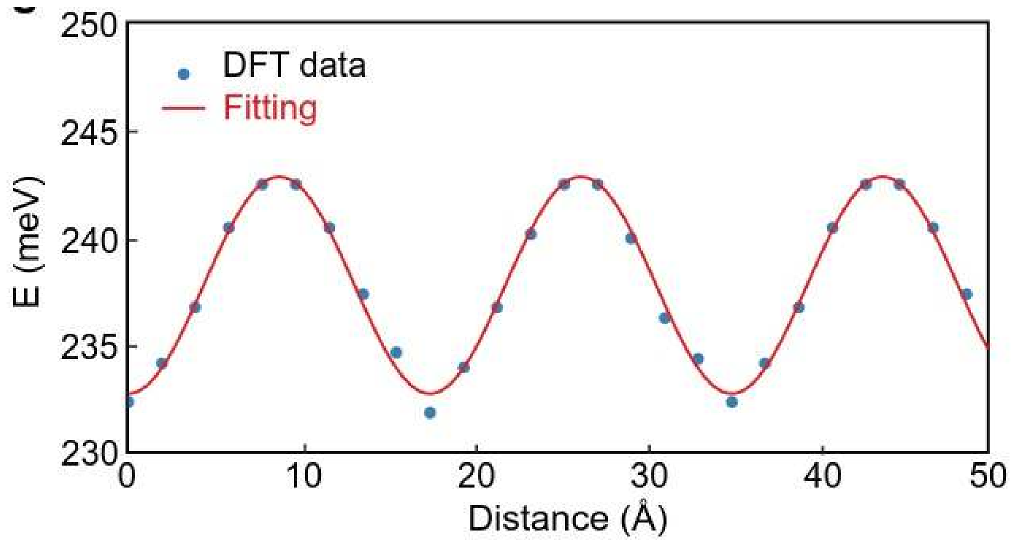

$$\mathbf{P} = \Lambda \frac{\mathbf{M} \times (\nabla \times \mathbf{M})}{\mathrm{M}^2} = \Lambda \mathrm{q}(-\sin(2\mathbf{q}\cdot\mathbf{r}), \sin^2(\mathbf{q}\cdot\mathbf{r}), 0)$$

Advanced Materials, 2311342 (2024)

Controlling multiferroic domains with an STM tip

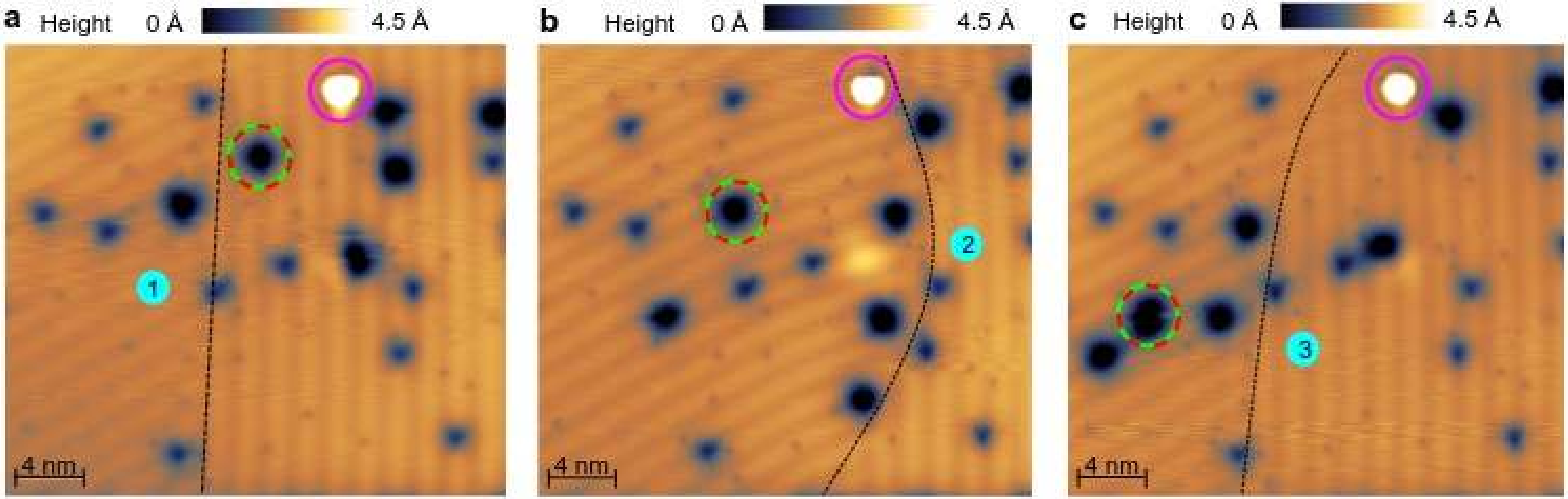

An STM bias allows to control the multiferroic domains

Advanced Materials, 2311342 (2024)

Engineering artificial multiferroics with twisted van der Waals materials

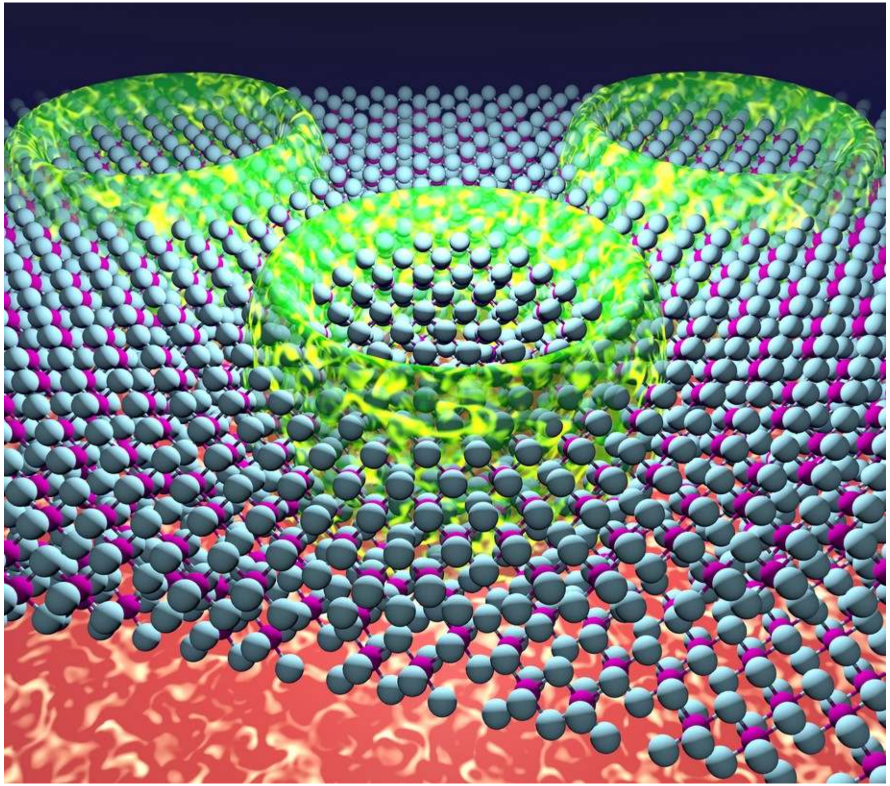

A. Fumega

2D Materials 10 025026 (2023)

Twisted 2D trihalides

$CrBr_3$

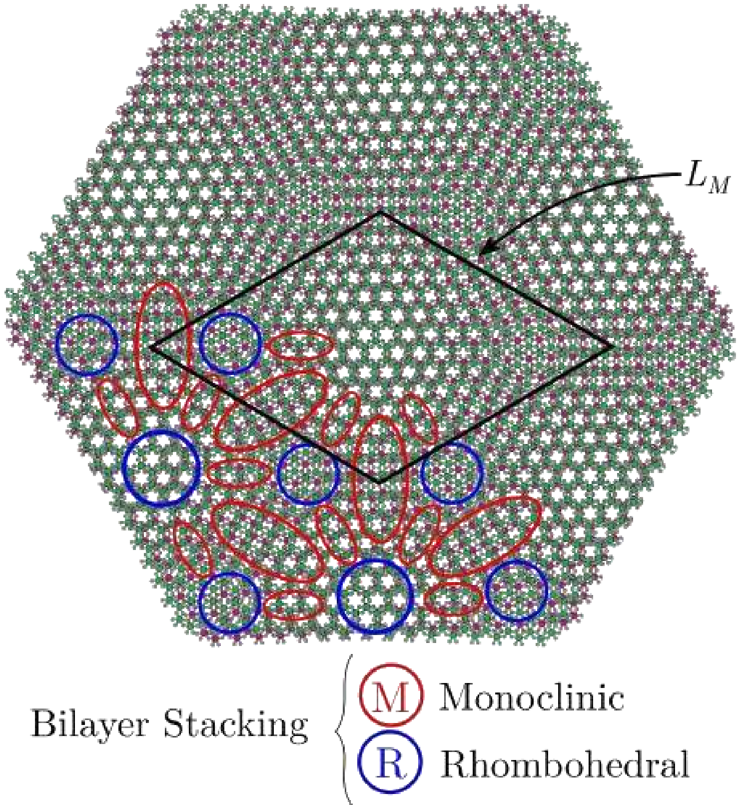

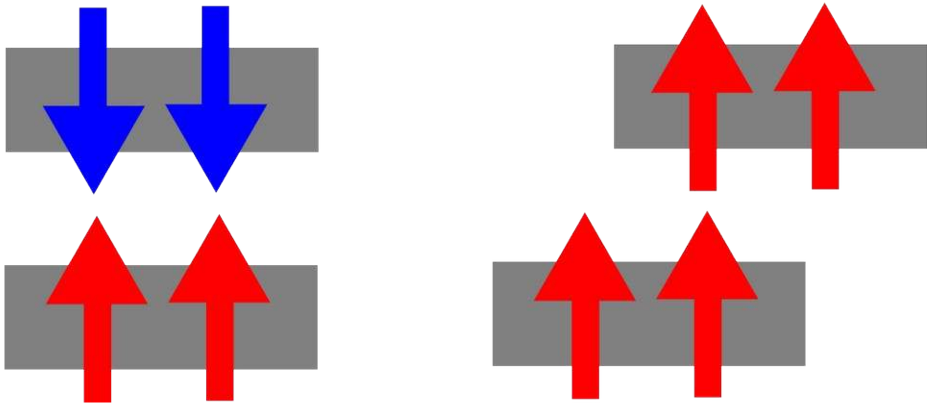

The local stacking determines
the coupling between layers

Nature Nanotechnology 17, 143–147 (2022)

Non-collinear magnetism at domain walls

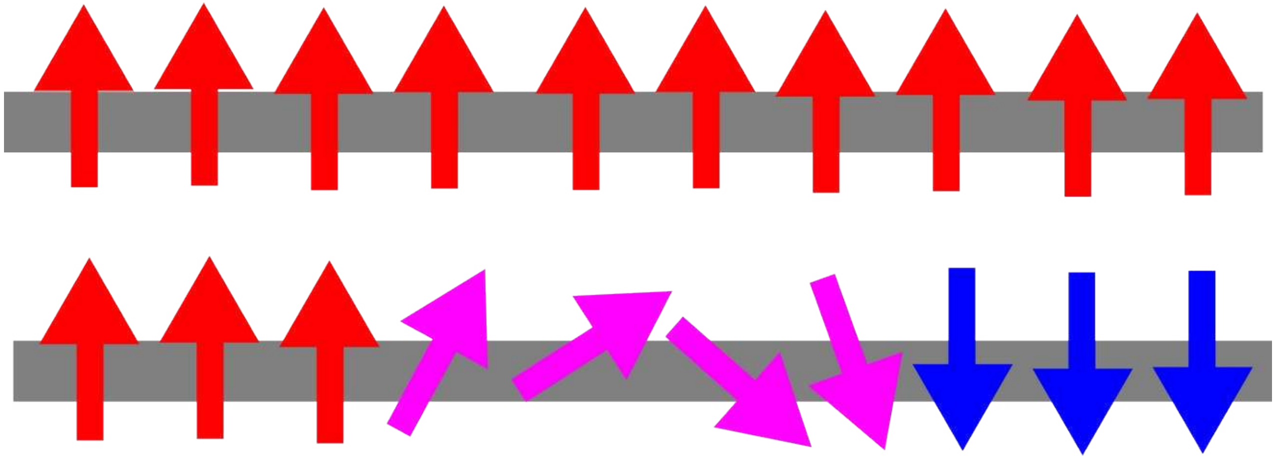

Stacking #1

Stacking #2

Mixed FE/AF domains

Nature Nanotechnology 17, 143–147 (2022)

Non-collinear magnetism

arXiv:2204.01636

Twisted 2D magnetic materials

Non-collinear magnetism and multiferroic order appear due to the moire

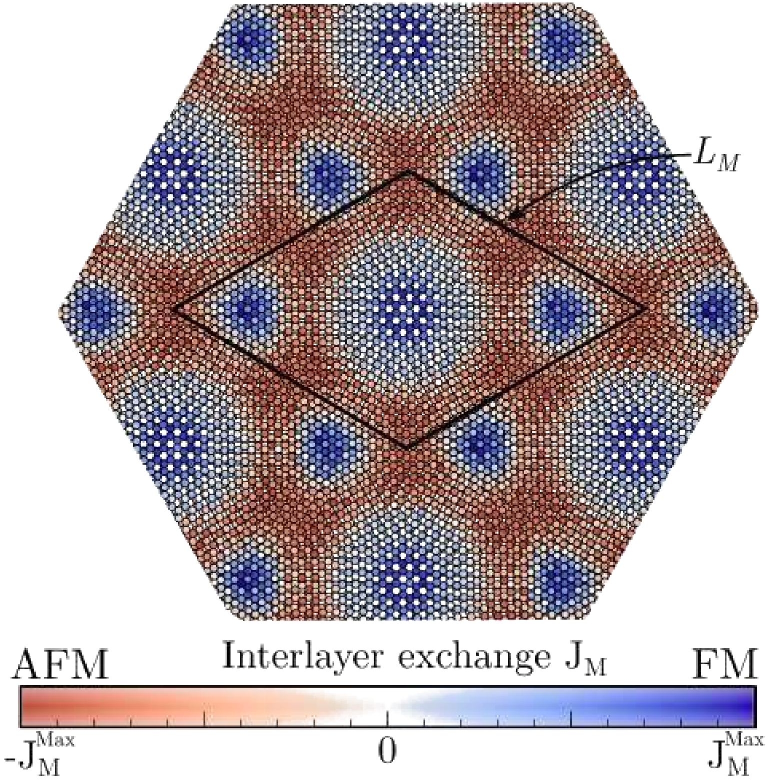

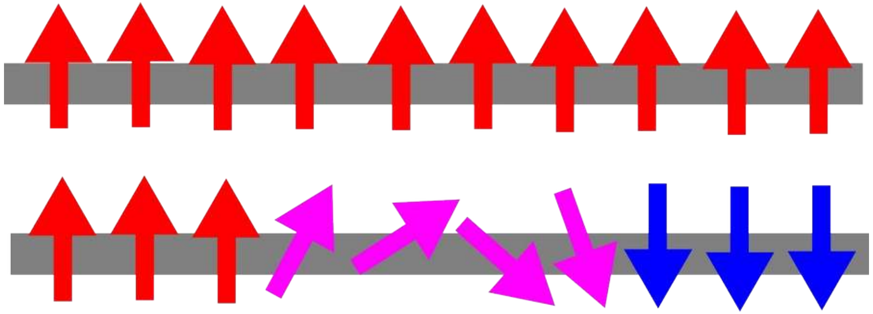

$$\mathbf{P} = \xi \mathbf{q} \times \mathbf{e}$$

Electric polarization

SOC driven

Wavevector of the spin spiral

Spin rotation axis

Stacking, magnetic order and electric polarization

Structure

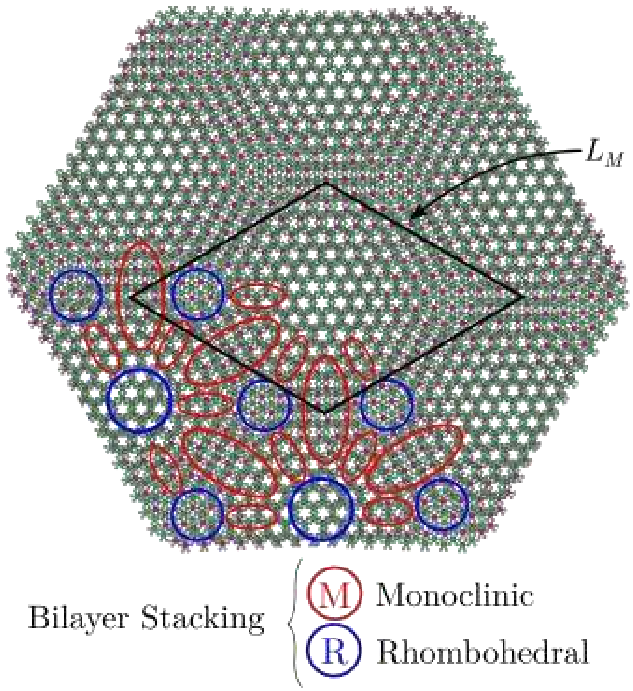

Magnetic order

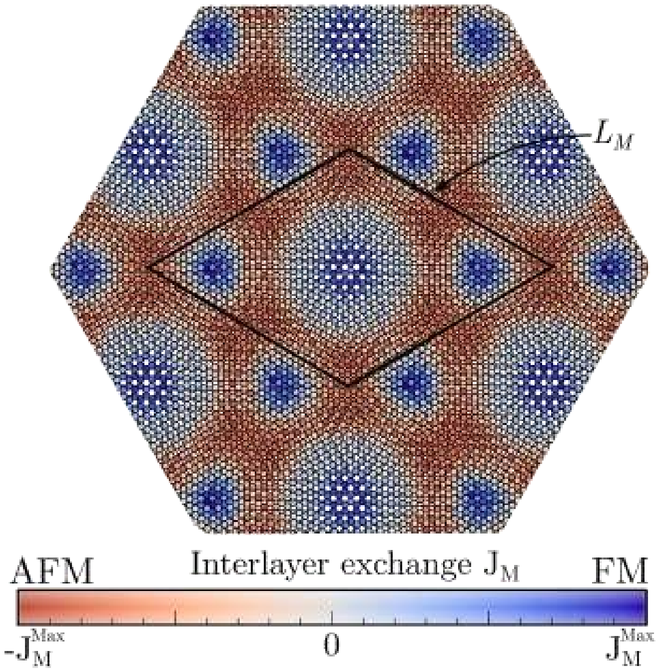

Ferroelectric order

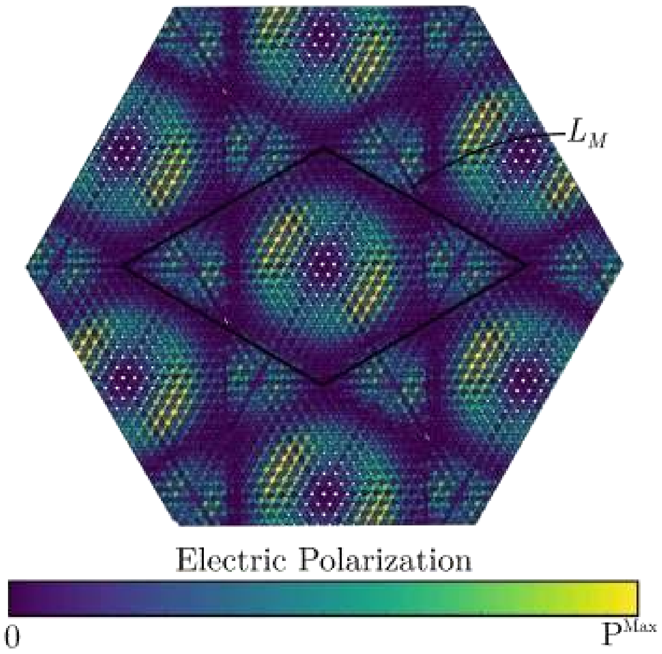

Stacking, magntic structure and ferroelectric order are correlated

Magnetization and ferroelectricity

Magnetization

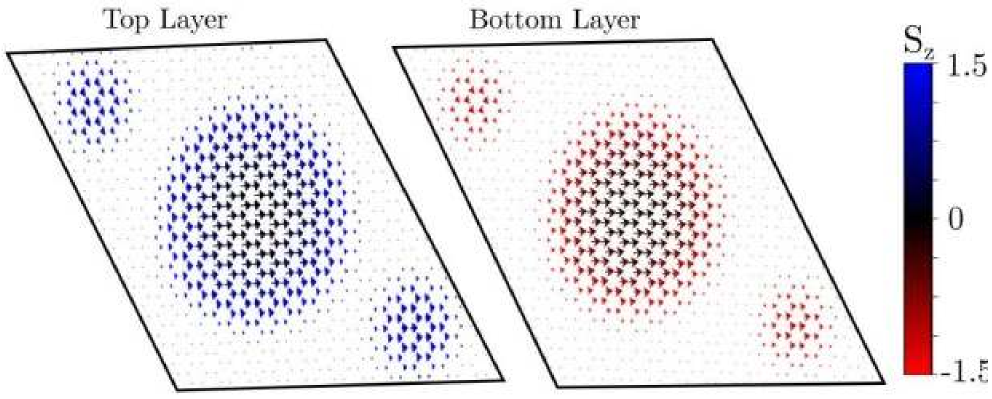

Ferroelectric order

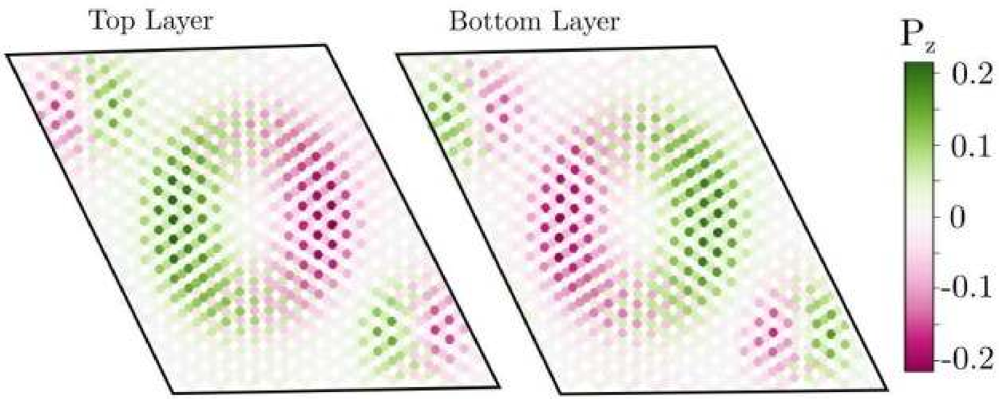

The ferroelectric order appear at the domain walls between magnetic domains

Tracking the emergence of ferroelectricity

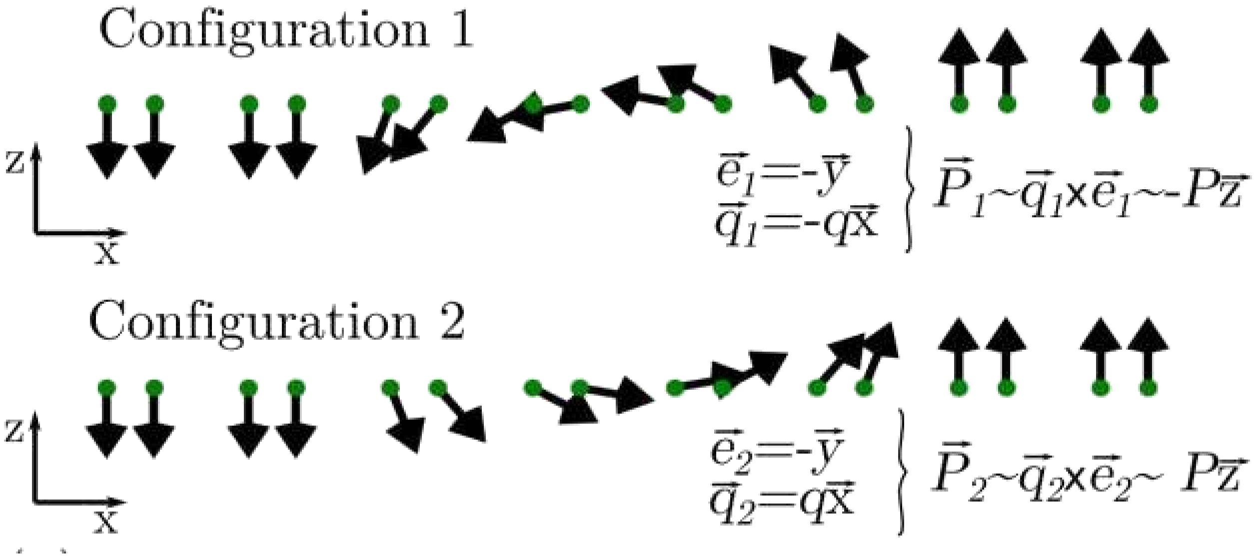

Ferroelectric electronic density

$$\delta\rho = \rho[\mathbf{q}_1] - \rho[\mathbf{q}_2]$$

Ferroelectric force

$$\boldsymbol{\mathcal{F}}_\alpha = \frac{1}{2}(\mathbf{F}_\alpha[\mathbf{q}_1] - \mathbf{F}_\alpha[\mathbf{q}_2]),$$

The ferroelectric electronic correction

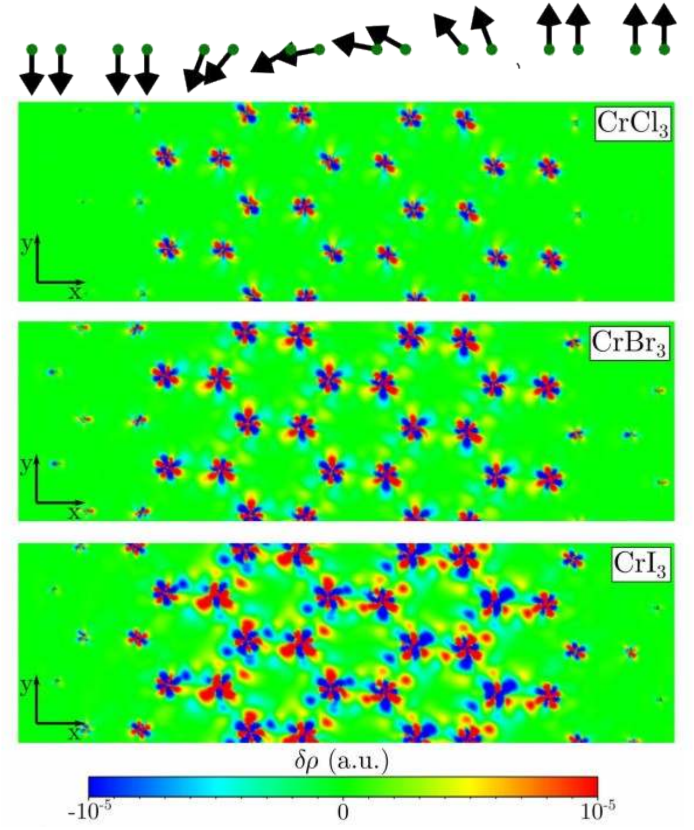

Ferroelectric electronic density

$$\delta\rho = \rho[\mathbf{q}_1] - \rho[\mathbf{q}_2]$$

The ferroelectric electronic correction emerges in the region with non-collinear magnetization

It becomes stronger the heavier the halide

The ferroelectric force

Magnetic configuration

Ferroelectric force

$$\mathcal{F}_\alpha = \frac{1}{2}(\mathbf{F}_\alpha[\mathbf{q}_1] - \mathbf{F}_\alpha[\mathbf{q}_2]),$$

The ferroelectric force becomes
Stronger for heavier halides

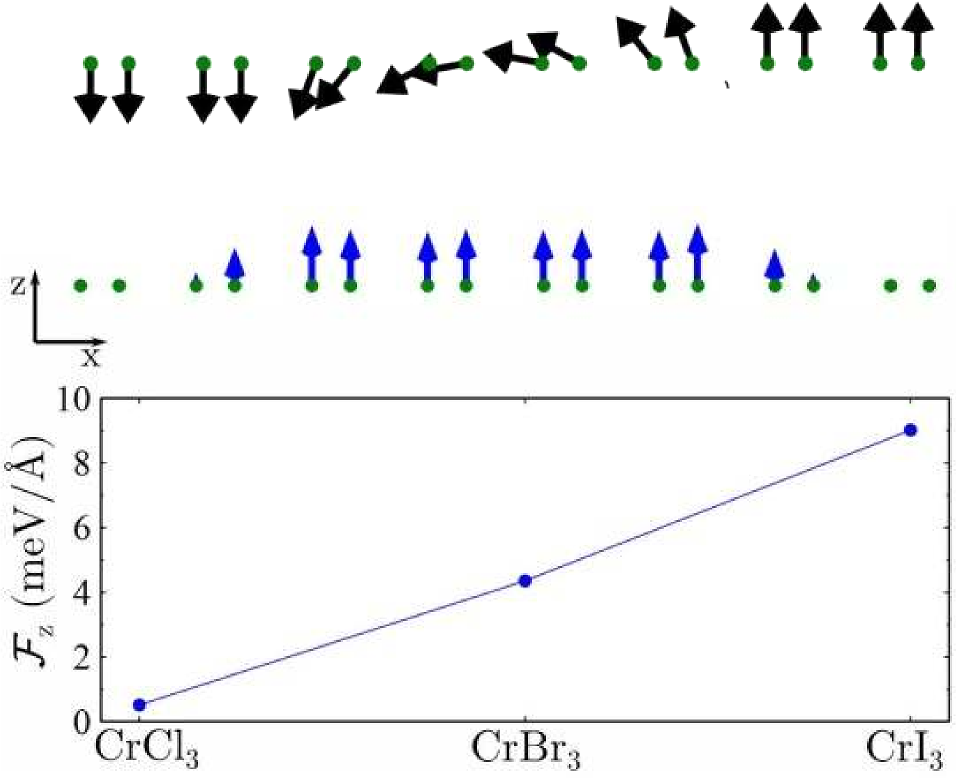

Electrically controllable skyrmions in twisted magnets

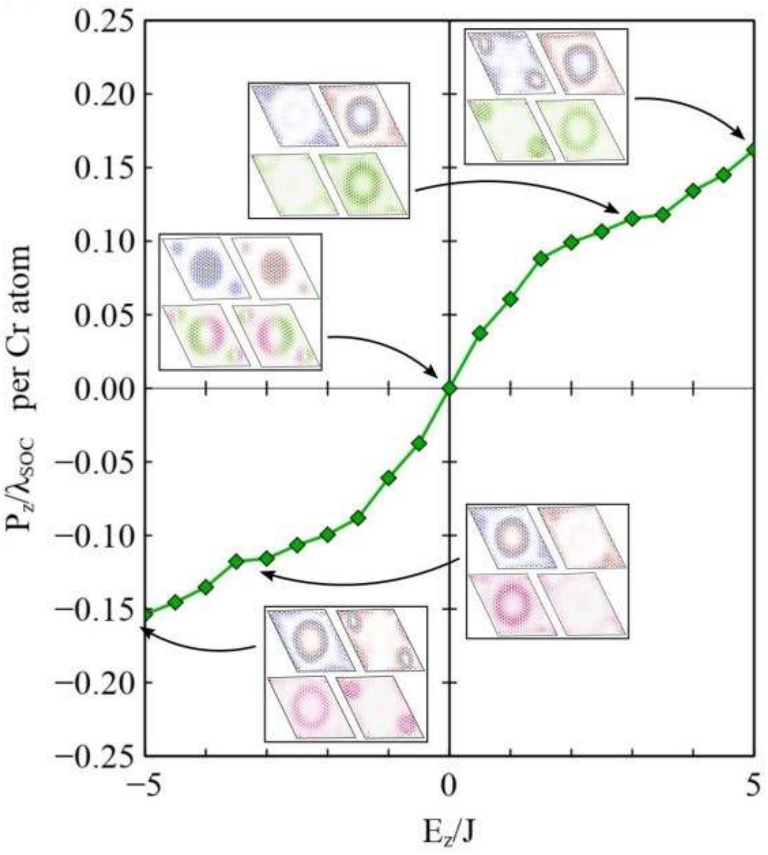

The electric polarization directly couples to an out-of plane electric field

$$\mathcal{H}_E = \frac{1}{2}\sum_{ij}\mathbf{E}\cdot\mathbf{P}_{ij}.$$

Electrically controllable skyrmions in twisted magnets

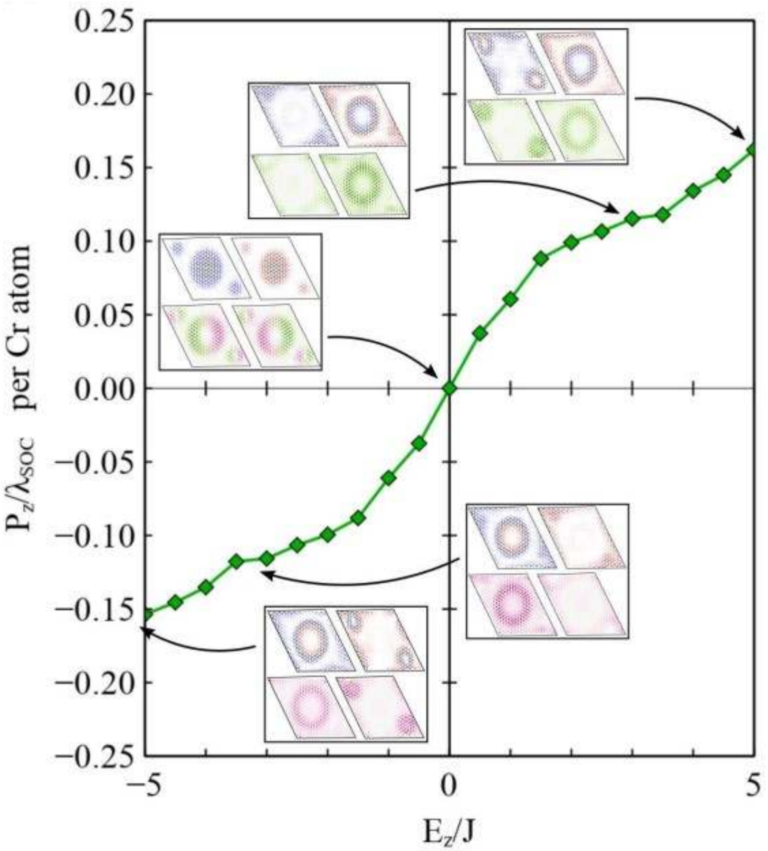

Skyrmions at finite interlayer bias

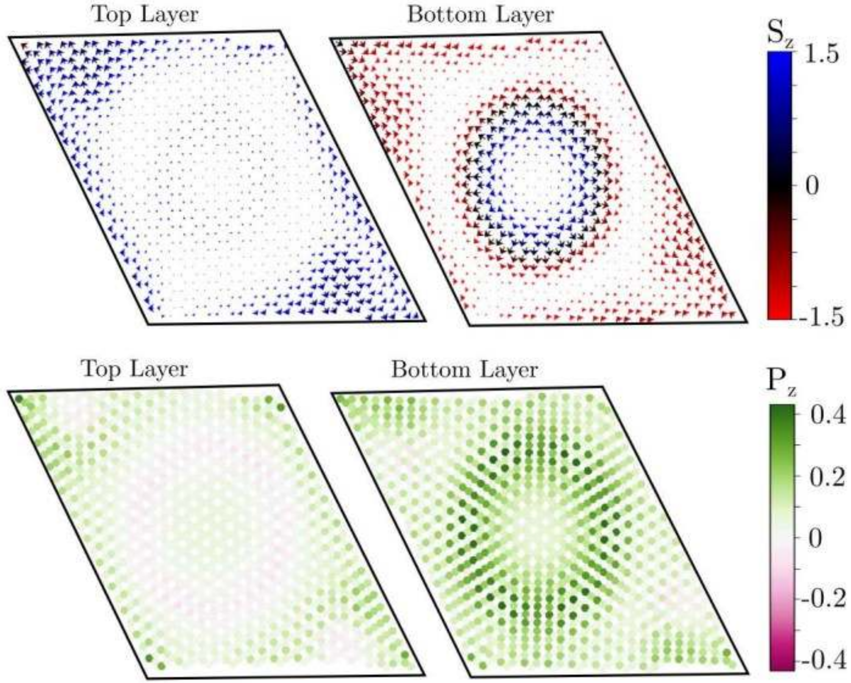

Van der Waals heavy-fermion Kondo magnets

The world of heavy fermion compounds

We have a rich family of bulk heavy-fermion compounds

$CeCoIn_5$
Science 375, 6576, 76-81 (2021)

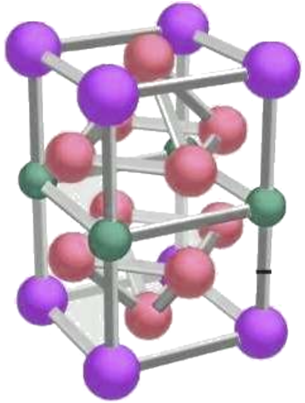

UTe_2
Nature 579, 523–527 (2020)

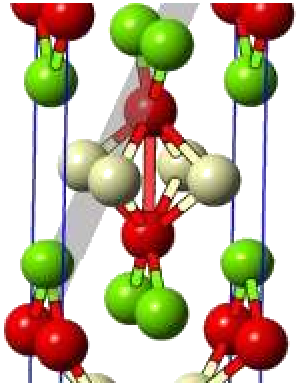

- Strongly correlated matter, dominated by Kondo lattice physics
- Unique system to realize quantum criticality and unconventional superconductivity
- Found in rare-earth compounds, such as UTe_2 or UPt_3

Searching for new heavy fermion compounds

We have a rich family of bulk heavy-fermion compounds

$CeCoIn_5$

Science 375, 6576, 76-81 (2021)

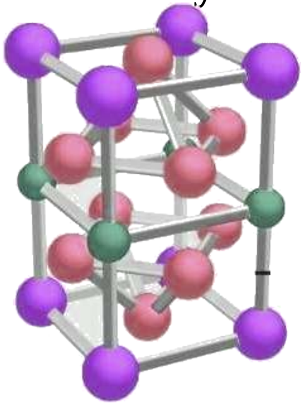

UTe_2

Nature 579, 523–527 (2020)

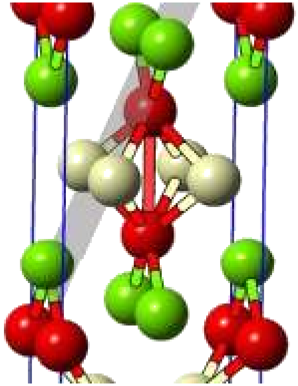

Can we realize heavy-fermion physics with two-dimensional materials?

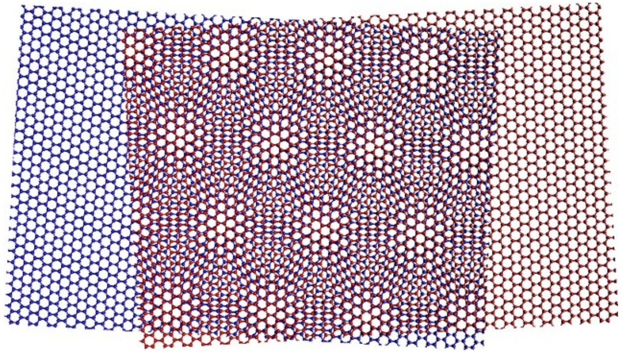

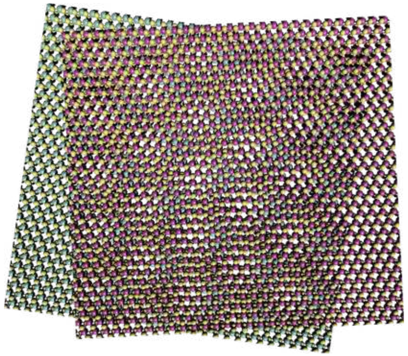

Phys. Rev. Lett. 127, 026401 (2021)
Nature 599, 582–586 (2021)
Phys. Rev. Research 3, 043173 (2021)
Phys. Rev. B 106, L041116 (2022)
Phys. Rev. Lett. 129, 047601 (2022)
Nature 616, 61–65 (2023)
Nature 625, 483−488 (2024)
Nano Letters 24 (14), 4272–4278 (2024)

Behind the scenes

Heavy fermions in twisted graphene trilayers

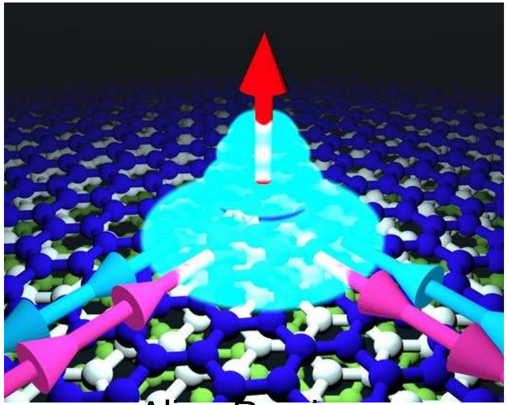

Aline Ramires

Phys. Rev. Lett. 127, 026401 (2021)

Heavy fermions in twisted dichalcogenide bilayers

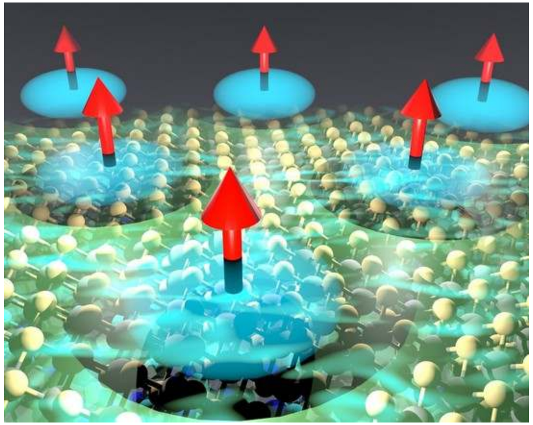

S. Ganguli

M. Amini

G. Chen

V. Vaňo

S. Kezilebieke

P. Liljeroth

Nature 599, 582–586 (2021)

Building an artificial heavy fermion state

Lattice of Kondo impurities

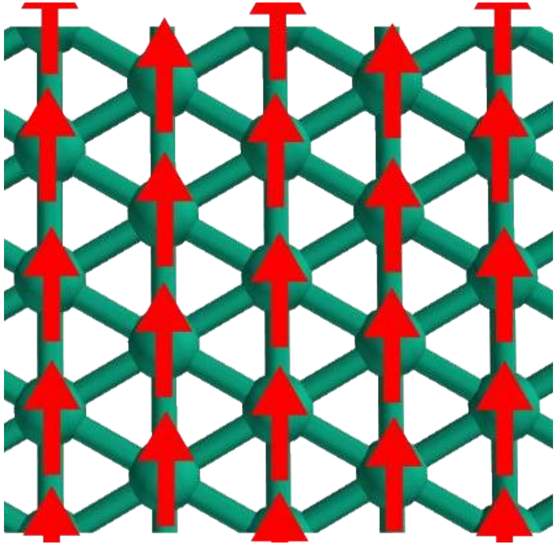

f-electrons in
rare-earth compounds

Dispersive electron gas

s/p/d-electrons in
rare-earth compounds

Building an artificial heavy fermion state

Conduction electrons form Kondo singlets with the impurities

Kondo-lattice model

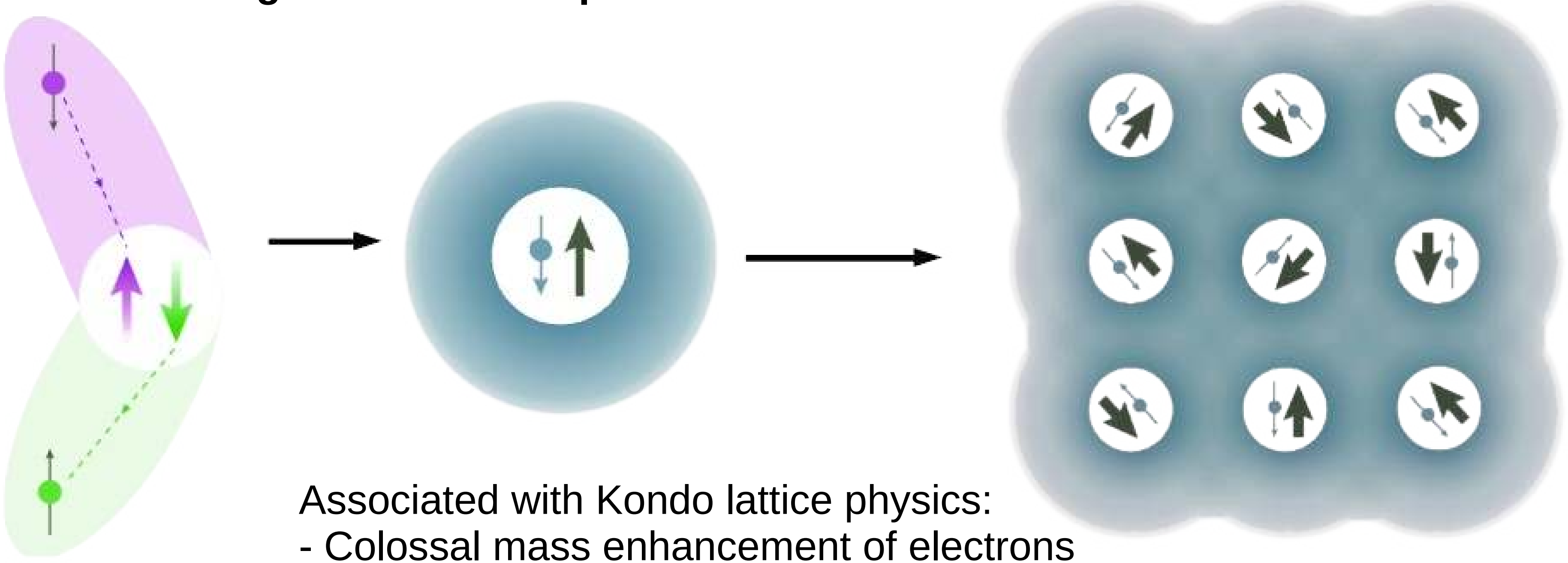

Associated with Kondo lattice physics:
- Colossal mass enhancement of electrons
- Quantum criticality
- Unconventional (topological) superconductivity

Basics of heavy fermion physics

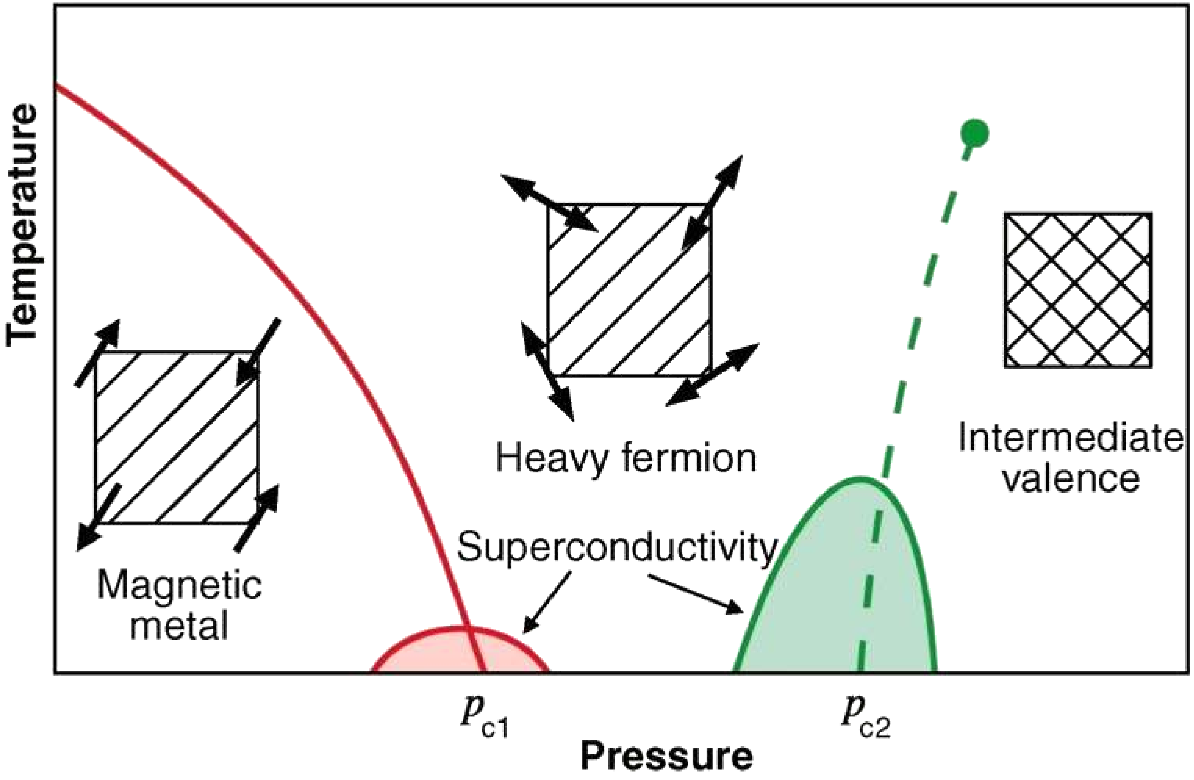

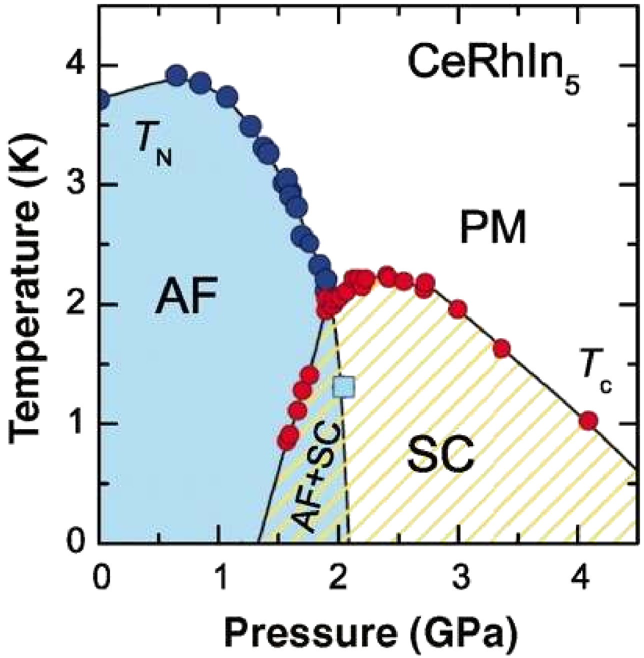

Science 332.6026, 196-200 (2011)

The Kondo problem

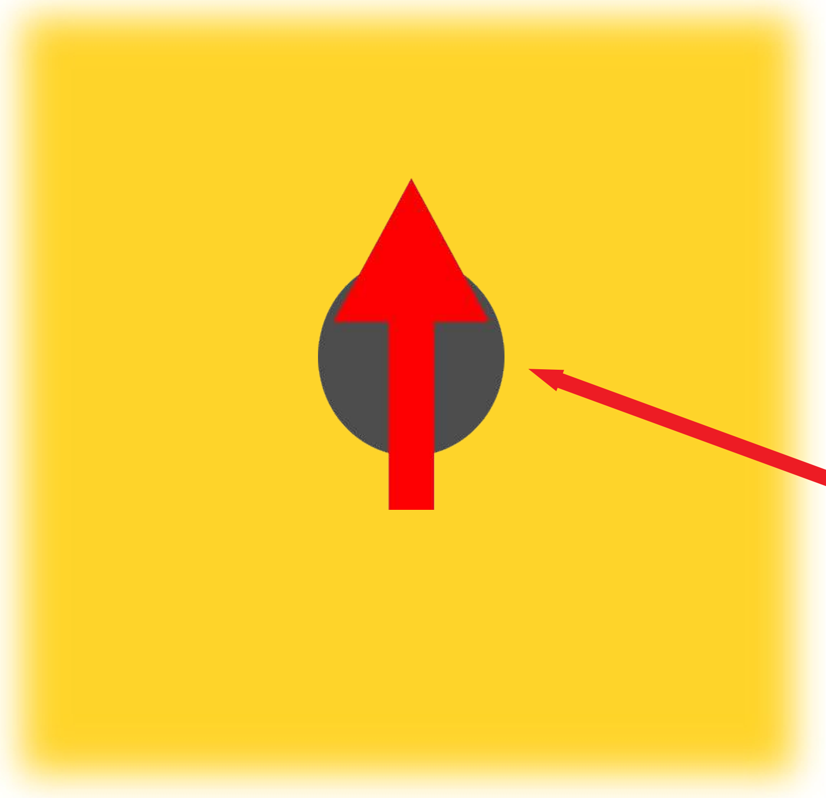

Conduction electrons

$$H = -t \sum_{(i,j)\sigma} \left(c^\dagger_{i\sigma} c_{j\sigma} + \text{ H.c } \right)$$

Kondo coupling

$$H_K = J_K \sum_{\alpha\beta} \left(c^\dagger_{0\beta} \vec{\sigma}_{\beta\alpha} c_{0\alpha} \right) \cdot \vec{S}$$

We now take a quantum spin S=1/2

$$|GS\rangle \sim \frac{1}{\sqrt{2}} [| \Uparrow \downarrow\rangle - | \Downarrow \uparrow\rangle]$$

The Kondo lattice problem

Lattice of Kondo impurities

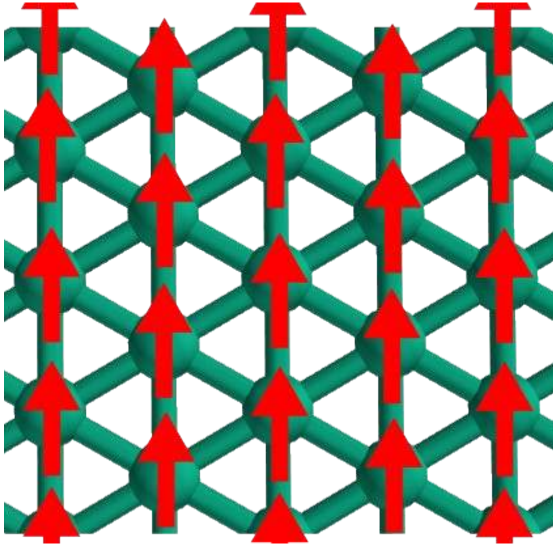

J_K

Dispersive electron gas

Both ingredients coupled through Kondo coupling

The Kondo lattice problem

The Kondo lattice problem

$$H = -t\sum_{(i,j)\sigma}\left(c^\dagger_{i\sigma}c_{j\sigma} + \text{ H.c }\right) + J_K\sum_{j,\alpha\beta}\left(c^\dagger_{j\beta}\vec{\sigma}_{\beta\alpha}c_{j\alpha}\right)\cdot\vec{S}_j$$

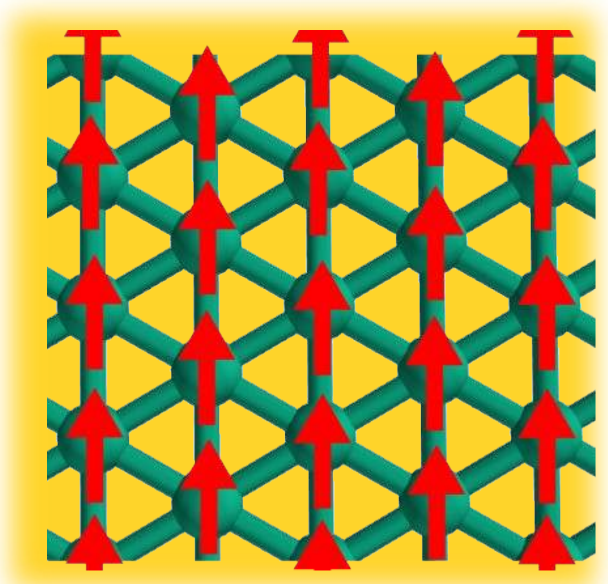

Conduction electrons

Kondo coupling

Kondo sites

Solving the Kondo lattice problem

$$H = -t\sum_{(i,j)\sigma}\left(c^{\dagger}_{i\sigma}c_{j\sigma} + \text{ H.c }\right) + J_K\sum_{j,\alpha\beta}\left(c^{\dagger}_{j\beta}\vec{\sigma}_{\beta\alpha}c_{j\alpha}\right)\cdot\vec{S}_j$$

Replace the spin sites by auxiliary fermions

$$S_{\alpha\beta}(j) \sim f^{\dagger}_{j\alpha}f_{j\beta} - \frac{n_f(j)}{N}\delta_{\alpha\beta}$$

This makes the effective Hamiltonian an “interacting” fermionic Hamiltonian

$$H \sim \sum_{\mathbf{k}\alpha}\epsilon_{\mathbf{k}}c^{\dagger}_{\mathbf{k}\alpha}c_{\mathbf{k}\alpha} - J_K\sum_{j,\alpha\beta}\left(c^{\dagger}_{j\beta}f_{j\beta}\right)\left(f^{\dagger}_{j\alpha}c_{j\alpha}\right)$$

Solving the Kondo lattice problem

Now we decouple the fermions with a mean-field approximation

$$H \sim \sum_{\mathbf{k}\alpha} \epsilon_{\mathbf{k}} c^{\dagger}_{\mathbf{k}\alpha} c_{\mathbf{k}\alpha} - J_K \sum_{j,\alpha\beta} \left(c^{\dagger}_{j\beta} f_{j\beta} \right) \left(f^{\dagger}_{j\alpha} c_{j\alpha} \right)$$

Obtaining a quadratic Hamiltonian

$$H \sim \sum_{\mathbf{k}\alpha} \epsilon_{\mathbf{k}} c^{\dagger}_{\mathbf{k}\alpha} c_{\mathbf{k}\alpha} - \gamma_K \sum_{\mathbf{k},\alpha} f^{\dagger}_{\mathbf{k}\alpha} c_{\mathbf{k}\alpha} + h.c.$$

Conduction band dispersion

Kondo hybridization

Electronic structure of the Kondo lattice problem

$$H \sim \sum_{\mathbf{k}\alpha} \epsilon_{\mathbf{k}} c^\dagger_{\mathbf{k}\alpha} c_{\mathbf{k}\alpha} - \gamma_K \sum_{\mathbf{k},\alpha\beta} f^\dagger_{\mathbf{k}\alpha} c_{\mathbf{k}\alpha} + h.c.$$

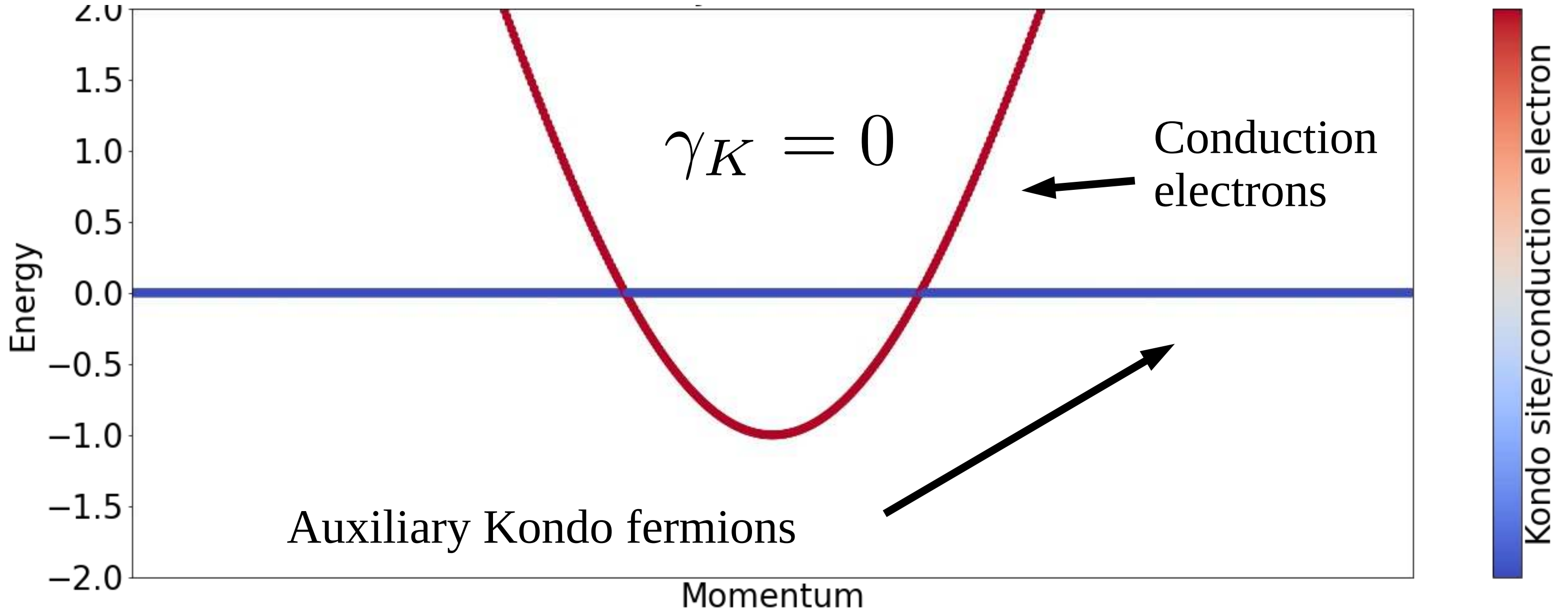

Electronic structure of the Kondo lattice problem

$$H \sim \sum_{\mathbf{k}\alpha} \epsilon_{\mathbf{k}} c^{\dagger}_{\mathbf{k}\alpha} c_{\mathbf{k}\alpha} - \gamma_K \sum_{\mathbf{k},\alpha\beta} f^{\dagger}_{\mathbf{k}\alpha} c_{\mathbf{k}\alpha} + h.c.$$

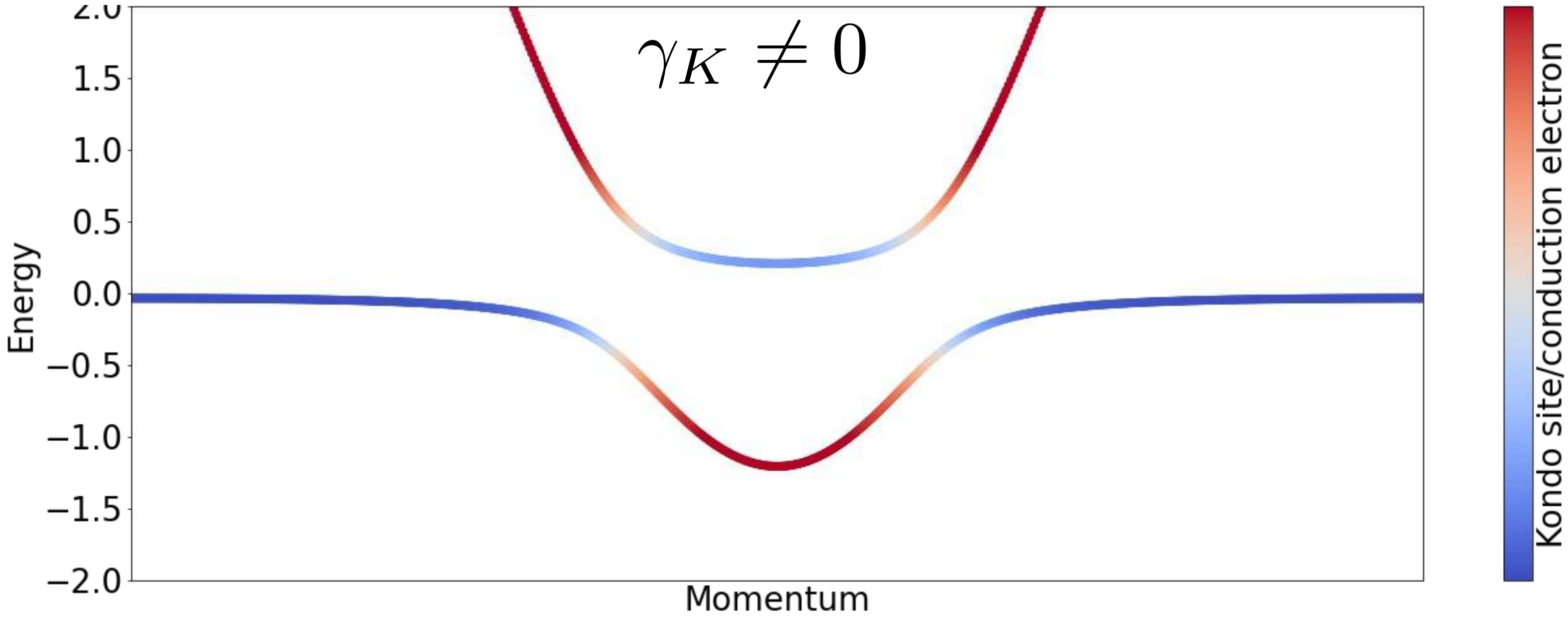

The Kondo coupling opens up a gap in the electronic structure

Electronic structure of a rare-earth van der Waals heavy-fermion material CeSiI

Ultrathin heavy-fermion isolated in

Nature 625, 483−488 (2024)

Heavy-fermion (gapped) electronic structure

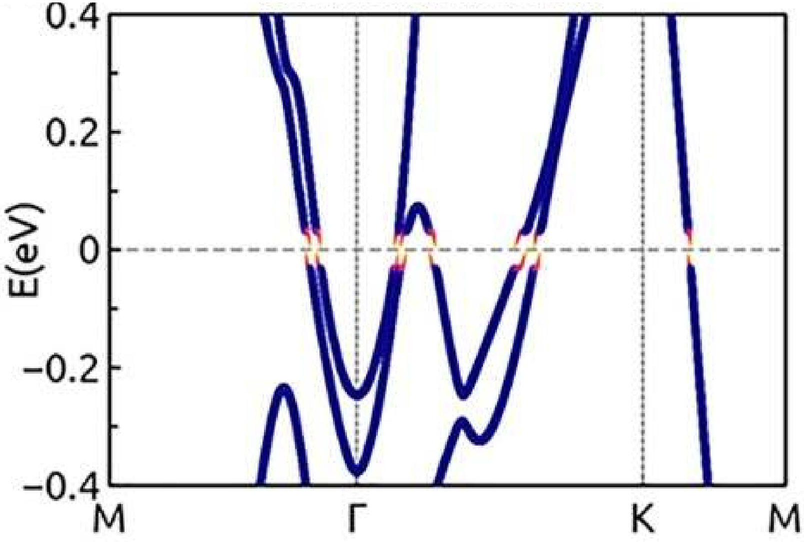

Nano Letters 24 (14), 4272–4278 (2024)

Heavy-fermions in twisted graphene trilayers

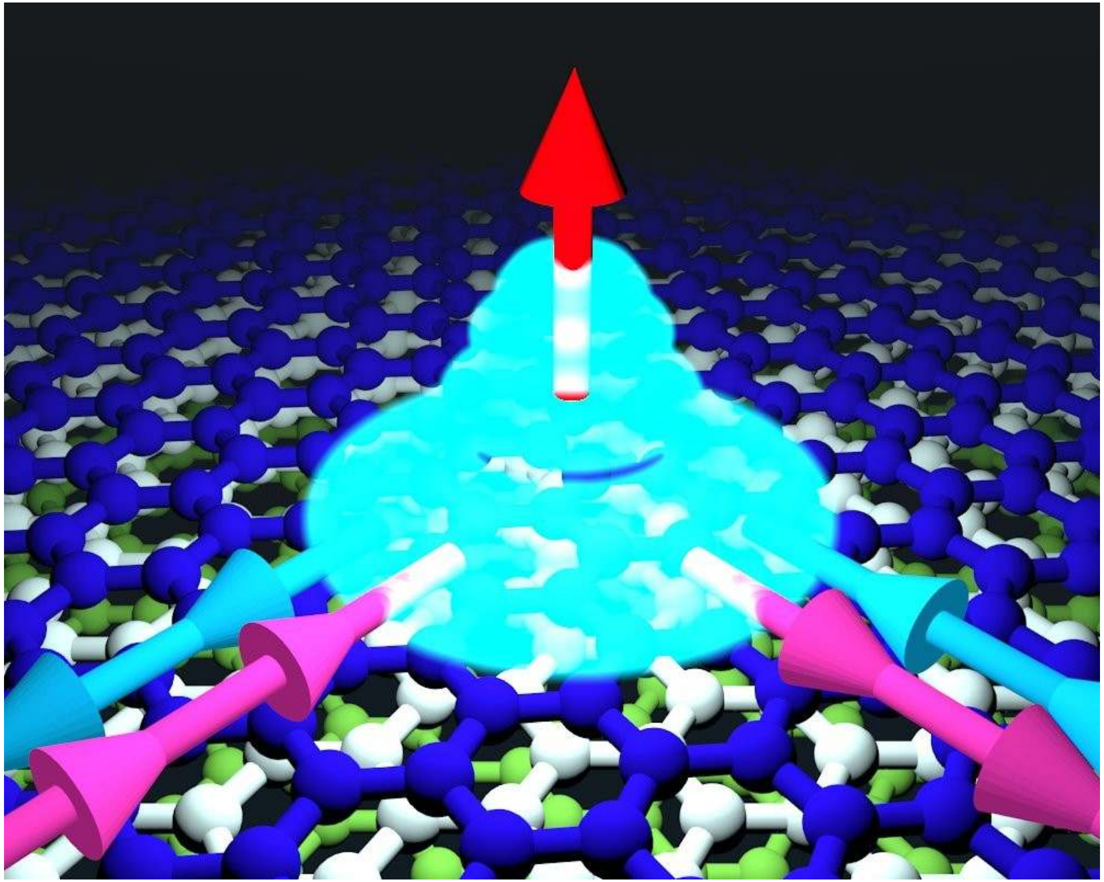

Aline Ramires

Phys. Rev. Lett. 127, 026401 (2021)

Heavy-fermions in twisted graphene trilayers

Top view

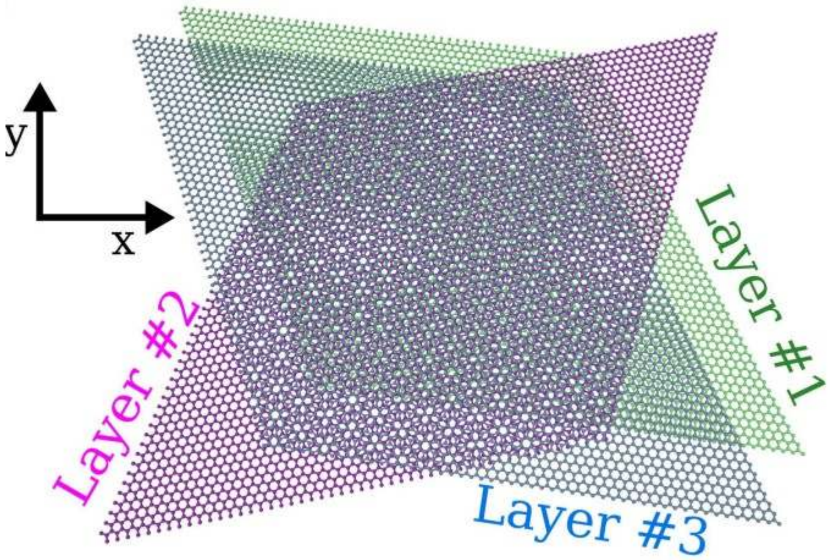

Lateral view

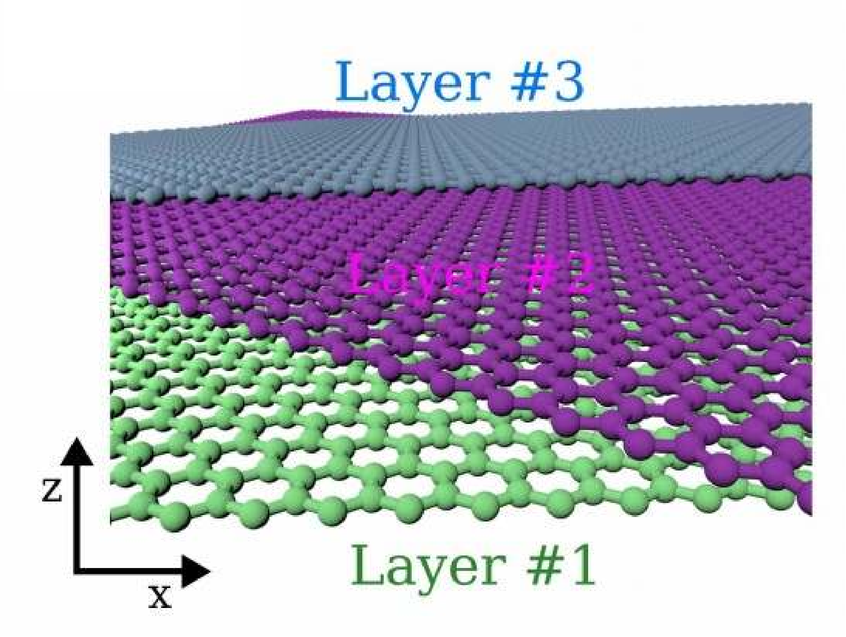

Heavy-fermions in twisted graphene trilayers

Top view

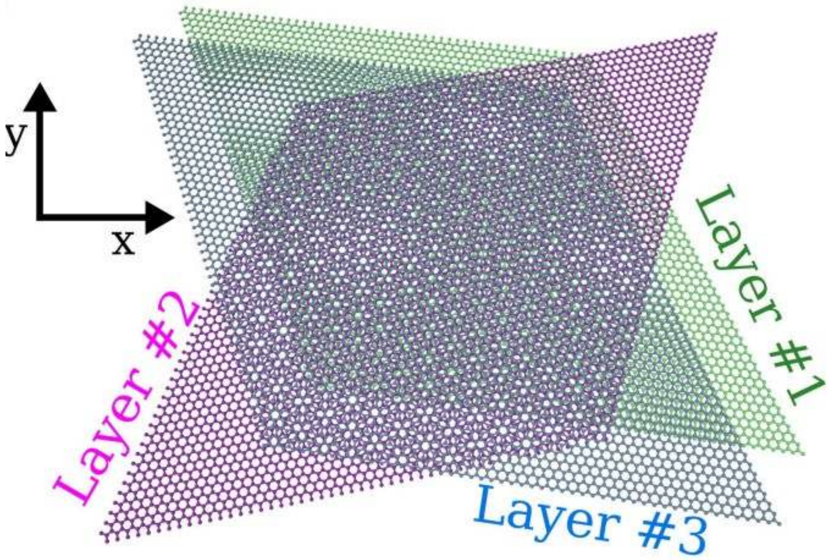

Band structure

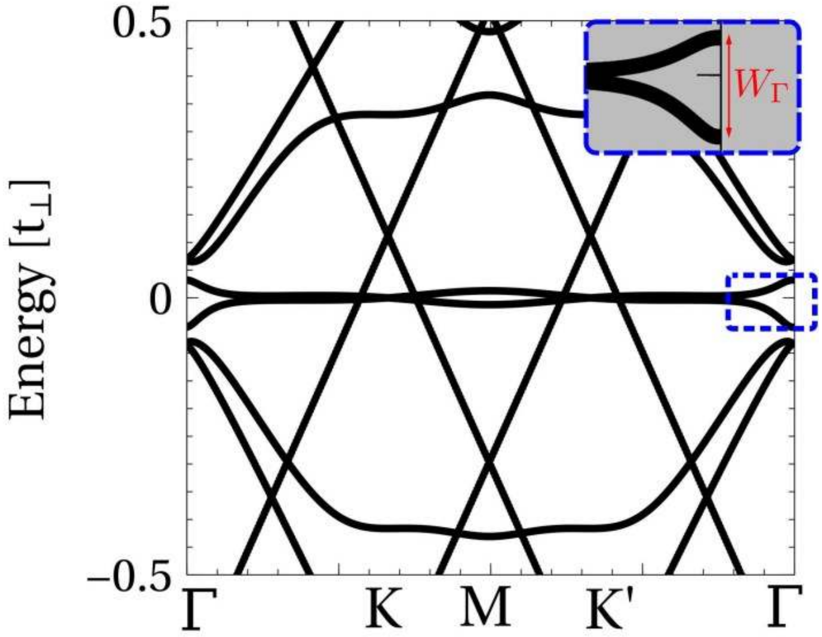

Heavy-fermions in twisted graphene trilayers

Top view

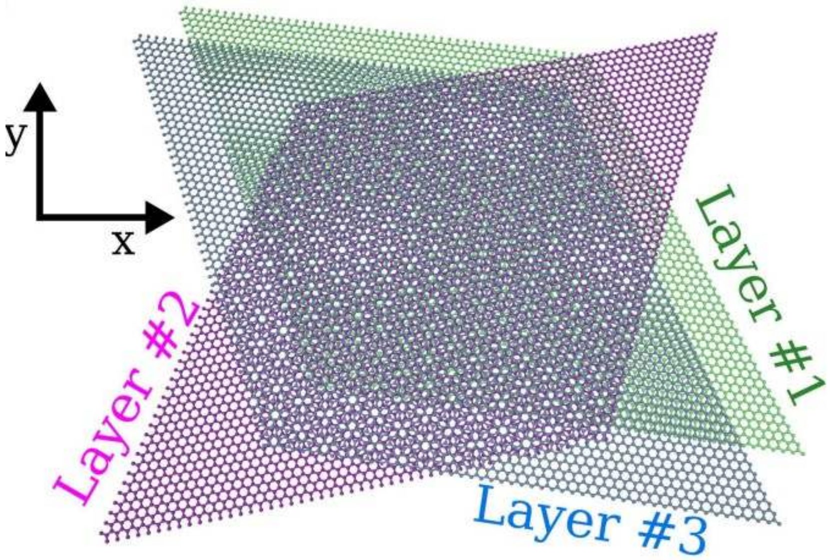

Electronic structure in the presence of an electric bias

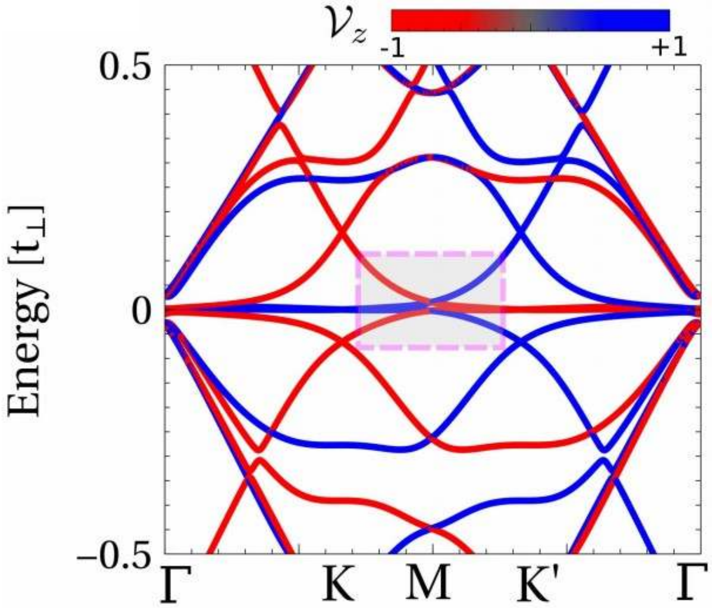

Heavy-fermions in twisted graphene trilayers

Low energy model

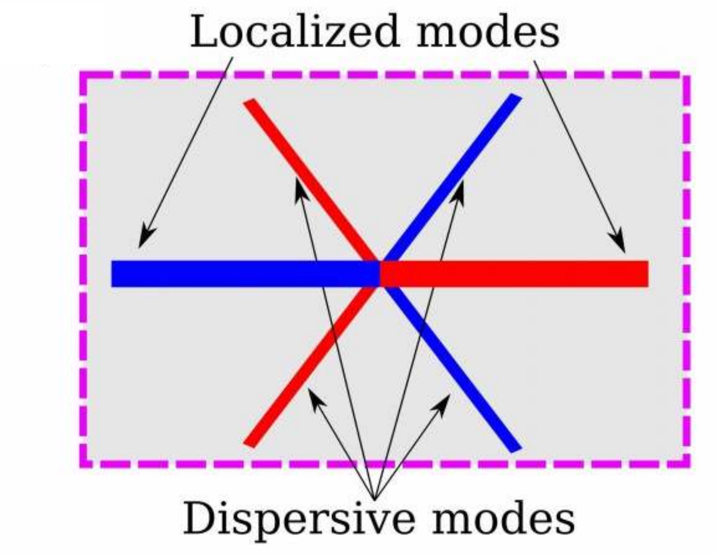

Electronic structure in the presence of an electric bias

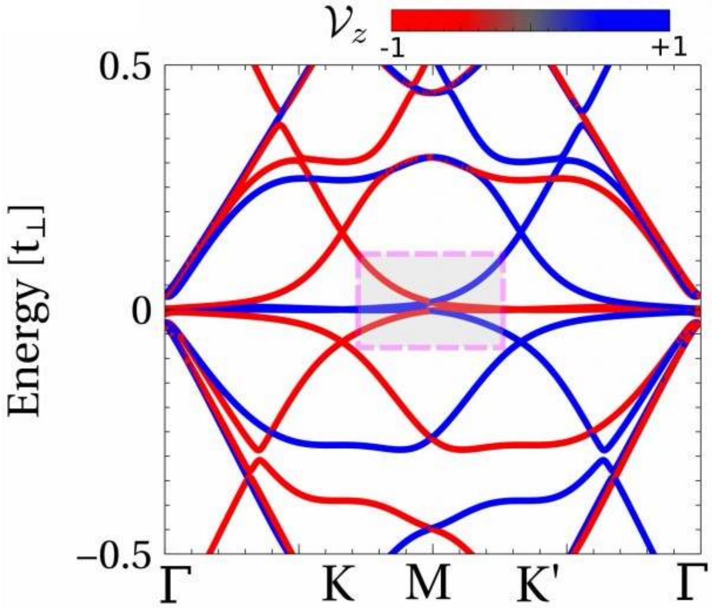

Kondo lattice model in the presence of interactions

Interactions of the Kondo lattice model

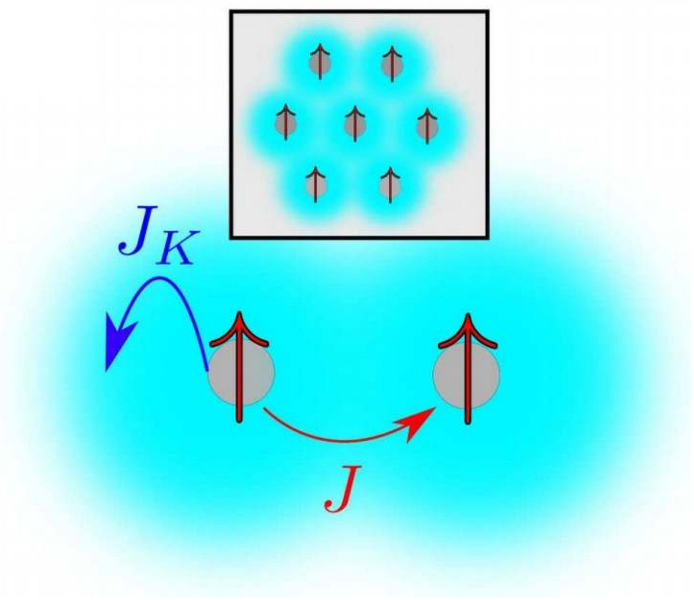

Kondo coupling

Exchange coupling

$$H = H_{\mathrm{dispersive}} + J_K \sum_{\langle i\alpha \rangle} \mathbf{S}_i \cdot \mathbf{s}_\alpha + J \sum_{\langle ij \rangle} \mathbf{S}_i \cdot \mathbf{S}_j$$

Promotes Kondo screening

Promotes magnetic order

A heavy fermion regime appears when the Kondo coupling dominates over the exchange coupling

$$|J/J_K| < 1$$

Kondo lattice model in the presence of interactions

Interactions of the Kondo lattice model

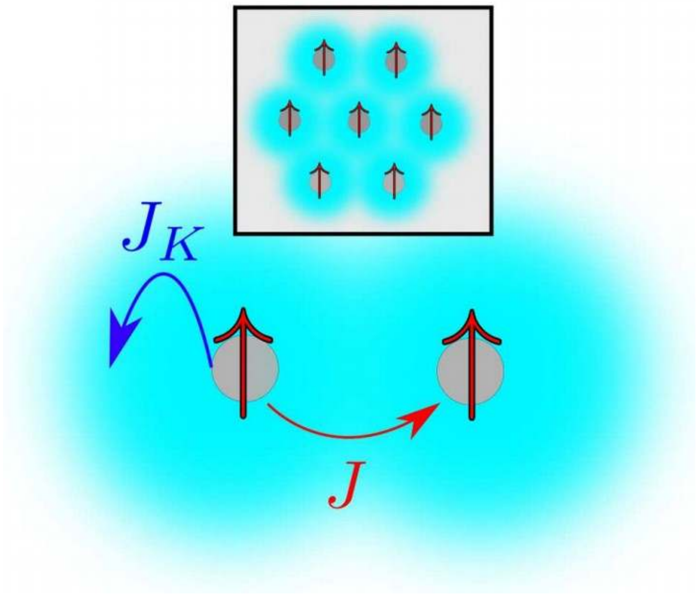

Electric control of the Kondo regime

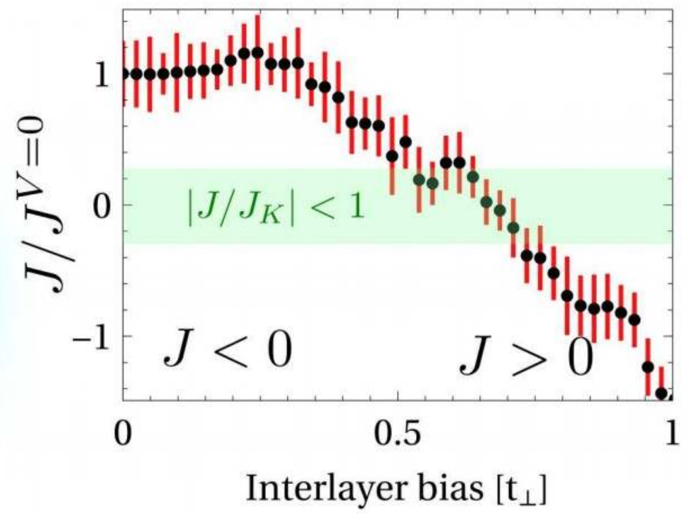

A heavy fermion regime appears when the Kondo coupling dominates over the exchange coupling

$$|J/J_K| < 1$$

Heavy-fermions in twisted graphene trilayers

Heavy-fermion (Doniach) phase diagram

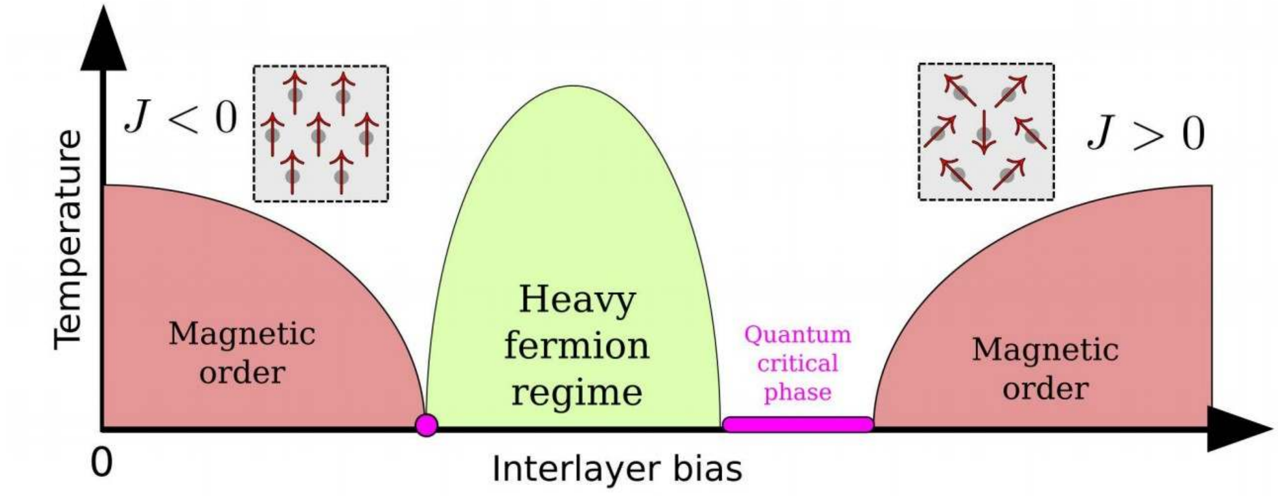

Electric control of the Kondo regime

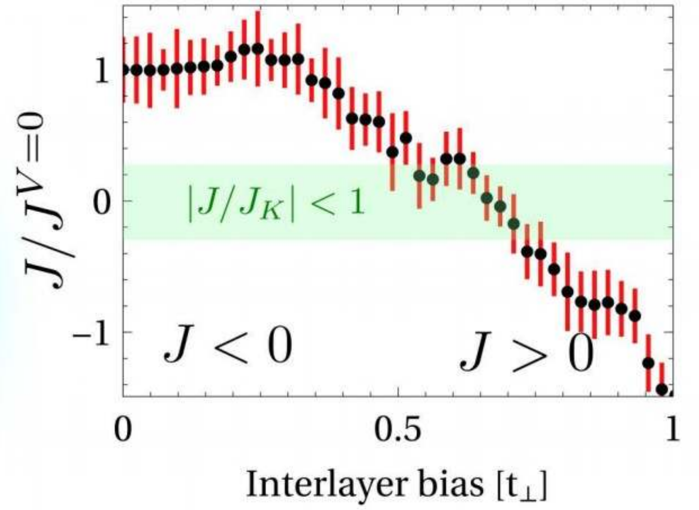

The full phase diagram of the heavy fermion system can be explored in a single twisted graphene, by tuning the system with an electric bias

An experimental signature of heavy-fermion physics: spin-triplet superconductivity

Reentrant superconductivity in twisted trilayer graphene

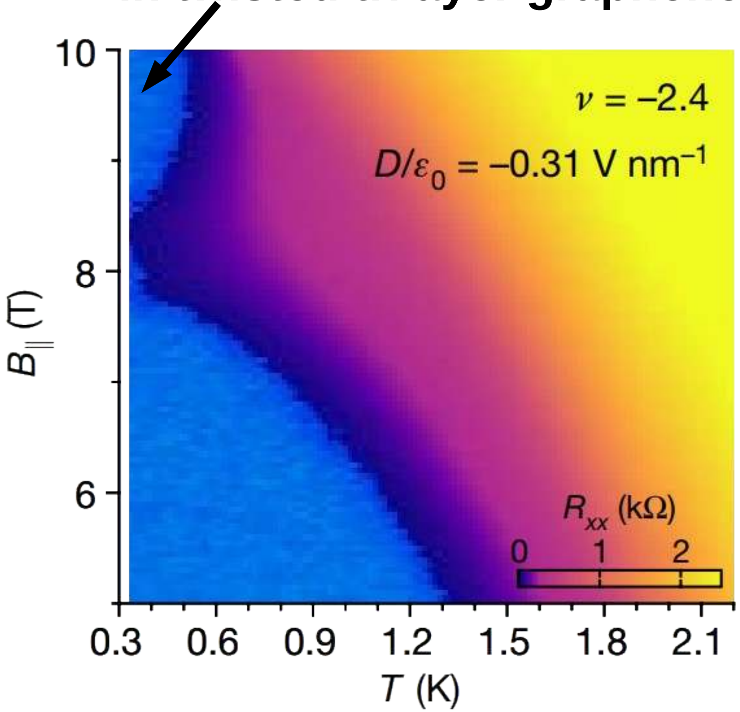

Nature 595, 526–531 (2021)

Reentrant superconductivity in UTe_2

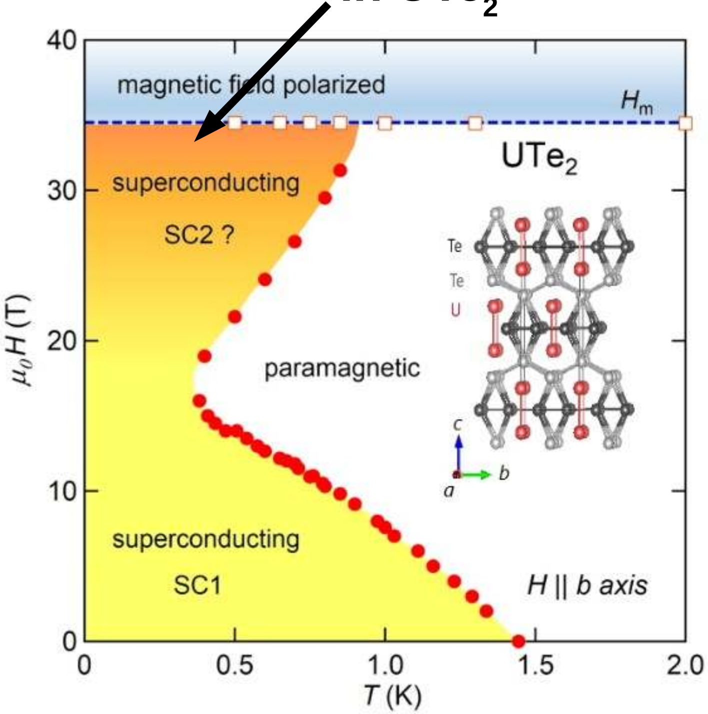

Nat. Phys. 15, 1250 (2019)
Science 365, 684 (2019)

Heavy-fermions in a van der Waals dichalcogenide heterostructure

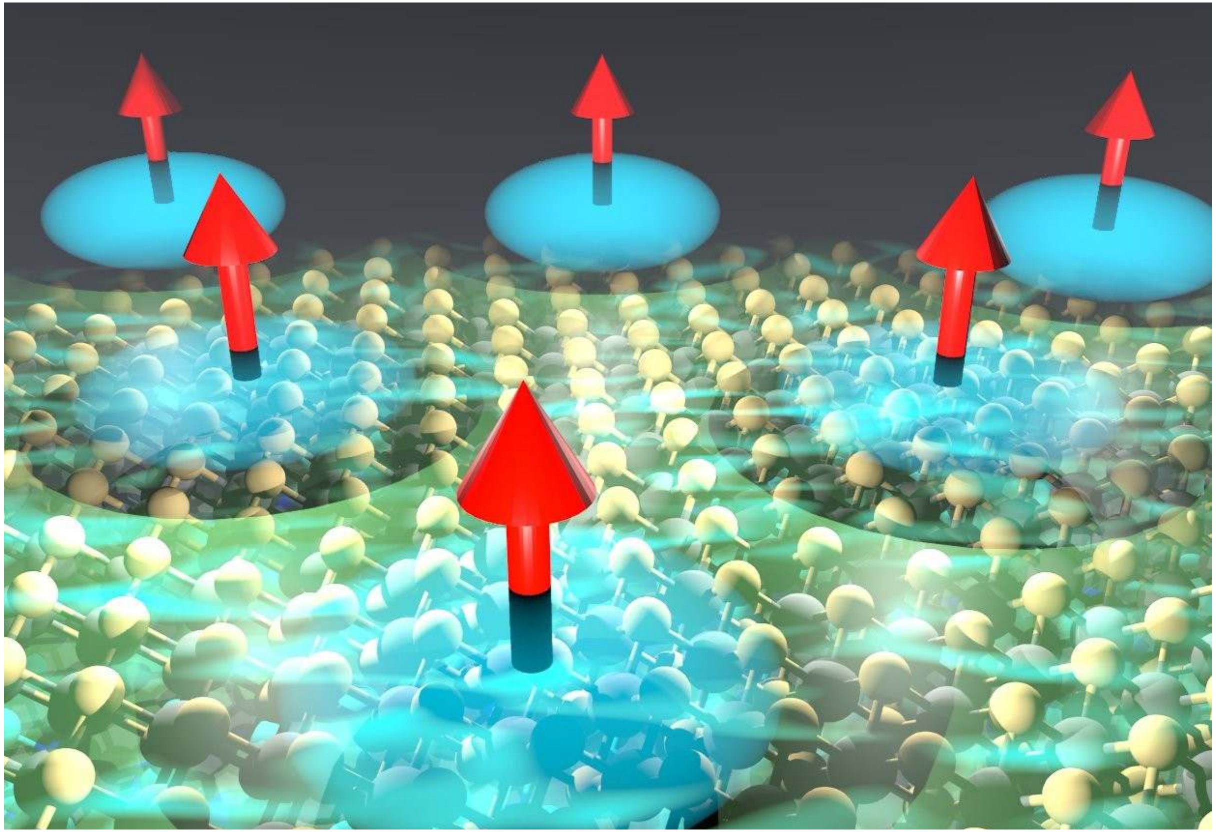

V. Vaňo

M. Amini

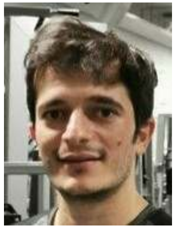

G. Chen

S. Ganguli

S. Kezilebieke

P. Liljeroth

Nature 599, 582–586 (2021)

Heavy-fermions in dichalcogenide bilayers

Triangular lattice of local magnetic moments

$1T\text{-}TaS_2$

Two-dimensional electron gas

$1H\text{-}TaS_2$

Moment formation in 1T-TaS_2

Charge-density wave reconstruction, leading to a localized orbital in a $\sqrt{13}\times\sqrt{13}$ unit c

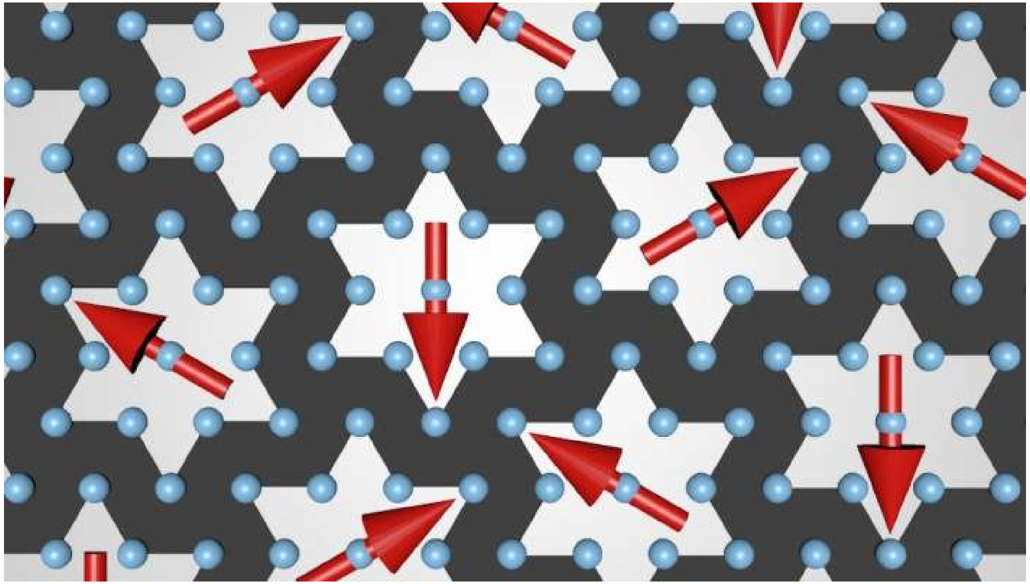

Ta

Strong interactions give rise to local moment formation

Effectively a S=1/2 Heisenberg model in a triangular lattice

PNAS 114.27 (2017)
Phys. Rev. X 7, 041054 (2017)
Phys. Rev. B 96, 195131 (2017)

Heavy-fermions in dichalcogenide bilayers

Interlayer coupling creates the Kondo coupling

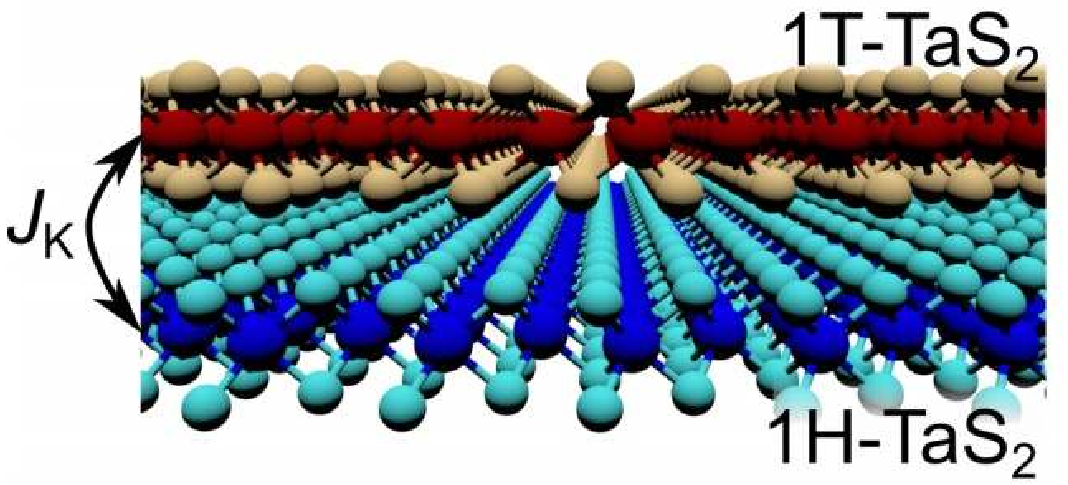

Intralayer exchange between local moments

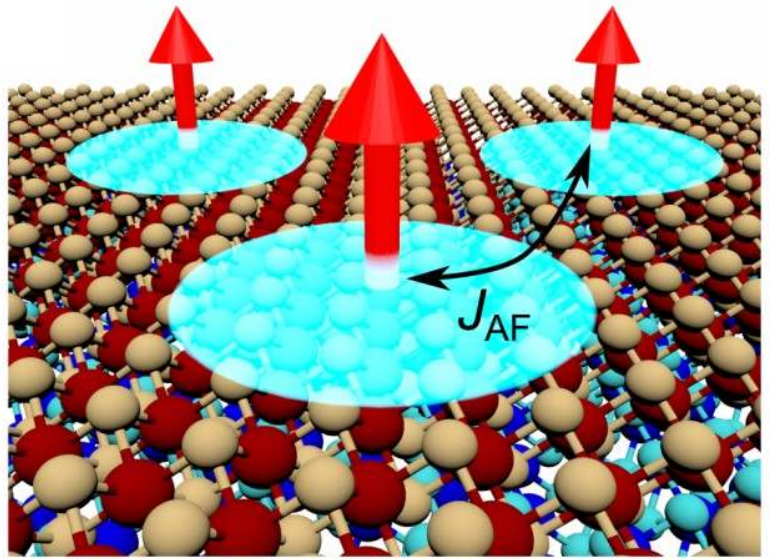

The bilayer realizes all the ingredients for heavy-fermion physics

Experimental signatures of heavy-fermion physics

- Kondo physics in the magnetic lattice
- Gap opening in the metallic layer

Both signatures can be probed with scanning tunnel microscopy by growing two heterostructures

Probing the Kondo peak

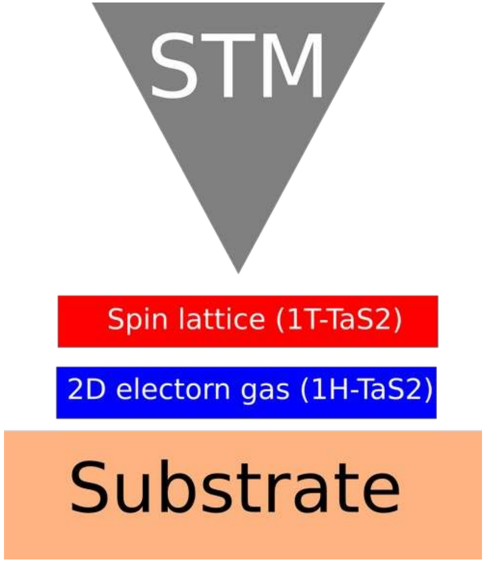

Probing the heavy-fermion gap

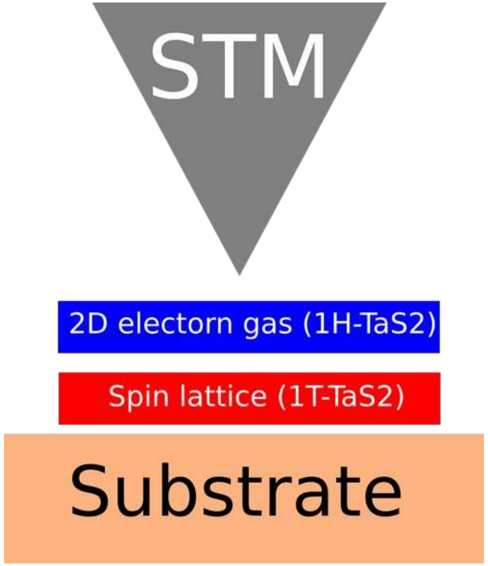

Grid spectroscopy of 1T-1H

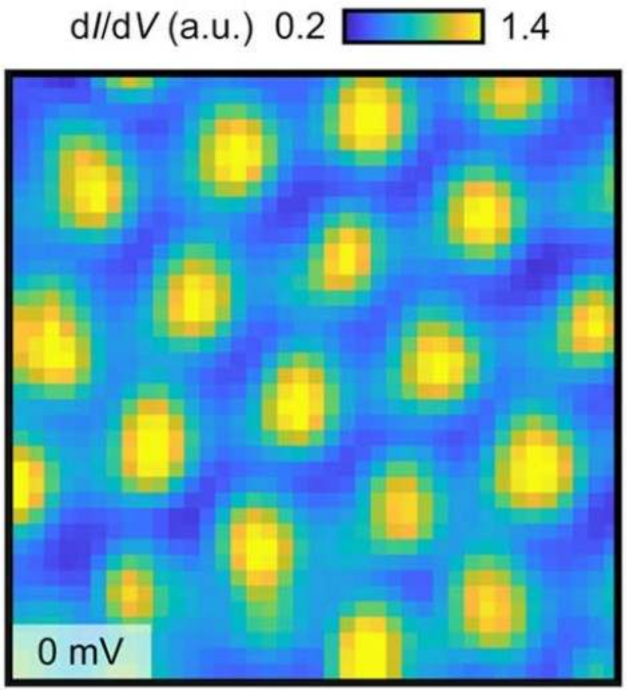

dI/dV (V=0)

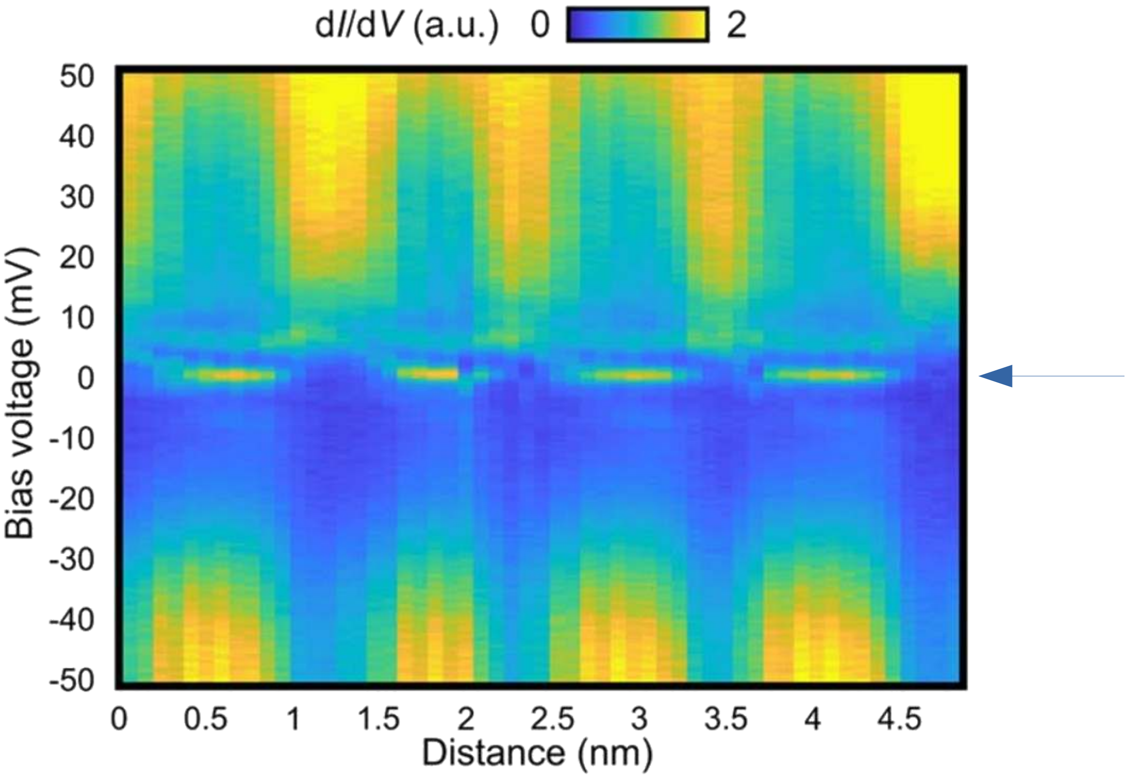

Zero bias (Kondo) peak appearing with the CDW periodicity

Kondo physics in the magnetic lattice

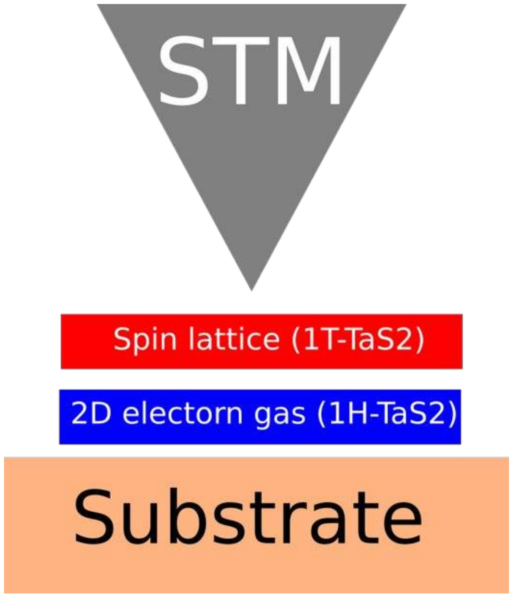

Sample

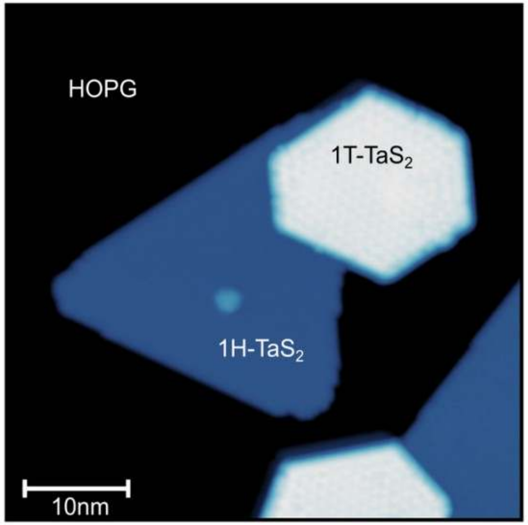

Differential conductance

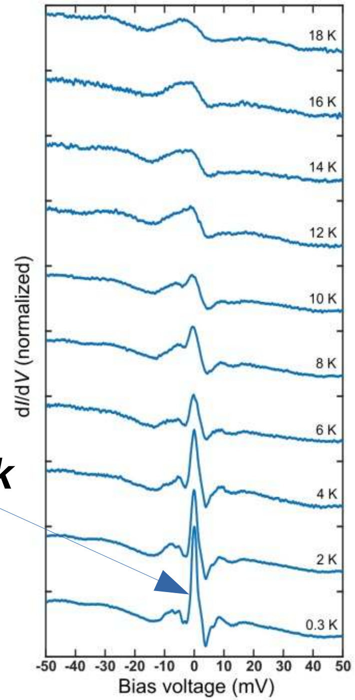

Kondo peak

The system shows a Kondo peak when the local moments are probed

Temperature and field dependence consistent with Kondo

Kondo physics in the magnetic lattice

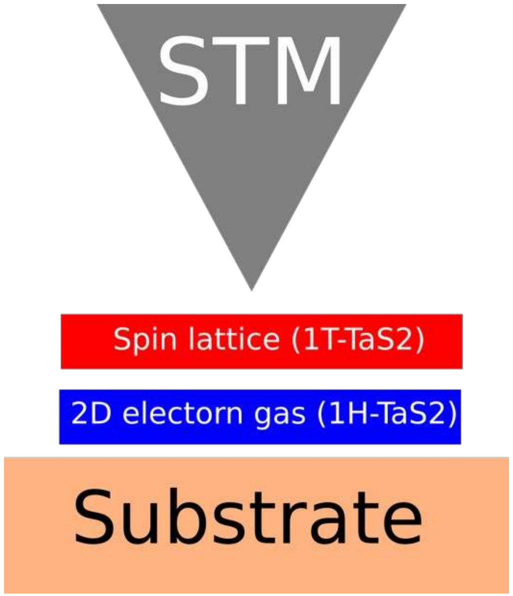

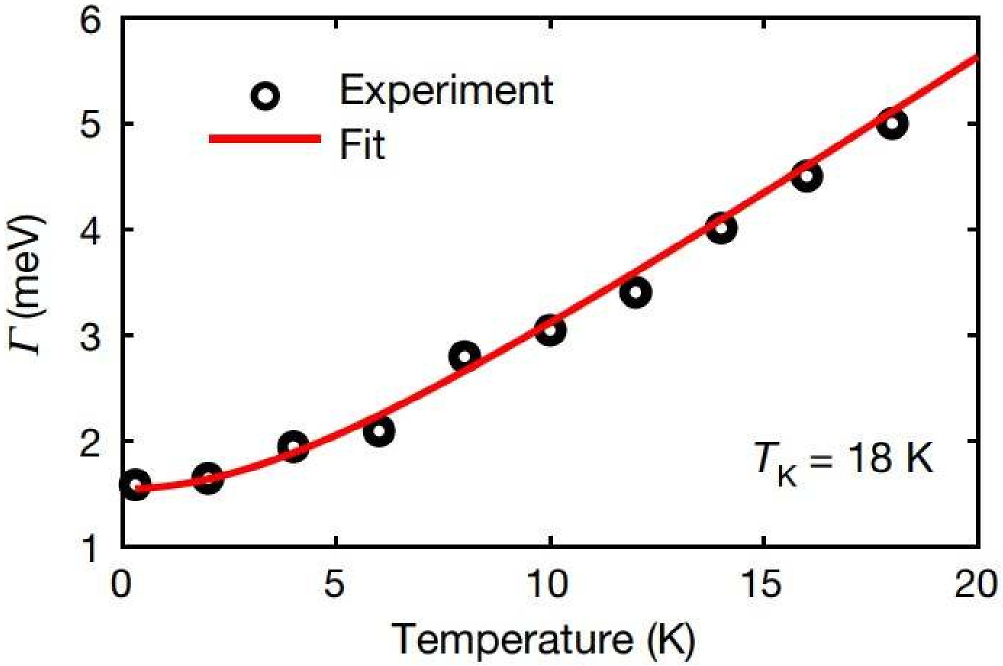

The Kondo peak follows the expected temperature dependence

Heavy-fermion gap in the 2D electron gas

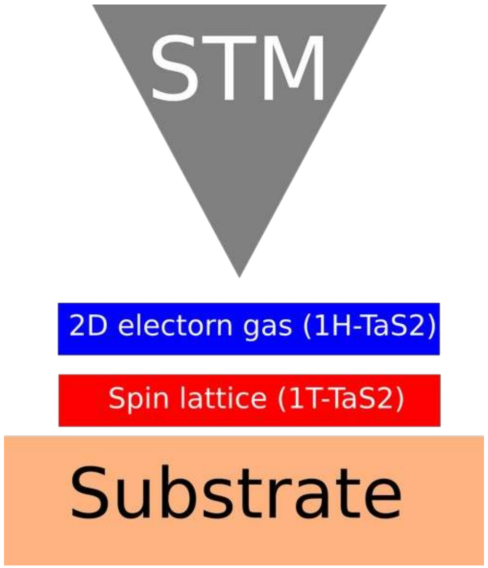

Sample

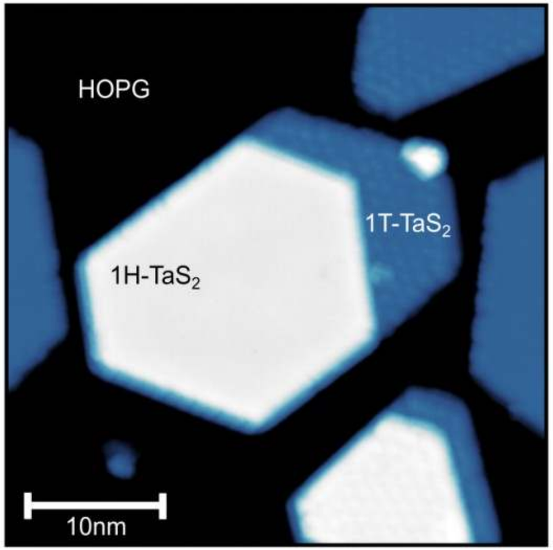

Differential conductance

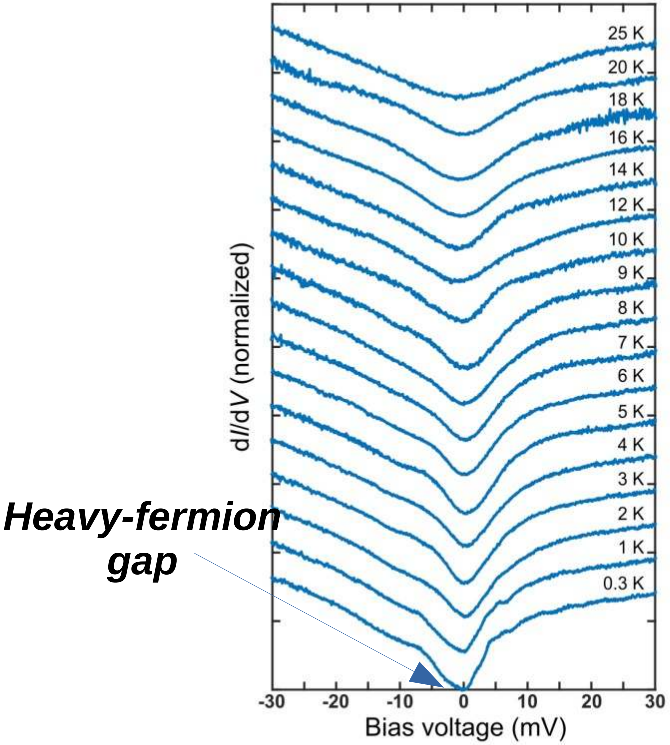

A heavy-fermion gap appears on the metal side

Temperature and field dependence consistent with a heavy-fermion gap

Heavy-fermion gap in the 2D electron gas

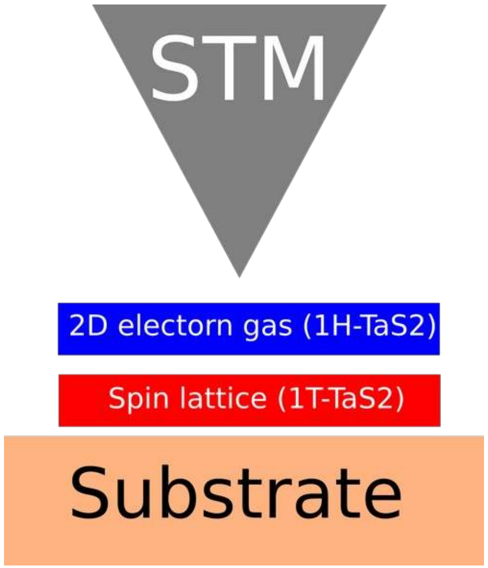

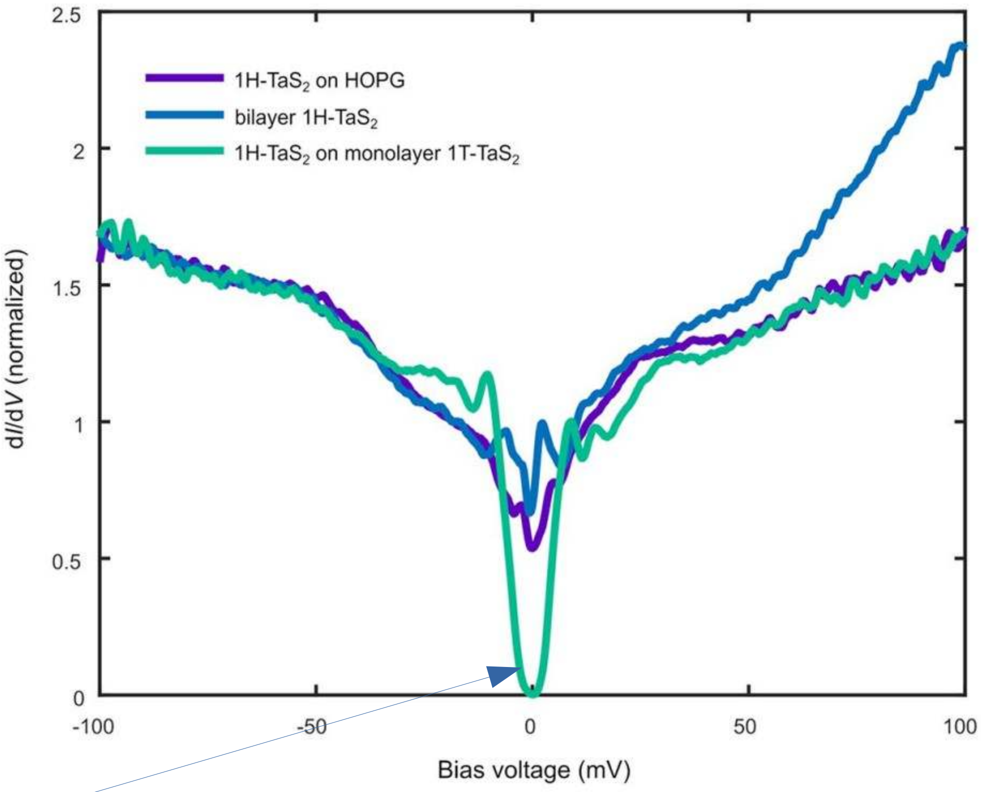

Heavy-fermion gap

Heavy-fermion gap in the 2D electron gas

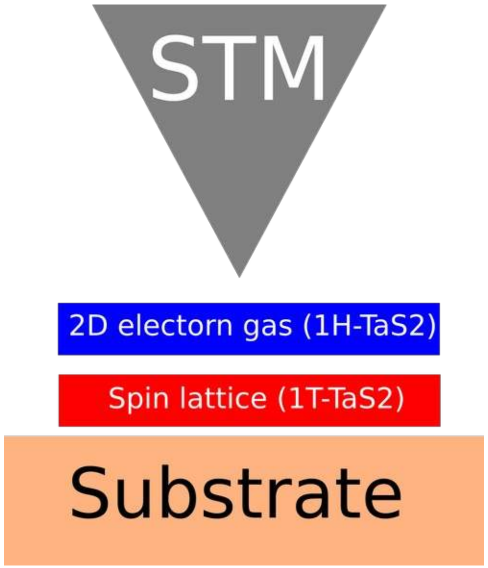

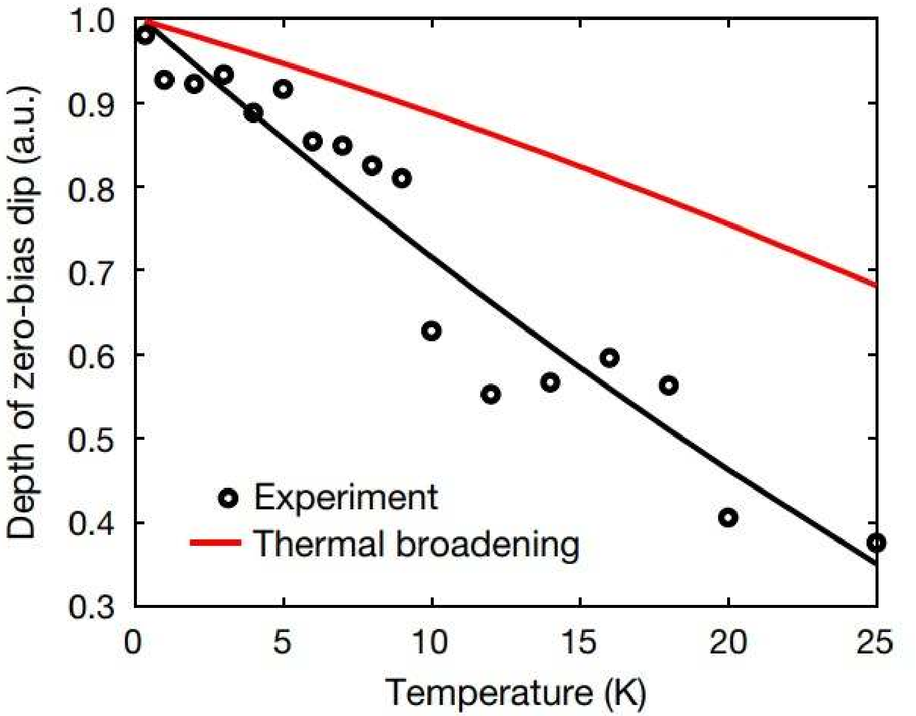

The gap shows a temperature dependence beyond thermal broadening, expected from a heavy-fermion gap

The phase diagram van der Waals heavy-fermions

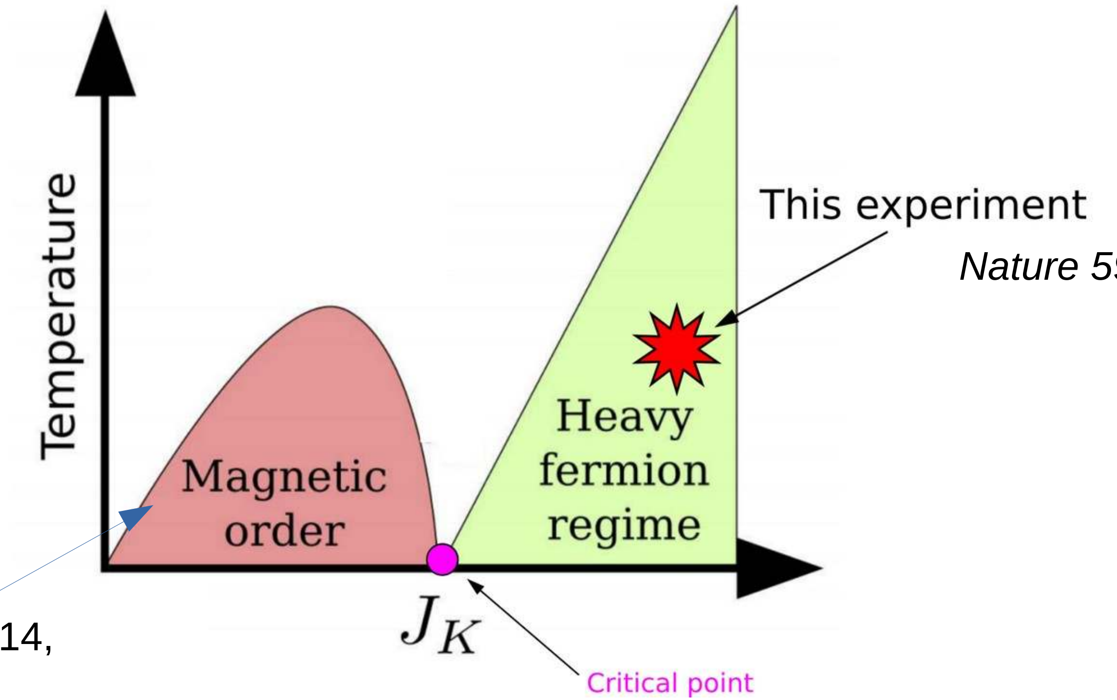

Nature 599, 582–586 (2021)

Nature Communications 14, 7005 (2023)

Can we push this system to critical and different unconventional superconducting regimes?

Controlling the heavy-fermion state

Of course, we can use the typical knobs of bulk heavy fermion compounds (pressure, chemical doping, etc)

Most importantly, we can exploit the full tunability of van der Waals materials

Gating

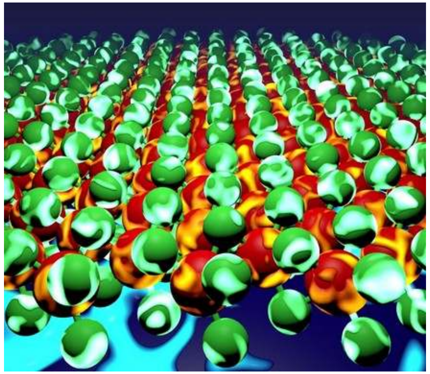

Science 306, 5696, 666-669 (2004)

Twist engineering

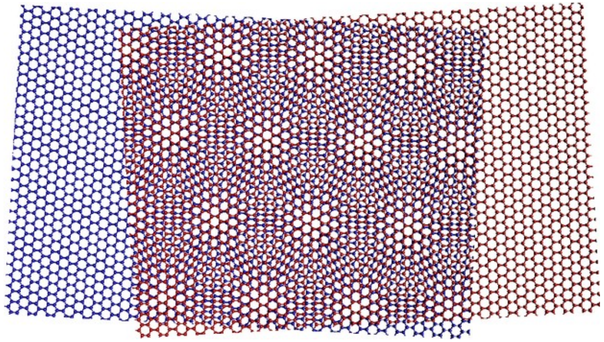

Nature Reviews Materials 6, 201–206 (2021)

Materials engineering

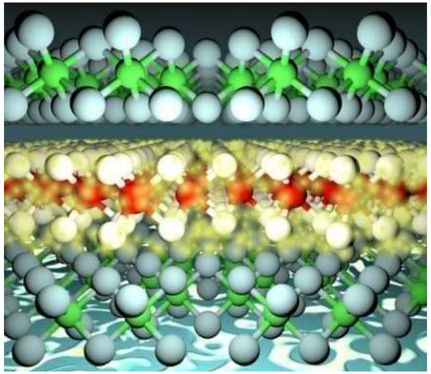

Nature 499, 419–425 (2013)

Allowing to independently control Kondo coupling, exchange coupling, doping and electronic dispersion

Open-source software for van der Waals materials

Quantum Lattice: A user interface to compute electronic properties

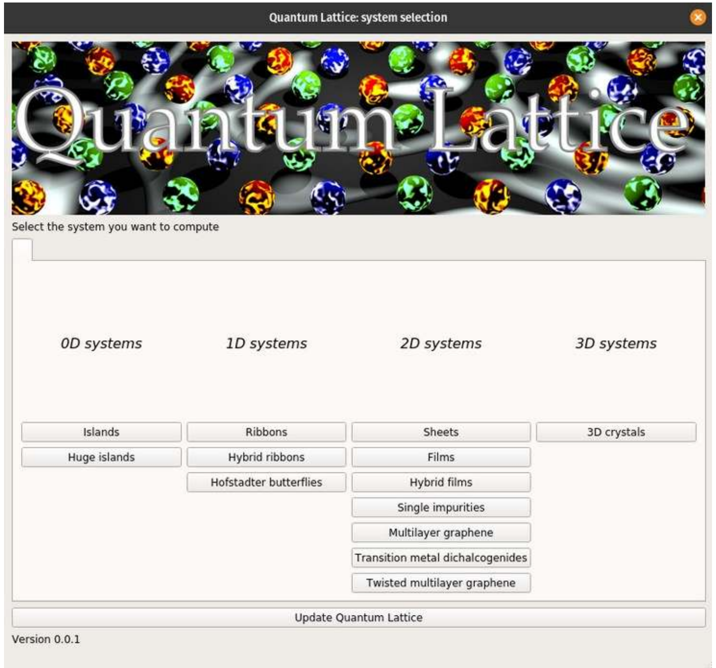

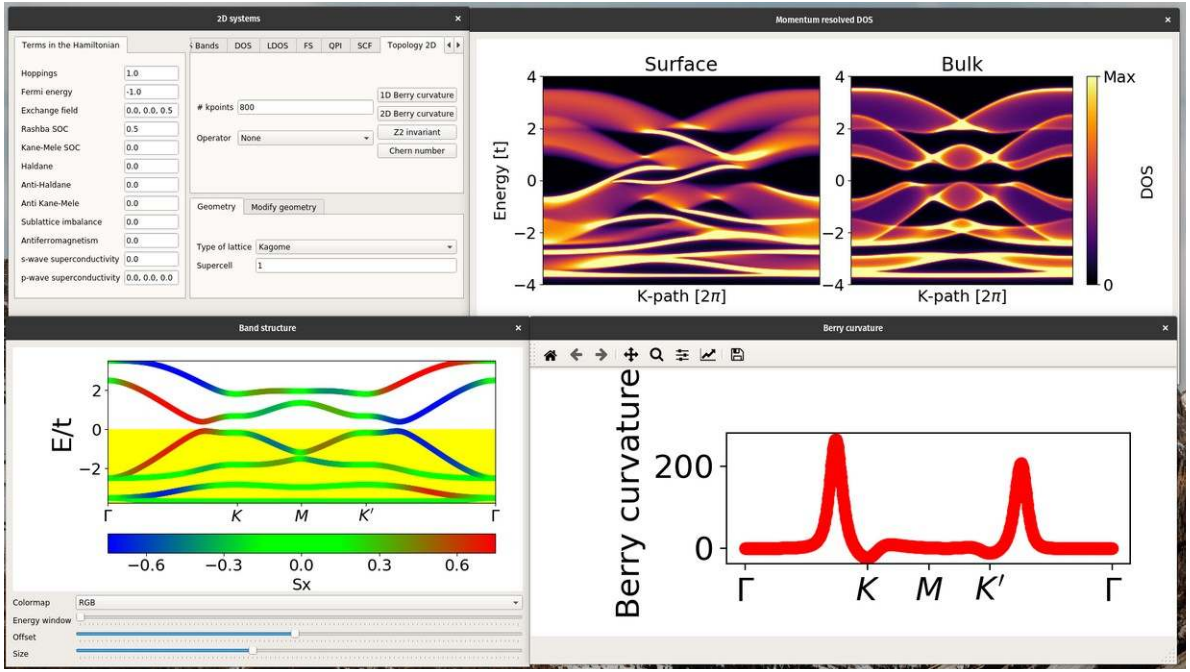

Quantum Lattice: open source interactive interface for tight binding modeling

https://github.com/joselado/quantum-lattice

Quantum matter in van der Waals materials school

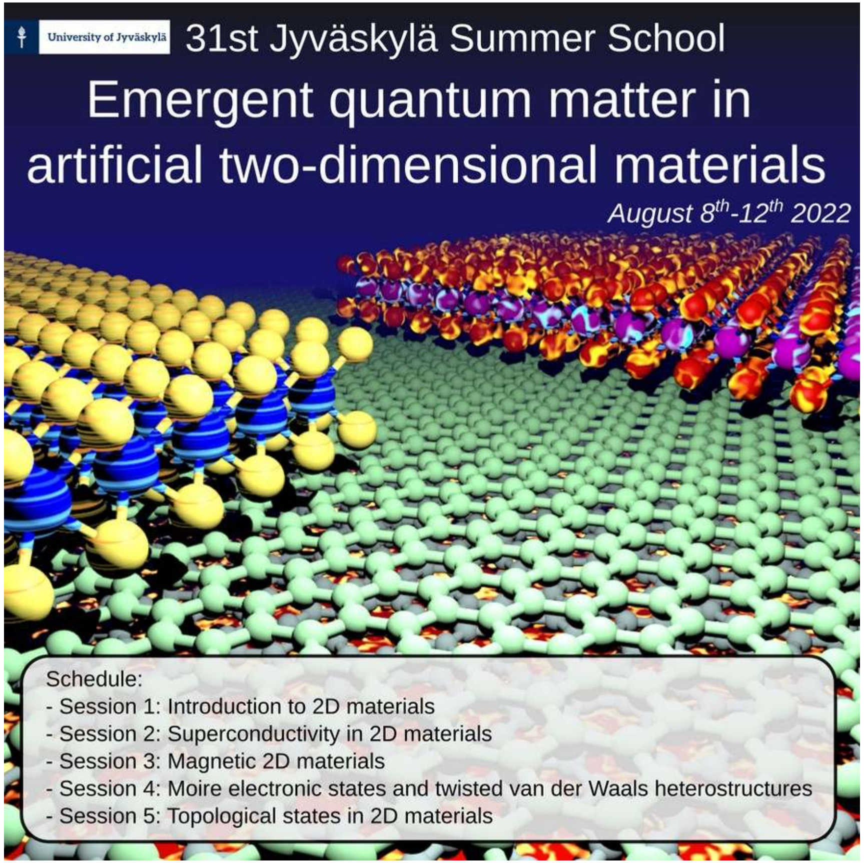

Recordings available at

https://www.youtube.com/channel/UCgnB-4CcqRQnvTi7P0cUakQ

- Session 1: Introduction to 2D materials
- Session 2: Superconductivity in 2D materials
- Session 3: Magnetic 2D materials
- Session 4: Moire electronic states and twisted van der Waals heterostructures
- Session 5: Topological states in 2D materials

Take home

Van der Waals materials provide a new platform to engineer exotic matter, including multiferroics and heavy-fermion Kondo lattices

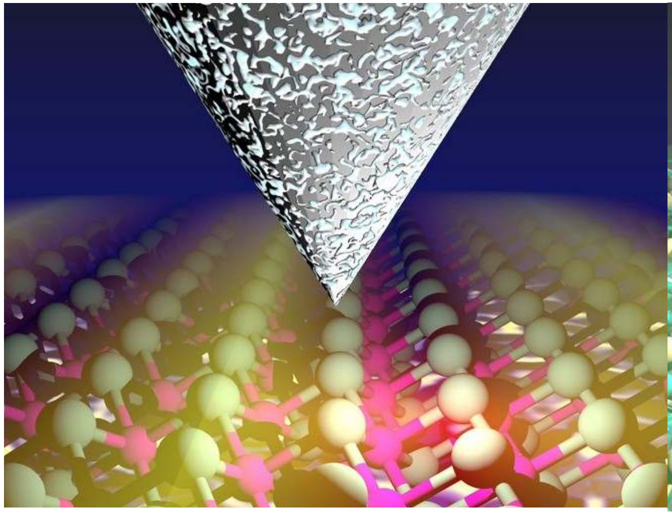

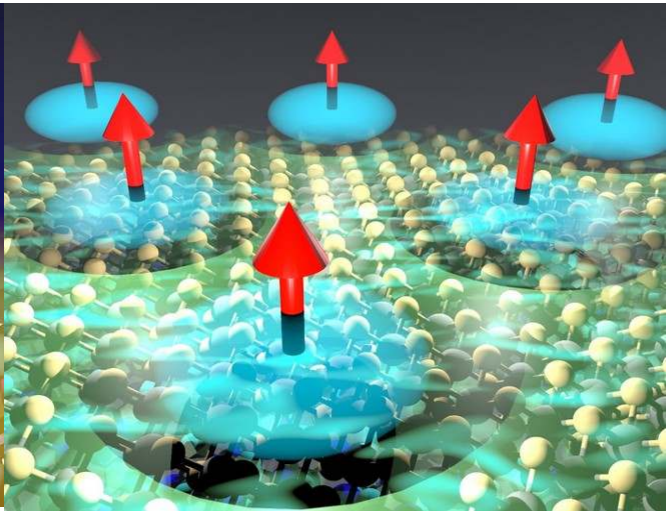

2D Materials 9 (2), 025010 (2022)
2D Materials 10 (2), 025026 (2023)
Advanced Materials, 2311342 (2024)

Phys. Rev. Lett. 127, 026401 (2021)
Nature 599, 582–586 (2021)
Nano Letters 24 (14), 4272–4278 (2024)

Thank you

Funding from

J&AE JANE AND AATOS ERKKO FOUNDATION

SUOMEN AKATEMIA